Charles University

Second Faculty of Medicine

Doctoral study programme: Medical Biophysics

Aleksei Pashchenko

Bionanosensors in early-stage theragnostics

Bionanosenzory v časné teragnostice

Dissertation Thesis

Supervisor at CUNI: prof. Evžen Amler, PhD

Supervisor at UNISS: Prof.ssa Margherita Maioli

Prague and Sassari, 2025

UNIVERSITÀ DEGLI STUDI DI SASSARI

Scuola di dottorato di ricerca in Scienze Biomediche

Curriculum: Biologia e Genetica

XXXVII° ciclo

"Bionanosensori nella teranostica in fase iniziale"

"Bionanosensors in early-stage theragnostics"

Dottorande: *Dott. Aleksei Pashchenko*

Tutor: *Prof.ssa Margherita Maioli*

Co-Tutor*: Prof. Even Amler PhD*

Coordinatore del corso di dottorato: Prof.ssa Margherita Maioli

Anno Accademico 2024/2025

CHARLES UNIVERSITY

SECOND FACULTY OF MEDICINE

DEPARTMENT OF BIOPHYSICS

and

UNIVERSITY OF SASSARI

DEPARTMENT OF BIOMEDICAL SCIENCES

Aleksei Pashchenko

Bionanosensors in early-stage theragnostics

Co-Tutelle Dissertation Thesis

Supervisor at CUNI: Prof. Even Amler PhD

Supervisor at UNISS: Prof. Margherita Maioli, PhD

Prague and Sassari 2025

Declaration

I declare hereby that I made this dissertation thesis by myself and that I mentioned and cited properly all the sources and literature. At the same time, I declare that this thesis was not used to obtain another or the same title.

I agree with permanent deposition of an electronic version of my thesis in the system database of interuniversity project Thesis.cz for a permanent control of similarities of theses.

In Prague on 8.4.2025

Aleksei Pashchenko

Acknowledgments

Firstly, I would like to express my gratitude to both of my supervisors, Prof. Evžen Amler, PhD, and Prof. Margherita Maioli, PhD, for their invaluable guidance throughout my Co-tutelle Doctoral Study. The synergy of their expertise and unwavering commitment truly fueled my motivation, especially during the challenging times. Their support was a beacon that guided me forward.

Thank you to the faculties, staff, and colleagues from both universities for their support. I am especially grateful to the laboratory teams for their assistance during my experiments and to the outstanding orthopedic surgeon, the late Fedoruk G.V. Lastly, I would like to acknowledge my family for their unwavering love and belief in me. Their support has been my greatest inspiration.

Bionanosensors in early-stage theragnostics

Abstract

The thesis focuses on the development and application of nanomaterials in the field of theranostics, combining diagnostics and targeted drug delivery within the framework of personalized medicine. The primary objective is to design and test ultrasensitive and mechanically stable bionanosensors based on nanofiber membranes that are able to detect the early stages of diseases. These sensors, functionally modified with specific molecular binding agents, will enable the accurate detection of biomarkers such as proteins, antibodies, bacteria, and microRNAs, significantly enhancing and expanding diagnostic capabilities. The secondary goal is to develop and test systems for active targeted drug delivery, including implantable gels, protective/prophylactic devices, and on-tissue systems such as regenerative skin coverings.

The theoretical section summarizes current knowledge on biomarkers, nanotechnology, and targeted drug delivery methods, particularly in oncology and degenerative diseases.

The experimental section demonstrates the detection of bacterial contamination using nanofiber-based sensors that are able to identify *Escherichia coli* and other biomolecules in various model fluids. The results confirm the potential of these technologies not only for the early diagnosis of infections and cancer but also for the advancement of active targeted drug delivery delivery systems in regenerative medicine. The research also addresses the limitations of traditional methods, such as the low specificity and limited accessibility of imaging techniques and the side effects of passive drug delivery. It offers a promising direction for modern diagnostic and therapeutic strategies.

Keywords

bionanosensors, biomarkers, chemotherapy, electrospun nanofibers, microRNA, nanofiber membranes, personalized medicine, theranostics

Bionanosenzory v časné teragnostice

Abstrakt

Dizertační práce se zaměřuje na vývoj a použití nanomateriálů v oblasti teragnostiky, tedy propojení diagnostiky a cílené terapie v kontextu personalizované medicíny. Hlavním cílem je navrhnout a otestovat ultrasenzitivní a mechanicky stabilní bionanosenzory na bázi nanovlákenných membrán, které jsou schopny detekovat časná stádia onemocnění. Tyto senzory, funkčně modifikované specifickými molekulárními — vazebnými látkami, umožňují přesnou detekci biomarkerů, jako jsou proteiny, protilátky, bakterie, mikroRNA apod., čímž výrazně zlepšují a zpřístupňují diagnostické možnosti. Druhým cílem je vývoj a testování systémů pro aktivní cílené dodávání léčiv, včetně implantovatelných gelů, protektivních/profylaktických prostředků a „on-tissue“ aplikací, jako jsou regenerační kožní kryty.

Teoretická část shrnuje současné poznatky o biomarkerech, nanotechnologiích a možnostech cíleného dodávání léčiv, zejména v onkologii a degenerativních onemocněních.

Experimentální část prokazuje detekci bakteriální kontaminace pomocí nanovlákenných senzorů, schopných identifikovat *Escherichia coli* a další molekuly v různých modelových tekutinách. Výsledky potvrzují potenciál těchto technologií nejen pro včasnou diagnostiku infekcí a nádorových onemocnění, ale také pro rozvoj systémů cílené léčby a regenerativní medicíny. Výzkum zároveň reaguje na omezení běžných metod, jako je nízká specifita a dostupnost zobrazovacích technik, současně na vedlejší účinky pasivního dodávání léčiv, a navrhuje perspektivní směr pro moderní diagnosticko-terapeutické strategie.

Klíčová slova:

bionanosenzory, biomarkery, chemoterapie, electrospun nanovlákna, mikroRNA, nanovlákenné membrány, personalizovaná medicína, teragnostika

Bionanosensori nella teranostica in fase iniziale

l'abstract

La tesi si concentra sullo sviluppo e l'applicazione di nanomateriali nell'ambito della teragnostica, combinando diagnostica e somministrazione mirata di farmaci nel contesto della medicina personalizzata. L'obiettivo principale è progettare e testare bionanosensori ultrasensibili e meccanicamente stabili, basati su membrane di nanofibre, in grado di rilevare le fasi iniziali delle malattie. Questi sensori, modificati funzionalmente con specifici agenti molecolari leganti, consentono un rilevamento accurato di biomarcatori come proteine, anticorpi, batteri e microRNA, migliorando e ampliando significativamente le capacità diagnostiche. Il secondo obiettivo è lo sviluppo e il test di sistemi per la somministrazione attiva e mirata di farmaci, compresi gel impiantabili, dispositivi protettivi/profilattici e sistemi "on-tissue", come coperture cutanee rigenerative.

La parte teorica riassume le conoscenze attuali sui biomarcatori, sulle nanotecnologie e sulle metodologie di somministrazione mirata, in particolare in oncologia e nelle malattie degenerative.

La parte sperimentale dimostra la rilevazione di contaminazioni batteriche mediante sensori a base di nanofibre, capaci di identificare *Escherichia coli* e altre biomolecole in vari fluidi modello. I risultati confermano il potenziale di queste tecnologie non solo per la diagnosi precoce di infezioni e tumori, ma anche per l'evoluzione di sistemi attivi di somministrazione terapeutica nella medicina rigenerativa. La ricerca affronta inoltre i limiti dei metodi tradizionali, come la bassa specificità e l'accessibilità limitata delle tecniche di imaging, nonché gli effetti collaterali della somministrazione passiva di farmaci, offrendo una direzione promettente per strategie diagnostico-terapeutiche moderne.

Parole chiave

bionanosensori, biomarcatori, chemioterapia, nanofibre elettrofilate, microRNA, membrane di nanofibre, medicina personalizzata, teragnostica

List of Abbreviations

ADT – Androgen Deprivation Therapy

API – Active Pharmaceutical Ingredient

AR – Androgen Receptor

AST – Aspartate Transaminase

ATP – Adenosine Triphosphate

BIPEDs – Burden of disease, Investigative, Prognostic, Efficacy of intervention, Diagnostic, Safety

BPH – Benign Prostatic Hyperplasia

CDKN1A – Cyclin-Dependent Kinase Inhibitor 1A

CDx – Companion Diagnostics

CK – Creatinine Kinase

CRP – C-Reactive Protein

CQDs – Carbon Quantum Dots

CRPC – Castration-Resistant Prostate Cancer

CS-MB – Chitosan-Molecular Beacon

DNA – Deoxyribonucleic Acid

EGFR – Epidermal Growth Factor Receptor

ELISA – Enzyme-Linked Immunosorbent Assay

ESR – Erythrocyte Sedimentation Rate

FNIH – Foundation for the National Institutes of Health

FRET – Fluorescence Resonance Energy Transfer

GPC-3 – Glypican-3

HER2 – Human Epidermal Growth Factor Receptor 2

ITPR2 – Inositol 1,4,5-Trisphosphate Receptor Type 2

LDH – Lactate Dehydrogenase

LSPR – Localized Surface Plasmon Resonance

MB – Molecular Beacon

MD – Musculoskeletal Disorder

MSC – Mesenchymal stem cell

miRNA – MicroRNA

NMs – Nanomaterials

NP – Nanoparticle

OA – Osteoarthritis

PAN – polyakrylonitril

PCL – Polycaprolactone

PCa – Prostate Cancer

PCSC – Prostate Cancer Stem Cell

PEG – Polyethylene Glycol

PL – Precancerous Lesion

PLD5 – Phospholipase D5

PMC – PubMed Central

POCT – Point-of-Care Testing

PSA – Prostate-Specific Antigen

PVA– Polyvinyl Alcohol

QCM – Quartz Crystal Microbalance

RA – Rheumatoid Arthritis

RNA – Ribonucleic Acid

ROC – Receiver Operating Characteristic

SC – Stem cell

SERS – Surface-Enhanced Raman Scattering

SF – Synovial Fluid

SPR – Surface Plasmon Resonance

SSC – Skin Stem Cell

TMJ – Temporomandibular Joint

WBC – White Blood Cell

WOMAC – Western Ontario and McMaster Universities Arthritis Index

Table of Contents

1. INTRODUCTION

1.1 Role of nanotheragnostics in personalized medicine.

Nanothergnostics is a technological process/system based on functionalized nanofibers or other scaffolding systems for diagnostic and therapeutic applications, particularly for the targeted delivery of drugs.

In the rapidly progressing field of medicine, nanotheragnostics has begun an advanced technological course that simultaneously integrates therapeutic and diagnostic experiences. This innovative approach impacts nanotechnology's unique properties to transform how we diagnose and treat diseases, with a particular focus on early diagnosing and targeted drug administration. Nanotheragnostics combines 'nano,' referring to the scale of the used technology, with 'theragnostics,' a multiuse of therapy and diagnostics.(Wiesing 2019) The essence of nanotheragnostics lies in its ability to functionalize scaffolding materials, such as nano-sized liposome-functionalized nanofibers, to perform dual roles (Figure 1). These materials can be engineered to target specific cells or tissues, enhancing the precision and efficacy of treatment while minimizing side effects. Coupling diagnostic and therapeutic functions into a single platform optimizes patient care through personalized medicine approaches.

The theragnostic interdisciplinary field aims to simultaneously diagnose, deliver drugs, and monitor therapeutic responses at the nanoscale. Due to the molecular scale of interaction, it is very important to realize the dominance of different physical principles in biological systems(Liu et al. 2024a). Understanding that upscale models will be partly representative is especially important in developing drug delivery systems, even minor details can have a significant impact. This concept is evident in the study of Na+, K+, and ATPase translocation. (Amler et al. 1992)Due to the membrane surface potential, the water molecule structure and orientation in the closest membrane vicinity differ significantly from the structure of bulk/oriented water molecules. (Hua et al. 2014; Watson et al. 2023)The surface membrane potential generates a unique arrangement of water molecules, resulting in distinct structural and dynamic properties compared to oriented water. (Liu et al. 2024b)This nanolayer can exhibit altered dielectric properties, increased viscosity, and alterations in hydrogen bonding patterns. This phenomenon is widely spread throughout nature, and, for example, effective production of ATP would not exist without this water nanolayer. The nanolayer thickness is only a few nanometers and, thus, comparable with the size of antigens and, generally, proteins and nucleic acids. Importantly, there is a clear domination of the surface tension, which influences the properties of this layer, which has to be overcome

during the targeted drug delivery. Water availability is crucial for protein function, and macromolecules impact water potential within cells. Biomolecular condensation of disordered proteins buffers water potential, suggesting an evolutionary driver for protein disorder and function.(Watson et al. 2023)

MicroRNAs (miRNAs) are small, non-coding RNA molecules that play a key role in regulating gene expression, influencing numerous physiological and pathological processes. MiRNAs are promising tools in nanotheragnostics for targeted therapy. Biomimetic systems emulate natural interactions for effective intracellular delivery. With their small size and specific targeting capabilities, miRNAs can be incorporated into electrospun nanofibrous drug delivery systems, enabling precise gene regulation at the site of pathological tissues and working as a label–targeting address.

Electrospun nanomaterial-based theragnostic systems present several advantages for clinical applications. They are minimally invasive, injectable, and adaptable for delivery through parenteral, transdermal, mucosal, or laparoscopic and other ways of administration in the form of gels, fluidic interfaces, or suspensions. Their portability and flexibility further improve their clinical utility.(Li et al. 2018; Guo et al. 2022) However, the success of these systems hinges on identifying appropriate disease-specific biomarkers. Knowledge of these biomarkers is major for designing an active targeting drug delivery system capable of addressing pathological states at the molecular level.

To develop these systems, it is imperative to determine the following:

- **Target site:** Identifying the specific site of action based on molecular biomarkers.
- **Load:** Designing the nanomaterials to carry therapeutic agents such as miRNAs or other payloads personalized to the disease context.
- **Release mechanism:** Engineering-controlled release mechanisms ensure precise delivery at the intended site.

The portability and injectable nature of these systems make them a promising solution for contemporary medical challenges. Their ability to deliver miRNA-based therapies with high specificity and minimal invasiveness underscores their potential to revolutionize targeted drug delivery in personolalized medicine.(Deshmukh et al. 2019) Combined with nanotechnologies, drug scaffold structures create a highly efficient system for drug delivery. Nanofibers provide a substantial surface area and high porosity, making them ideal for loading and releasing therapeutic agents in a controlled manner during post-production processing, such as fractionalization. Liposome-functionalized nanofibers enhance the stability and bioavailability of the therapeutic agents they carry. This hybrid system can be

engineered to target specific disease sites, such as cancerous tumors, where the liposomes release their payload precisely where needed, thereby reducing systemic toxicity. Nanofibrous membranes undergo external characterization and optimization to enhance functionality and stability during delivery. This process minimizes off-target effects and maximizes therapeutic efficacy. Consequently, nanotheragnostics, which deals with nanometer drug delivery and targeted systems, open new possibilities for precision and personalized medicine.

1.2. Usage of Nanomaterials in Biomedicine

Nanomaterials are characterized as substances with at least one dimension measuring under 100 nanometers. (Figure 1) Their unique physical, chemical, and biological properties, which vary with scale, possess the potential to transform biomedicine. According to ISO 80004-1:2023, the classification of nanomaterials encompasses nano-objects and nanostructured substances, identified through various descriptors such as particles, assemblies, coatings, films, and layers. SO(ISO 80004-1:2023(en), Nanotechnologies) This classification promotes a standardized vocabulary within both research and industry. The revised definition from the European Commission (2022) asserts that a nanomaterial may be natural, incidental, or engineered, consisting of solid particles that exist separately or as discernible components within aggregates or agglomerates.(European Observatory for Nanomaterials) To meet the criteria as a nanomaterial, at least 50% of its particles must exhibit external dimensions ranging from 1 nm to 100 nm. Furthermore, this definition includes materials exhibiting elongated or plate-like morphologies, wherein certain dimensions may either be below or exceed 100 nm. In 2023, the Joint Research Centre (JRC) issued guidance to facilitate the application of this revised framework. The integration of nanomaterials within biomedical practices necessitates compliance with regulatory standards set forth by organizations such as the U.S. Food and Drug Administration (FDA) and the European Medicines Agency (EMA). These agencies require comprehensive evaluations of toxicity, biocompatibility, efficacy, and long-term stability. The FDA provides product-specific, scientifically grounded guidance for nanotechnology applications, while the EMA emphasizes thorough physicochemical characterization.

By addressing both the scientific complexity and evolving regulatory landscape, understanding nanomaterials' applications and their transformative role in biomedicine is essential for spreading innovative applications in important fields.

1.2.1. Classification, Synthesis, Properties, and Biomedical Applications.

Nanomaterials have noticeably transformed healthcare by offering innovative solutions in medical devices and pharmaceuticals. These materials are characterized by their nanoscale size, which imparts unique physical and chemical properties that can be leveraged in various biomedical applications. Common nanomaterials include nanoparticles, nanofibers, nanocomposites, and nanotubes, each possessing distinct characteristics such as high surface area to volume ratio, enhanced mechanical strength, and unique optical properties.

Figure 1. Size comparison of biosynthesized nanoparticles.

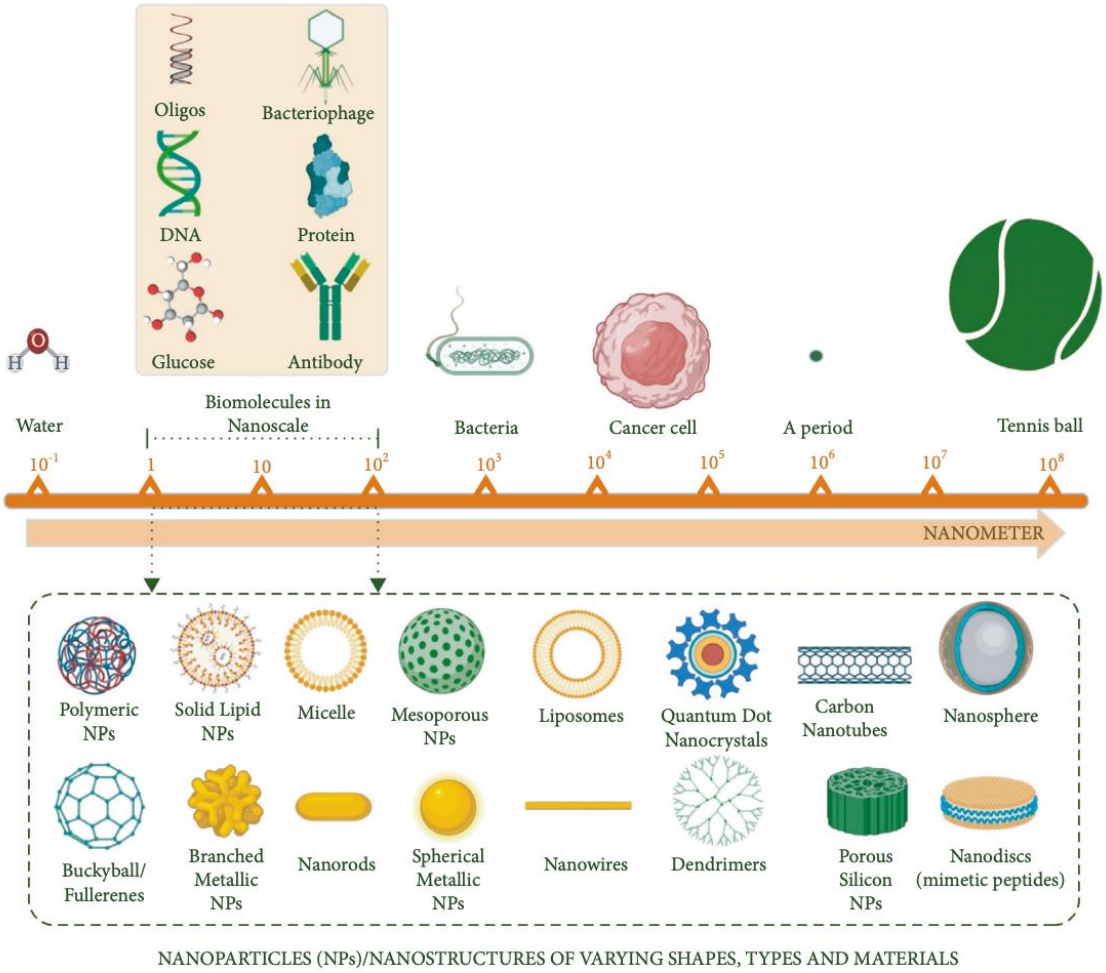

Reproduced from Ravindran et al. (2021) under CC BY 4.0." Schematic diagram exhibiting size comparison of nanoparticles (NPs) typically in the range of 1–100 nm, as compared to the otherstructures. Created with BioRender.com with publication license."(Mahmood Ansari et al. 2021)

Nanomaterials exists in different types, *including nanoparticles, nanofibers, nanocomposites, and nanotubes*. Each type has specific features that make it useful for particular applications. Nanoparticles are often used for drug delivery because they can move easily through the body and target specific cells. Nanofibers are commonly used in tissue repair and wound healing because they resemble natural body tissues. Nanocomposites

combine different nanomaterials to create stronger or more flexible materials, while nanotubes, especially carbon-based ones.

Nanomaterials are typically synthesized using either *top-down* or *bottom-up* approaches. *Top-down* techniques involve breaking down bulk materials into nanoscale particles using methods like milling, lithography, or laser ablation, which are advantageous for large-scale production but may introduce defects or limit shape control. Conversely, *bottom-up* techniques, such as sol-gel synthesis, self-assembly, and chemical vapor deposition, construct nanomaterials atom-by-atom or molecule-by-molecule, allowing for more precise control over size, morphology, and functionality.

In this thesis, we will concentrate more on bottom-up techniques for producing nanofibers, there a few of them:

1. **Drawing Fibers from a Viscous Polymer**: This method involves the mechanical stretching of fibers derived from either a polymer solution or melt, allowing for precise control over both fiber thickness and orientation.

2. **Bacterial Synthesis**: specific bacteria that naturally generate nanofibers as part of their extracellular structures. Although this approach is eco-friendly, it is constrained to the materials that these particular bacteria produce.

3. **Phase Separation**: the separation of polymer solutions to fabricate nanofiber structures. It is adaptable for a range of polymer types; nevertheless, managing fiber diameter and orientation presents challenges.

4. **Self-Assembly**: molecular interactions to construct nanofiber structures, enabling precise control at the molecular scale. However, it is limited to materials that exhibit self-assembling capabilities.

5. **Centrifugal Spinning**: centrifugal forces to generate nanofibers from polymer solutions or melts. While it provides high production rates, controlling the diameter and orientation of the fibers may prove difficult.

These materials' application areas span diagnostic imaging to therapeutic delivery systems. In diagnostics, nanomaterials improve imaging modalities' sensitivity and specificity, facilitating early disease detection. In therapeutics, they play a crucial role in drug delivery systems, where their ability to target specific cells or tissues enhances the efficacy and reduces the side effects of treatments. Moreover, integrating nanomaterials in biosensors has advanced the field of point-of-care testing by providing rapid and accurate results.

Nanomaterials are produced using different techniques*, including chemical reactions, vapor-based methods, and electrospinning (F*igure 2). The method used affects the structure and properties of the final product, which in turn influences its medical applications. Scientists also modify nanomaterials by attaching biological molecules or polymers to improve their safety and ability to target specific cells.

Regulatory approvals are critical in ensuring nanomaterial innovations meet international health standards, guaranteeing safety and efficacy in biomedical applications. As research progresses, the development of new nanomaterials continues to push the boundaries of medical science, offering promising avenues for improved patient outcomes.

1.3 Electrospun Nanomaterials biomedical applications

Electrostatic spinning is an adaptable technique utilized for the fabrication of nanofibers by leveraging electrostatic forces to transform polymer solutions or melts into extremely fine fibers. This method entails applying a high voltage between a rotating electrode and a collector electrode, which polarizes the polymer solution or melt and forms a shape referred to as the Taylor cone.(Figure 10) Consequently, a slender stream of polymer solution is extracted from the apex of the cone and elongated into a fiber due to the influence of the electric field. As the fiber progresses toward the collector electrode, the solvent evaporates or the melt solidifies, culminating in the creation of a solid nanofiber on the collector surface.

The characteristics of the polymer solution, which encompass concentration, viscosity, molecular polarity, and ionic strength, have a significant bearing on the electrospinning outcome. Elevated polymer molecular weights and concentrations generally promote fiber formation, whereas lower viscosity may result in spraying rather than fiber generation. Furthermore, enhanced electrical conductivity or diminished surface tension can improve fiber yield. Additionally, the boiling point and evaporation rate of the solvent are vital parameters that influence the final structure and characteristics of the fibers produced. Modern electrospun-produced nanomaterials have passed a significant milestone in their various applications in biomedicine. Electrospinning is an adjustable technique used to produce polymer fibers with diameters ranging from nanometers to micrometers. These fibers are characterized by high surface area-to-volume ratios and significant porosity. These attributes make them exceptionally suited for biomedical uses, including tissue engineering, drug delivery, and diagnostic systems.

In tissue engineering, electrospun nanofibers serve as scaffolds that mimic the extracellular matrix, providing structural support conducive to cell adhesion, proliferation, and differentiation. This biomimicry facilitates the regeneration of various tissues, such as

skin, bone, and cartilage. Additionally, these nanofibers can be functionalized with bioactive molecules to further enhance tissue repair processes.

Electrospun nanofibers have been employed in drug delivery systems due to their capacity to encapsulate therapeutic agents and release them in a controlled manner.(Figure 11) The high porosity and customizable surface properties of these fibers allow for the incorporation of a wide range of drugs, including small-molecule pharmaceuticals, proteins, and nucleic acids. By adjusting the fiber composition and structure, it is possible to tailor the release kinetics, achieving sustained or stimuli-responsive drug release profiles. This targeted delivery approach enhances therapeutic efficacy while minimizing systemic side effects.

Figure 2. Schematic illustration of the measures to endow NMs with sensing properties throughout the electrospinning process

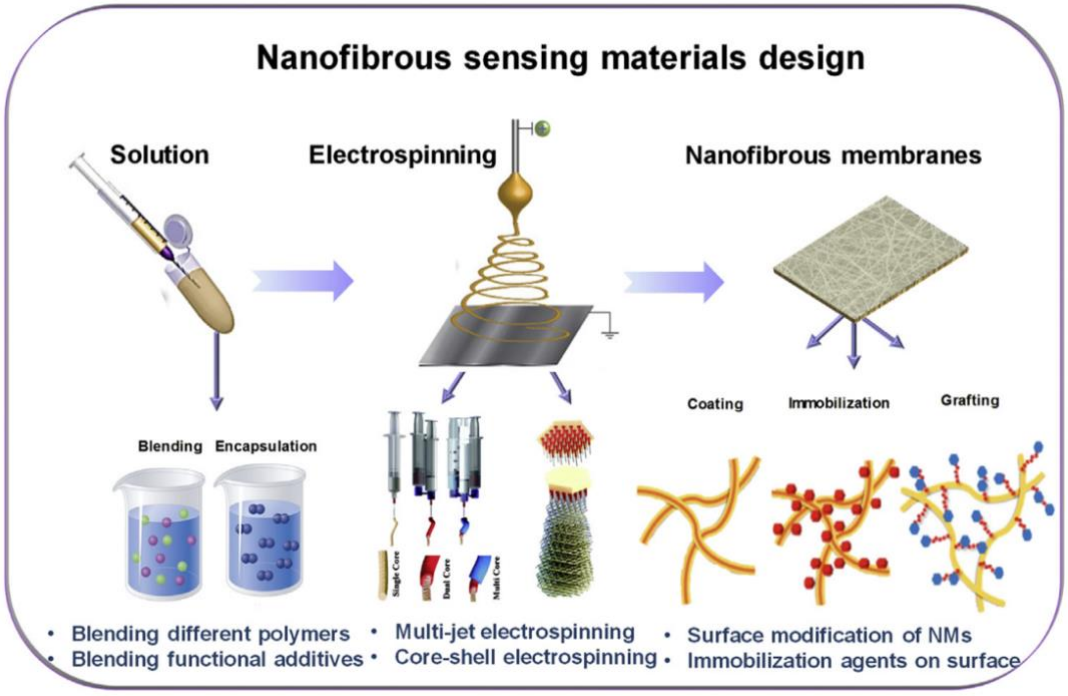

Reprinted from Electrospun Nanofibers for Sensors, Sharma, G.K., & James, N.R. (2022), Chapter 18, Elsevier, Copyright (2022), with permission from Elsevier (in the appendix)(Sharma et al. 2022)

Modifying the surfaces of polymer nanofibers through a procedure called **functionalization** enables the customization of these materials for targeted biomedical applications. This customization enhances their versatility and efficacy. By incorporating bioactive agents—such as growth factors, cell adhesion proteins, differentiation cues, and therapeutic agents—researchers can produce nanofibers that significantly impact biological responses. In the field of regenerative medicine, these functionalized fibers are essential for

eliciting beneficial cellular reactions, as they replicate the characteristics of the natural extracellular matrix, thereby facilitating cell adhesion, proliferation, and tissue regeneration.

Functionalization relates to the enhancement of medication effectiveness. (Figure 2) To accomplish this aim, various functionalization methods may be utilized, outlined as follows:

1. **Surface Coating**: Chemical modification or plasma treatment significantly boosts biocompatibility and drug adsorption. Plasma treatment introduces functional groups that increase hydrophilicity, whereas chemical grafting allows for the attachment of bioactive molecules, thereby enabling customized drug interactions.

2. **Incorporation of Polymers**: Biocompatible and biodegradable polymers—such as polycaprolactone (PCL), polylactic acid (PLA), polyethylene glycol (PEG), and chitosan—are integrated into nanofibers to modulate drug release kinetics. These polymers enhance structural integrity and influence degradation rates, facilitating controlled release mechanisms.

3. **Nanoparticle Integration**: The incorporation of metallic nanoparticles (e.g., gold, silver) or ceramic nanoparticles (e.g., silica, hydroxyapatite) enables stimuli-responsive drug release. These nanoparticles facilitate regulated drug discharge based on external stimuli, including variances in pH, temperature alterations, or enzymatic activity.

4. **Layer-by-Layer** (LbL) Assembly: Sequential layering of oppositely charged polymers and bioactive molecules constructs multilayered nanofibers with adjustable drug release characteristics. This methodology enhances stability and provides sustained release over prolonged periods.

5. **Covalent Functionalization**: The direct chemical bonding of drugs or targeting ligands to the surfaces of nanofibers ensures accurate localization and extended drug retention. Functional groups, such as amines, carboxyls, or thiols, can be introduced to enhance targeting precision and bioavailability.

In diagnostic applications, electrospun nanofibers contribute to the development of highly sensitive biosensors. Their extensive surface area facilitates the immobilization of recognition elements, such as antibodies or aptamers, leading to improved detection of biomarkers. These nanofiber-based sensors have been utilized in detecting various analytes, including proteins, pathogens, and small molecules, thereby aiding in early disease diagnosis and monitoring.

Overall, the integration of electrospun nanofibers in biomedicine exemplifies nanotechnology's potential to revolutionize healthcare. As research in this area continues to

evolve, it promises to bring about further innovations that will enhance the quality of life for patients worldwide.

1.3 Biosensors and bionanosensors: Design, Functionality, and Life Cycle

Biosensors are excellent for clinical usage due to their low cost, quick reaction time, mobility, automation, and potential for serial manufacturing. Compared to traditional biomarker detection techniques, biosensors provide many benefits. (Nicu and Lechĺ 2008)nt research has demonstrated the value of biosensors in rheumatoid arthritis, cancer diagnosis, and pathogen detection. Lastly, biosensors could be the optimal strategy for particular disorders like juvenile idiopathic arthritis, which call for a quick and accurate diagnosis. (Longo et al. 2021).

The concept of biosensors for disease detection has been extensively explored over the past few decades. However, a new generation —bionanosensors—is redefining early diagnostics and theragnostics by combining diagnostic precision with therapeutic potential. (Pashchenko et al. 2022). These nanoscale sensors can detect minute concentrations of disease biomarkers in real time, providing earlier and more accurate diagnoses than conventional techniques.

One of the keys enabling technologies behind these advanced systems is the use of electrospun nanofibers. These nanofibers serve as highly porous and surface-rich materials, exhibiting an exceptionally high surface area-to-volume ratio and submicron-scale pore sizes. As a result, they function as ultra-efficient filters and sensing platforms. Additionally, they mimic the physical dimensions of biological structures and allow for straightforward surface and core functionalization. This means that active biological molecules—such as enzymes, antibodies, or DNA—can be stably attached to enhance sensitivity and specificity.(Chen et al. 2014; Naresh and Lee 2021)

Bionanosensors are advanced devices that combine biological components with nanoscale materials. By enhancing the receptor components and increasing the number of binding agents, these sensors significantly improve sensitivity and selectivity. They can effectively bind biological molecules to electronic systems, making them valuable tools in various fields such as medical diagnostics, environmental monitoring, and food safety. (Figure 3).(Van Dorst et al. 2010; Sharma et al. 2015; Wang et al. 2019b)

Figure 3. Typical structure of a biosensor (biorecognition, interface and transduction)

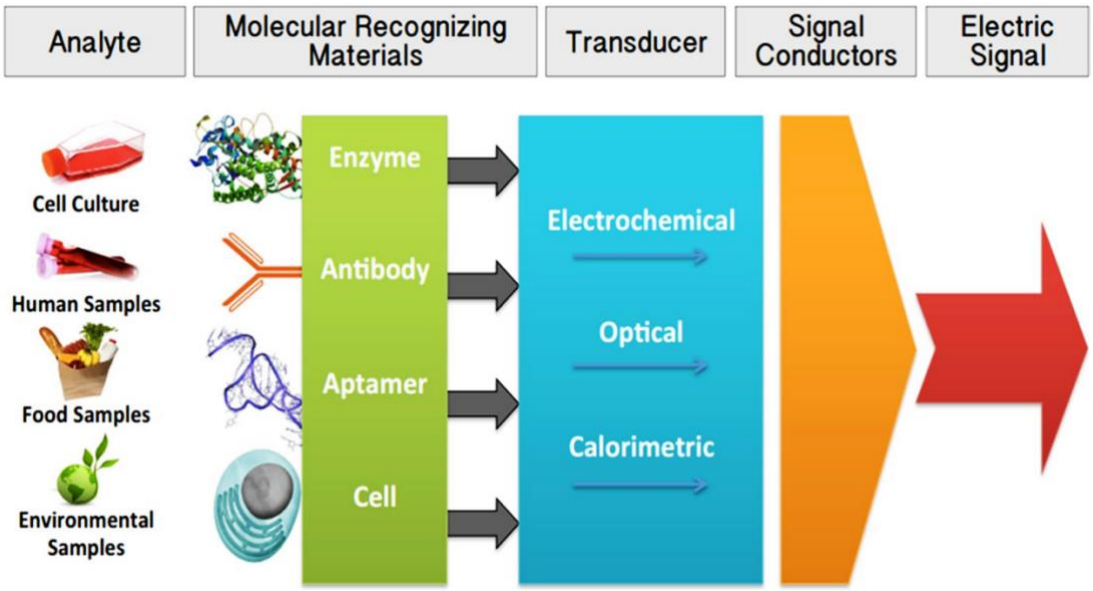

This figure is reproduced from Hassani, S., Momtaz, S., Vakhshiteh, F., Salek Maghsoudi, A., Ganjali, M. R., Norouzi, P., & Abdollahi, M. (2017). Biosensors and their applications in detection of organophosphorus pesticides in the environment. Archives of Toxicology, 91(1), 109–130. https://doi.org/10.1007/s00204-016-1875-8. Licensed under the Springer Nature License. With permission from Springer Nature (in the appendix).(Hassani et al. 2016)

Bionanosensors are emerging as pivotal tools in the early detection and monitoring of treatment of diseases, particularly in the field of theranostics, which combines therapeutic and diagnostic capabilities for personalized medicine. (Martino et al. 2025)These sensors integrate biological recognition elements—such as enzymes, antibodies, or nucleic acids—with nanomaterials like gold nanoparticles, carbon nanotubes, and quantum dots. This combination allows for the precise detection of biomarkers associated with various diseases, including cancer, by converting biological responses into measurable signals, such as optical or electrical outputs and thermal or acoustic outputs (Figure 5).

The development lifecycle of bionanosensors includes several key phases:

1. The initial phase involves **conceptualizing and designing** the sensor based on the target analyte, its concentration, and the specific environment in which it will be detected. Precise selection of appropriate biological elements and nanomaterials is paramount. Fabrication techniques, such as lithography, self-assembly, or chemical vapor deposition, are employed to construct the sensor at the nanoscale.

2. **Functionalization** includes attaching biological molecules to the nanomaterial. This step is crucial to ensure that the sensor maintains its high

specificity and sensitivity. Surface chemistry plays a pivotal role in this phase, ensuring stable and efficient interaction between biological components and the sensor surface.

3. Bionanosensors undergo **validation and calibration** to ensure they accurately respond to predetermined concentrations of analytes. This phase involves extensive testing to verify the sensor's reliability and reproducibility across diverse environments and conditions. During this stage, bionanosensors are deployed in real-world settings, where their compact size allows for integration into various devices and systems, including portable and wearable electronics. Continuous monitoring is conducted to maintain sensor accuracy and to collect data for analysis.

Regular maintenance checks are important to keep sensors accurate and lasting longer. These checks include cleaning, recalibrating, and sometimes replacing parts. When bionanosensors reach the end of their life, they are safely disposed of or recycled to reduce their impact on the environment.

Bionanosensors offer many advantages, but they face several challenges, including stability under varying conditions, potential biocompatibility issues, and the need for standardization across different applications. Future research efforts aim to tackle these challenges by enhancing the robustness of sensors, expanding their range of applications, and incorporating advanced data analysis technologies, such as artificial intelligence.

The operation of bionanosensors involves a sequence of events(Figure 3):

- The biological **recognition** element binds specifically to the target analyte.
- This **binding** event induces a change in the nanomaterial's properties, such as alterations in electrical conductivity or light emission.
- The transducer **detects these changes** and **converts** them into a quantifiable signal, which is then processed and displayed, indicating the presence and concentration of the analyte.

Upgrading of sensing technology with Nano-Receptors emphasize a groundbreaking advancement in sensing technology, characterized by their ability to detect and analyze substances at the nanoscale with exceptional precision. (Figure 4) These sensors integrate biological components with nanomaterials, enabling them to interact with a wide range of biological and chemical substances. The ongoing research aims to address existing challenges, such as improving sensitivity, minimizing cross-reactivity, and enhancing stability, which are critical for successful real-world applications.

Figure 4. Conceptual model of biosensing principle.

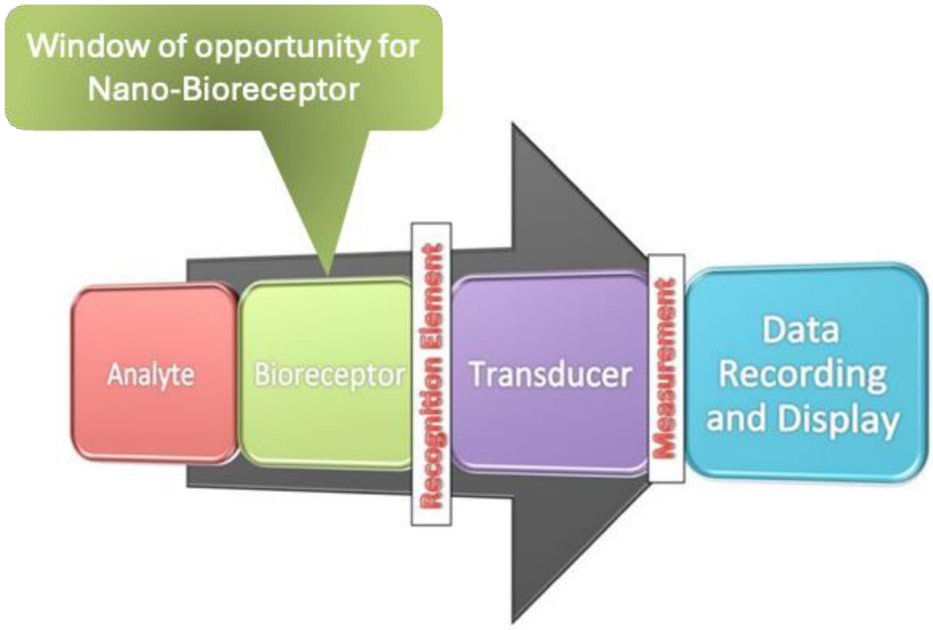

This figure is adapted from Hassani, S., Momtaz, S., Vakhshiteh, F., Salek Maghsoudi, A., Ganjali, M. R., Norouzi, P., & Abdollahi, M. (2017). Biosensors and their applications in detection of organophosphorus pesticides in the environment. Archives of Toxicology, 91(1), 109–130. https://doi.org/10.1007/s00204-016-1875-8. Licensed under the Springer Nature License. With permission from Springer Nature (in the appendix).(Hassani et al. 2016)

Fundamental characteristics and Applications of Biosensors

The main characteristics of biosensors are(Bhalla et al. 2016)

- **Selectivity** describes the detection of a particular analyte within a sample containing other compounds and contaminants.
- **Reproducibility** is the ability to produce identical responses in repeated test setups.
- **Stability** is the degree of resistance to environmental changes outside the detection system.
- **Sensitivity** defines the limit of detection (LOD) and is characterized by the minimum amount of analyte that can be detected by the biosensor. (“Introduction to biosensors - PMC”)
- **Linearity** is an attribute that indicates the accuracy of the measurement response.

All these characteristics describe us as the primary points of characterization of biosensors. This well-established field has already penetrated numerous domains, including environmental sensors and food quality sensors, and numerous sensors are utilized in veterinary and manufacturing industries.

Figure 5. Classification of biosensors based on transducer systems

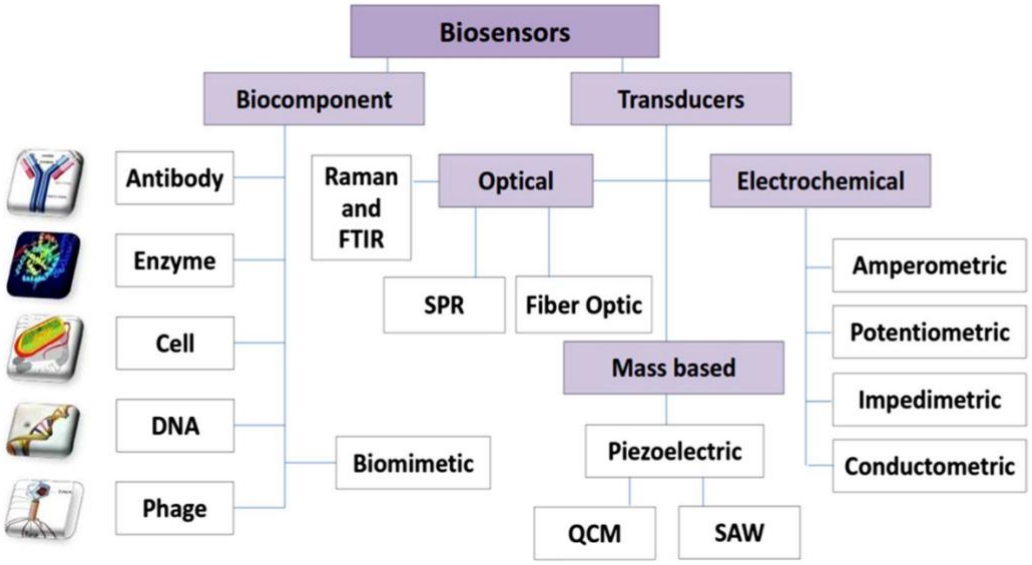

This figure is reproduced from Hassani, S., Momtaz, S., Vakhshiteh, F., Salek Maghsoudi, A., Ganjali, M. R., Norouzi, P., & Abdollahi, M. (2017). Biosensors and their applications in detection of organophosphorus pesticides in the environment. Archives of Toxicology, 91(1), 109–130. https://doi.org/10.1007/s00204-016-1875-8. Licensed under the Springer Nature License. With permission from Springer Nature (in the appendix).(Hassani et al. 2016)

The application of biosensors in unconventional areas has inspired knowledge transfer from other fields to medicine, benefiting many research groups and even in everyday patients' lives. However, the intricate certification process and clinical studies mandated for various device groups hinder the rapid adoption of new technology in the medical sector compared to other domains. Nevertheless, this fact facilitates the accelerated utilization of knowledge from other medical fields, thereby reducing the duration of research and development processes.

Figure 6. Overview of NMs applications in sensors. NP, nanoparticle; QCM, quartz crystal microbalance

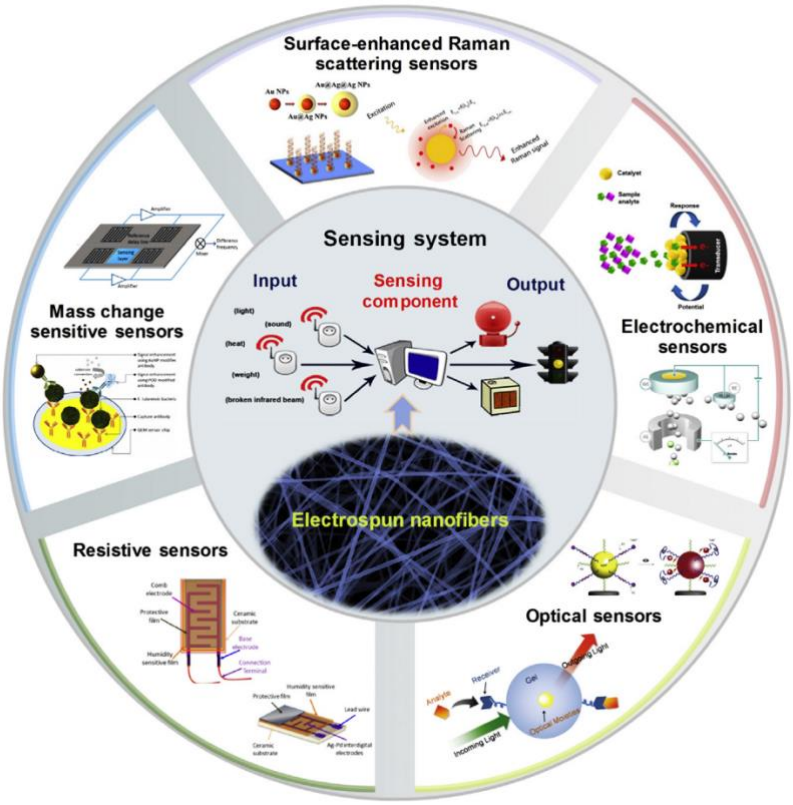

Reprinted from Electrospun Nanofibers for Sensors, Sharma, G.K., & James, N.R. (2022), Chapter 18, Elsevier, Copyright (2022), with permission from Elsevier (in the appendix)(Sharma et al. 2022)

Nanofiber-based bionanosensors are particularly beneficial for applications that require rapid and accurate detection of low-abundance biomolecules in bodily fluids like blood, saliva, or sweat. When correctly functionalized, these fibers enable detection without complex sample preparation or pre-concentration steps, which is crucial for point-of-care testing and wearable diagnostic systems. Moreover, their compatibility with multiple signal transduction mechanisms (such as optical, electrochemical, mass-sensitive, and resistive) allows them to be integrated into a wide range of devices for versatile use.(Figure 6) Thus, their functionalization and smart systems formation significantly increase their application potential. Specific treatments or functionalization of nanofibers surface and/or core provide nanofibers with new parameters and properties. (Figure 7)

Figure 7. Integrated Nano-Receptor design for ultrasensitive detection of labelled biomarkers.

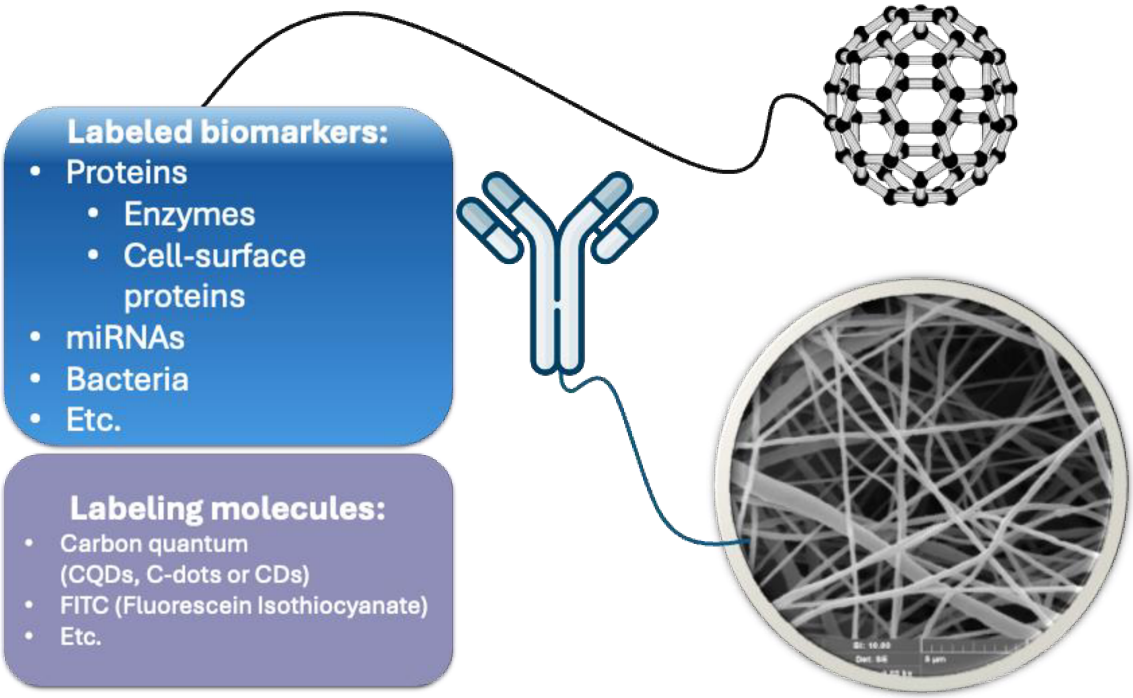

Nano-Receptor *– part of biosensor, based on functionalized PAN (polyacrylonitrile) nanofibers with linker attached on whole dept of nanomembrane. This membrane is a semi-ready product, with the availability to be completed by binding agents.*

Bionanosensors are composed of three primary components(Figure 4,5):

1. **Biological Recognition Elements:** These include enzymes, antibodies, nucleic acids, and aptamers that specifically interact with target analytes, ensuring the sensor's selectivity.
2. **Bioreceptor and Nanomaterials-based Bioreceptor (window of opportunity for improvement):** Materials such as gold nanoparticles, carbon nanotubes, and quantum dots are employed for their unique properties, including high surface area, electrical conductivity, and optical characteristics, which enhance the sensor's sensitivity and enable effective signal transduction.
3. **Transducers:** These convert the biological interaction into a measurable signal. Depending on the application, transducers can function through various mechanisms, including optical, electrochemical, piezoelectric, or thermal methods.

The integration of gold nanoparticles with electrospun fibers enhances the sensitivity of these biosensors, allowing them to detect even the most minute quantities of biological markers. Gold nanoparticles improve the electrical conductivity and optical properties of the fibers, thereby increasing their effectiveness in bio-detection and therapy. This integration

supports the development of more sophisticated diagnostic tools that are capable of simultaneous detection and treatment. In addition to gold nanoparticles, carbon dots also play a crucial role in enhancing the performance of these biosensors. Carbon dots, known for their excellent photoluminescent properties, contribute to better imaging and tracking of biological processes. They offer high chemical stability, low toxicity, and the ability to be easily functionalized, making them ideal for a wide range of biomedical applications. The incorporation of carbon dots into electrospun fibers further improves the biosensors' sensitivity and selectivity, providing a dual enhancement in both optical and electrical properties.

Optical biosensors employ the interaction of light with biological elements to detect the presence or concentration of substances. The principle of these sensors often involves the use of optical signals, such as changes in absorbance, fluorescence, or refractive index, to identify specific analytes. Optical biosensors are known for their high sensitivity and rapid response times, attributes that make them suitable for real-time monitoring applications. Recent advancements in optical technology have led to the development of miniaturized and portable optical biosensors, which are being increasingly used in point-of-care diagnostics and remote sensing.

Electrochemical biosensors are enhanced tools in the analysis of biological samples and have diverse applications in medical diagnostics. These sensors work by transducing a biochemical reaction into an electrical signal, which can be quantitatively measured. The incorporation of membrane technologies in electrochemical biosensors has revolutionized their functionality. Membranes serve as selective barriers that enhance the specificity of the sensors, allowing them to target specific molecules or ions within complex biological matrices. As a result, electrochemical biosensors are capable of precise and reliable analysis, making them indispensable in the field of clinical diagnostics and environmental monitoring.

1.4 Modern POCT diagnostics.

In recent decades, molecular diagnostics have reached their zenith in medical diagnosis, particularly in the global diagnosis of early stages of infections during the COVID-19 pandemic. The impact of rapid and easy-to-use diagnostics tools must be considered—some of them are performed in hospitals and laboratories, and some at points of care (POCT). Still, there were qualitative and needed more accurate, as antigen tests for viruses were also performed at home or work. The testing objectives were also different; in the case of POCT and home/workplace - testing, the primary purpose was to eliminate the spread of communal disease. Other tests have shown a continuation of the disease and the ability to return to

work. Even with the use of different test systems diagnostic workflow proof, this idea of classification of biological markers has its place in medical care algorithms. Even if we talk about diagnosis, monitoring, prognosis or risk/prediction, and other described types of biomarkers. Some medical fields have already found a balance between the diagnostic methods and patient clinical pathways; a good example is an appropriate implementation of cardiac markers and the identification of the most specific troponins, which have replaced previously used aspartate transaminase (AST), lactate dehydrogenase (LDH), and creatinine kinase (CK). This is because of the long-lasting story of research and intense inquiry into early diagnosis in cardiological emergencies with broad patient populations. Although troponins were discovered in 1965, a reliable immunoassay to determine their blood levels was developed in the late 1990s. (Ohtsuki and Morimoto 2022). Nowadays, the measurement of cardiac troponin I (cTnI) and cardiac troponin T (cTnT) are markers of acute myocardial infarction (AMI), (Wang et al. 2020). and they are the gold standard in AMI diagnosing and even the easy-accessible method in the office of general practitioner (GP).

The imbalance between imaging, molecular diagnostics, and physical examination is evident in various critical areas, which is confirmed with posthumous diagnosis. For example, the Kallen-Laurents scale is used to evaluate osteoarthritis, or its widely used synonym, osteoarthrosis, but the signs and clinical manifestations of the disease usually differ from the imaging methods' results. Its heterogeneity in identifying, validating, and monitoring even increases the gap between on-site and diagnosing specialists.

Especially significant is the extension of the relatively young term "liquid biopsy." It presently involves detecting circulating tumor DNA, metastatic/hematogenic circulating cancer cells, and cancer-related biomarkers. This analysis could be performed using a minimally invasive bionanosensor assay and is available for risk stratification or treatment response monitoring in cancer patients (Valpione and Campana 2019). Measuring the biomarkers used to create the biosensor is already widely evaluated in research (Bernotiene et al. 2020)

A few pandemic years put healthcare systems under additional stress in wide geography and forced transformations in many clinical areas and related fields. These areas include personalized medicine, theragnostics, early-stage diagnosis, remote patient care, telemedicine, etc**.**

Logically evolution of the field will be the implementation of nanobiosensors and new theragnostic technologies in the usual workflow of the medical care provided, which can enable us to detect a smaller amount of a substance in a larger fluid volume, making more

significant numerous of examinations simply available for broad diagnostic and therapeutic applications of markers whose detection was previously costly and time-consuming. Biomarkers are the core issue that arises in biosensor development, and it is the right choice that makes the development viable and applicable in clinical practice.

1.4.1. Molecular biomarkers.

Biomarkers are becoming more applicable in routine clinical practice and have broad application potential to expand diagnostic options and further increase the effectiveness of therapy. Their main applications have already been identified. There are a few main types of biomarkers: susceptibility/risk, diagnostic, monitoring, prognostic, predictive, response, and safety biomarkers. (BEST (Biomarkers, EndpointS, and other Tools) Resource).

The application of biosensors and innovative nanomaterials is considered a section of future directions. Developments in technology allow us to consider markers that were previously impossible or difficult to analyze. Based on adequately selected biomarkers, nanobiosensors can be developed that, in turn, can detect extremely low concentrations of markers,

Nanomaterials are gaining popularity in molecular diagnostics. Moreover, methods of biomarker quality evaluation and standardization are developing. A synergy of molecular diagnostics and nanomaterials can be characterized as mainstreaming current medical concepts and a possible future in this area . (Kalogianni 2021).

Figure 8. Nanofibers integrated microfluidic analytical systems and their application in clinical and point-of-care cancer diagnostics based on liquid biopsy. CSF = cerebrospinal fluid

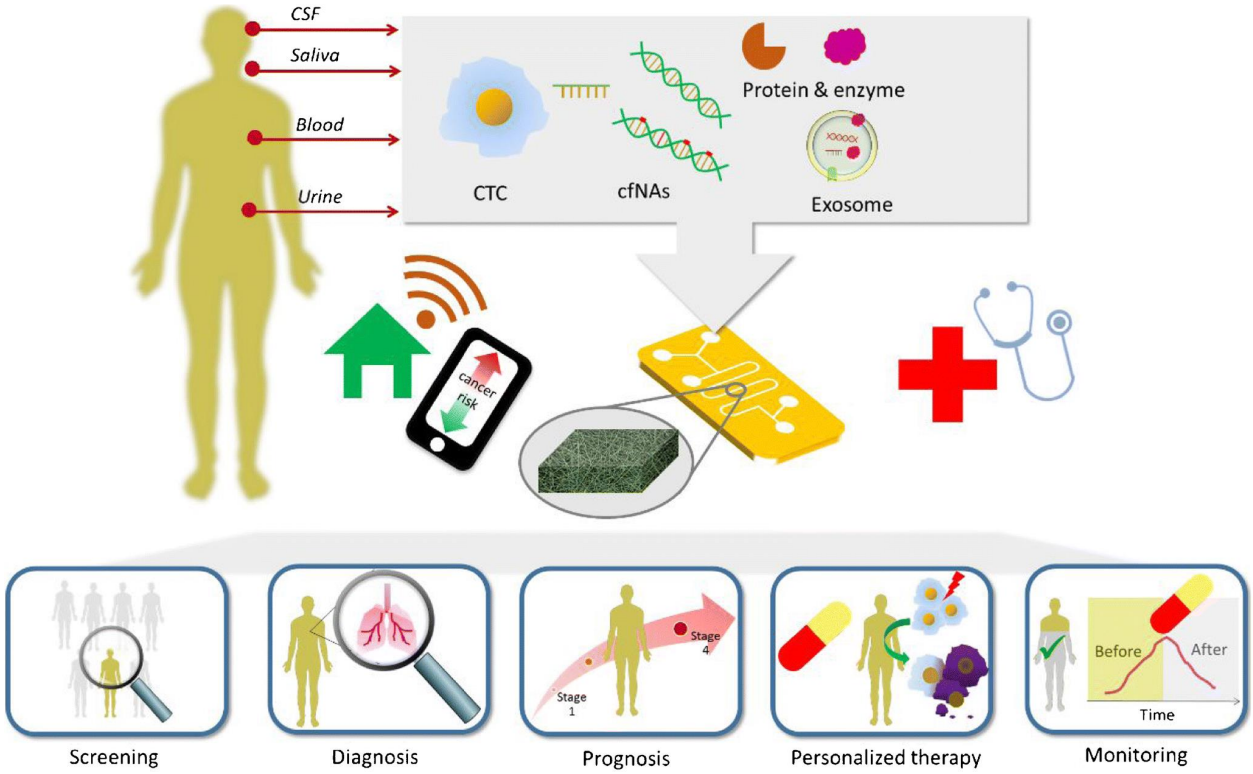

These figure is reproduced from Wongkaew, N. (2019). Nanofiber-integrated miniaturized systems: an intelligent platform for cancer diagnosis. Analytical and Bioanalytical Chemistry, 411(15), 3821–3832. https://doi.org/10.1007/s00216-019-01589-5. With permission from Springer Nature Link (in the appendix).(Wongkaew 2019)

1.4.2. Cancer biomarkers: detection and quantification.

The detection and quantification of cancer biomarkers are critical components in the personalized medicine approach for cancer diagnosis, prognosis, and therapy monitoring. Biomarkers serve as biological signatures that can indicate the presence of cancer, its progression, and the patient's response to treatment.

Cancer biomarkers are crucial tools in the diagnosis, prognosis, and monitoring of cancer. They can be categorized into several types based on the nature and methodology used to detect them.

- **Genomic Biomarkers:** These involve DNA mutations, gene amplifications, and chromosomal rearrangements. A well-known example is the BRCA1/2 mutations, which are linked to breast and ovarian cancer.

- **Proteomic Biomarkers:** These focus on protein expression and modifications. PSA, a proteomic marker, is widely used in prostate cancer screening.
- **Metabolic Biomarkers:** These are small molecules that can change in cancer cells, such as lactate or lipid levels, serving as indicators of cancer metabolism.

Prostate Cancer: PSA remains the most utilized biomarker for prostate cancer screening and monitoring. Research is focused on identifying markers like PCA3 to enhance specificity.miRNA: miRNAs are promising non-invasive biomarkers due to their stability in biological fluids. In prostate cancer, specific miRNA profiles have been linked to disease stage and progression. This makes them a valuable tool in early cancer detection and monitoring disease status.

Despite advancements, the identification and validation of reliable cancer biomarkers face challenges such as biological variability and the need for large-scale validation studies. The future direction involves integrating multi-omics data and using artificial intelligence to enhance biomarker discovery and clinical utility, especially in personalized cancer therapy.

1.4.3. Role of nano miRNAs in diagnostic and therapeutic.

Nanotechnology- MicroRNAs (miRNAs) are small non-coding RNAs that play a crucial role in gene regulation, particularly in cancer development and progression. Advances in nanotechnology have led to the development of highly sensitive and specific methods for miRNA detection, as well as novel therapeutic approaches for cancer treatment. Plasmonic sensor platforms, such as surface plasmon resonance (SPR) and localized surface plasmon resonance (LSPR), have demonstrated significant potential for miRNA detection. These platforms utilize the optical properties of nanoparticles to enable label-free, real-time detection of biomolecules, providing a powerful tool for early disease diagnosis and monitoring. In particular, SPR-based biosensors have been widely explored for detecting cancer biomarkers in liquid biopsy samples, offering a promising avenue for non-invasive diagnostic techniques. Colorimetric(optical) biosensors provide another valuable approach to miRNA detection by allowing analyte quantification through visible color changes. These biosensors enable real-time, sensitive detection of biomolecular interactions, which is essential for clinical diagnostics, environmental toxin detection, and proteomics. The miniaturization and multiplexing capabilities of nanotechnology enhance bioanalysis by enabling simultaneous detection of multiple analytes in smaller sample volumes. Several colorimetric and SPR-based biosensors have been developed to detect circulating miRNA biomarkers associated with cancer, including miR-21, miR-155, miR-141, and miR-148a. These biosensors, utilizing gold nanoparticles, graphene oxide, and other nanomaterials,

have demonstrated exceptional sensitivity and specificity, making them valuable tools for early cancer diagnosis and disease monitoring. Nanoplasmonic sensor chips and self-assembling nanostructures with controllable plasmonic functionalities have been developed to improve miRNA detection capabilities. These methods, employing DNA/miRNA hybridization techniques and surface-enhanced Raman spectroscopy (SERS) signaling, allow precise detection of miRNA biomarkers such as those implicated in lung cancer, including miR-107. Graphene-based biosensors, which take advantage of graphene's remarkable electronic and optical properties, have also emerged as highly sensitive platforms for detecting cancer-related miRNAs. Recent studies have demonstrated promising results in multiplex miRNA detection from human serum, HeLa cells, and patient urine, achieving detection limits as low as 0.05 pmol and 10 fM, respectively. Additional nanomaterials, such as carbon quantum dots (CQDs) and chitosan-molecular beacon (CS-MB) technology, are also being explored for highly sensitive miRNA detection, further advancing the prospects of early cancer diagnosis. Electrochemical biosensors, particularly those utilizing carbon-based nanomaterials, have gained attention for their high sensitivity and reproducibility in miRNA detection. These biosensors have been applied in the identification of breast cancer biomarkers, employing techniques such as nanohybrid formation, magnetic bar carbon paste electrodes, and graphene-polypyrrole-gold nanoparticle nanocomposites to enhance detection sensitivity and selectivity. One such sensor utilizes a modified three-screen-printed carbon electrode array functionalized with gold nanoparticles, graphene quantum dots, and graphene oxide. This system is capable of detecting miRNA-21, miRNA-155, and miRNA-210 simultaneously, demonstrating high sensitivity, selectivity, and multiplexing capabilities with promising diagnostic accuracy for early breast cancer detection. In addition, a dual-electrode electrochemical biosensor has been developed to simultaneously detect breast cancer biomarkers CA 15-3 and miRNA-21, further expanding the potential of nanotechnology in cancer diagnostics.Fluorescence-based biosensors, particularly those utilizing fluorescence resonance energy transfer (FRET), have emerged as valuable tools for miRNA detection. FRET sensors facilitate the study of intracellular processes and molecular interactions, enabling real-time monitoring of miRNA activity. One notable approach involves nanoflares, which are spherical gold nanoparticles functionalized with DNA for live-cell detection of intracellular mRNA. Two-color nanoflares, developed by Li et al. (2018), allow the simultaneous detection of miR-21 and miR-141 in live cancer cells, highlighting the potential of these platforms in cancer diagnostics. In another study, Esmaeili-Bandboni et al. (2018) designed an optical biosensor for detecting cancer-related

miR-155 based on cross-linking AuNP aggregation. This biosensor exhibited detection limits comparable to real-time PCR but provided a simpler and faster alternative. Further advancements in optical biosensing methods have led to the development of dual-mode sensors combining fluorescence and colorimetric detection, lateral flow assays with catalytic hairpin assembly, and photonic crystal biosensors, achieving ultra-low detection limits in the femtomolar to attomolar range. Beyond diagnostics, nanotechnology plays a crucial role in miRNA-based cancer therapies by addressing challenges related to miRNA delivery, stability, and targeting efficiency. Various nanocarriers, including lipid-based and non-viral vectors, have been developed to enhance the therapeutic potential of miRNAs. Dendritic nanocarriers, mesoporous magnetic clusters, and branched polyethylenimine nanoparticles have demonstrated significant potential in delivering miRNAs to cancer cells, effectively inhibiting tumor growth and inducing apoptosis in various cancer models. Extracellular vesicles, particularly exosomes, have also been explored as natural nanocarriers for targeted miRNA delivery, leveraging their ability to facilitate intercellular communication and transport therapeutic molecules.

1.5. Osteoarthritis (OA) is a widespread degenerative joint disease.

Osteoarthritis (OA) is a degenerative joint disease in which connective tissue and adjacent tissues are damaged. This disease is common in humans and animals as well. Given the high prevalence of this disease in the fauna, according to studies of two marine mammals and 22 land mammals(Nganvongpanit et al. 2017), we can assume that the etiology and prevalence of this disease are quite broad. Worldwide, about 250 million people suffer from osteoarthritis, representing 3.6% of the planet's population(Vos et al. 2012). This condition may be the most common joint disease in all mammalian species, which also opens space for research on animal models and sufficiently qualitative transfer of knowledge from experimental to clinical areas. In humans, the disease can develop not only because of external influences (post-traumatic stress) but also because of genetic predisposition or dysfunction of the body's systems. Therefore, the manifestations of this disease can be observed both in young people (athletes) and in patients of a certain age. Lifestyle contributes to the accumulation of risk factors, such as obesity, inactive lifestyle, or excessive physical activity. The development of an accurate and efficient diagnosis and treatment of this disease is an urgent task in modern medicine. Scientific articles with different geographies of origin were examined from European countries: Spain (Puigdellivol

et al. 2019), Czech Republic, Germany (Schadow et al. 2017), Austria, Denmark, Asia (China (Sun et al. 2019), Japan (Naraoka et al. 2013), India(Pal et al. 2016)) to North American countries: United States of America(Deshpande et al. 2016), Mexica (Furuzawa-Carballeda et al. 2009), considering this we can assume that the disease is very geographically widespread.

Furthermore, developing effective treatment strategies for modern medicine is significantly important because of the large-scale decline in quality of life and possible disability (increased number of disabled people) in the late stages of the disease and the costs the condition may cause in the future(Callahan et al. 2021). A combination of early detection and advanced treatment can promote health in sound adult patients with osteoarthritis.(Fedoruk G.V. 2012; Fedoruk G.V. 2013) However, this approach requires very tight specialization and a huge amount of experience. Additionally, the economic costs of disease and the epidemiological incidence of the population (Prevalence and most common causes of disability among adults--United States, 2005 ; Murray et al. 2013; Cui et al. 2020).

1.5.1. In-fluid Diagnostics of Arthritis

The diagnostic pathway follow a similar pattern for many musculoskeletal disorders (MDs). Most patient referrals and initial diagnoses become the general practitioner's responsibility (Primary care doctor). In turn, they shall be able to comprehensively collect the medical history, evaluate risk factors and disease development, and assess the patient's condition. After performing a physical examination, in which they can detect the signs of local inflammation and different abnormal findings, presenting irregularities in the skin near the joint, atypical joint axis and altered or restricted joint movement, assess the relationship between pain and collective activity, etc. They will also give lifestyle recommendations, prescribe therapy to relieve the acute condition (symptomatic treatment) and prescribe follow-up(additional) examinations. A continuation of the conditional patient management pathway is the referral of patients for a general blood test and biochemical test (detecting markers of rheumatological joint diseases is possible). Nowadays, the most frequently researched methods for monitoring the results of osteoarthritis treatment are WOMAC (Western Ontario and McMaster Universities Arthritis Index) for knee OA(osteoarthritis) and non-specific pain evaluation tests for TMJ(temporomandibular joint) OA(Nijhawan et al. 2014), which are a subjective questionnaire of treatment effectiveness or other pain questionnaires; However, for the evaluation of degenerative joint diseases, there are currently limited laboratory diagnostic possibilities.

The difficulty of diagnosis is caused by several factors, one of which is the broad etiology of the disease and the unknown exact trigger of the disease in an individual case. Also, recent studies argue for the existence of different phenotypes of osteoarthritis(Kjelgaard-Petersen et al. 2015). Early diagnosing allows us to use a "window of opportunities" for effective conservative treatment of the OA(Runhaar and Bierma-Zeinstra 2022).

The common biochemical laboratory tests of blood and other fluids give a basic image of what is happening in the body. Blood tests provide key diagnostic insights, and in the case of suspected rheumatological diseases, attention is paid to biochemical indicators, such as markers of general inflammation, which are reflected in the following blood markers:

- C-reactive protein (CRP). – a total inflammatory marker
- Erythrocyte sedimentation rate (ESR or sed rate).

Laboratory tests in non-comorbid OA are mostly normal, but some results may indicate other diseases (e.g., rheumatoid arthritis) or diagnose an underlying condition causing secondary OA or comorbid OA. In OA, involvement outside the normal joints indicates secondary OA; further investigation may be required to determine the underlying disease (e.g., endocrine, metabolic, neoplastic, or biomechanical abnormalities). (Garnero et al. 2001).

Specific markers for rheumatoid arthritis lesions, as differential diagnostic tests (Shen et al. 2015):

- Anti-cyclic citrullinated peptides (anti-CCP) antibodies. They signal bone damage caused by RA.
- Rheumatoid factor. Proteins are produced when it attacks healthy tissues.

The big advantage of laboratory tests is that they produce more relevant results with little human bias in the analysis of results. Also, these tests allow us to evaluate disease activity(Anderson et al. 2012).

The next useful diagnostic method for diagnosing arthritis in bigger joints is synovial fluid analysis. Synovial fluid is an integral part of synovial joints. Its volume, composition, and physical properties indicate pathological processes in the joints covered with the synovial layer. The fluid can contain all proteins that are found in plasma. Since it is an ultrafiltrate of blood plasma and a product of the metabolism of chondrocytes and synovial cells, this fluid plays a crucial role in joint metabolism. The synovial fluid composition will differ with common pathologies, an important diagnostic indicator for making an appropriate diagnosis. In the presence of synovitis caused by OA, synovial fluid sampling can help in the differential diagnosis from inflammatory arthritis, bacterial or traumatic. In

OA, synovial fluid is usually clear, viscous, and contains ≤ 2000 WBC/mcL (Meehan et al. 2021). The development of novel laboratory diagnostics should expand and complement existing diagnostic methods and bring a new trend into established areas of medicine, such as myofascial disorders like osteoarthritis.

1.5.2. Composite biomarkers and Companion diagnostics (CDx).

In diagnosing a complex disease such as osteoarthritis with a multifactor etiology, it is important to pre-determine the purpose of markers and evaluate their usefulness in clinical practice. (BEST- (Biomarkers, EndpointS, and other Tools, 2016))The Foundation for the National Institutes of Health/Osteoarthritis Research Society International (FNIH/OARSI) evaluated various biochemical indicators. However, because ELISAs can only assess a single molecule of interest at a time, it is extremely labor-intensive and difficult to simultaneously quantify many antigens in large cohorts of patient samples. For the dominant part of disorders, the presence of a single biochemical marker in blood, cerebrospinal fluid, synovial fluid, urine, or other body fluids is not an acceptable prognostic or diagnostic sign(Bernotiene et al. 2020).

Different classifications of biomarkers with the aim of standardization and sorting. Some of them use different criteria for dividing markers into categories by function, diagnostic purpose, and even classifications that take into account stages of disease developmentgroups of markers that include components of the pathogenetic process of the disease are created by many research groups (Lotz et al. 2014).

Classification of biomarkers is developed by the FDA-NIH Biomarker Working Group of National Institutes of Health (NIH) and the Food and Drug Administration (FDA), the U.S., - BEST (Biomarkers, EndpointS, and other Tools, 2016) Resource. Their classification covers quite a wide range of applications of biomarkers. In our review, we adhere to the more specialized classification for osteoarthrosis, the BIPEDs Criteria, which has common features. But also, some markers are supplemented with information that is not covered by this classification, such as Endpoint, composite markers and Companion diagnostics (CDx), and others.

One of the most suitable for arthritis is – the BIPEDs Criteria; BIPEDs classification was initially proposed by Bauer *et al. in 2006* (later modified by *Kraus et al.*)(Bauer et al. 2006; Kraus et al. 2024)

The classification includes the next groups of markers:

1. **Burden of disease** biomarkers: evaluate the amount or severity of the disease in people with OA, usually at one particular period. Studies including these markers must be compared to one or more gold-standard techniques for assessing the severity of the disease, such as clinical or radiographic criteria (i.e., Kellgren-Lawrence classification).
2. **Investigative biomarkers**: described as an investigation report if there is not enough data to place it in another category.
3. **Prognostic biomarkers**: a predictive biomarker indicates the development of OA in people without the condition or the development of OA in people who already have the condition. Longitudinal studies linking the marker's baseline risk of OA development or progression are necessary for its evaluation.
4. **Efficacy of intervention biomarkers**: can be used in randomized controlled trials to evaluate the alterations brought about by pharmaceutical treatments. These markers may serve as predictors or indicators of treatment effectiveness.
5. **Diagnostic biomarkers**: this type of markers can discriminate between those who have and don't have OA with a high degree of sensitivity and specificity. Individuals with OA and those with diseases that are easily mistaken for OA, such as rheumatoid arthritis, must be included in studies using these indicators.
6. **Safety biomarkers***:* those potential of representing tissue and/or organ toxicity after a given treatment, monitoring for early and advanced local and systemic adverse effects, setting therapeutic dosages without affecting physiology, and comprehending what "safe" ranges are for joint tissue biomarkers

To determine the disease accurately and most specifically, groups of markers can be used with the internal correlation between (Maren et al. 2022) between them(Hosnijeh et al. 2016). For example, by dividing interdependent markers into groups – pathway-related markers, miRNA markers, and others and creating and composite marker with these different groups or creating a score, using imagine methods will increase the accuracy of predicting individual symptoms. It is also possible to add markers of rheumatologic diseases and autoimmune markers for differential diagnosis.

Such groups of markers would give us a comprehensive, objective notion of the state of the tissues and the course of the disease.

Table 1. Potential categorization of marker groups by BIPEDs criteria. (Bay-Jensen et al. 2016)

Functional group of biomarkers	Candidate markers, group of markers, composite markers
Burden of disease	miRNA, genetic markers, cartilage metabolism markers
Investigative biomarkers	Markers of tissue stability, after conservative and surgical treatment, cartilage metabolism markers
Prognostic biomarkers	Monitoring of tissue stability
Efficacy of intervention	Monitoring of tissue stability, pro-inflamatory markers
Diagnostic	Disbalance in cartilage tissue, after injury monitoring
Safety biomarkers	Can reflect tissue and/or organ toxicity following a specific treatment, ("Synovial Fluid Biomarkers in Knee Osteoarthritis: A Systematic Review ...")

1.5.3 Serum, Synovial fluid (SF), Urine biomarkers of OA

These markers generally characterize tissue processes and help us to objectively understand and measure the activity of inflammation or cartilage stability. Screening and monitoring of such markers would be useful in individual clinical cases for early diagnosis and evaluation from the perspective of outcome intervention and as Endpoint markers. Many markers from this group have long been identified, and some have been well-researched. Many of these markers are already found reference values and defined correlations with other diagnostic methods, such as imaging methods or functional questionnaires. (Kraus and Karsdal 2021; Henrotin 2022)

Figure 9. Pathway-related markers

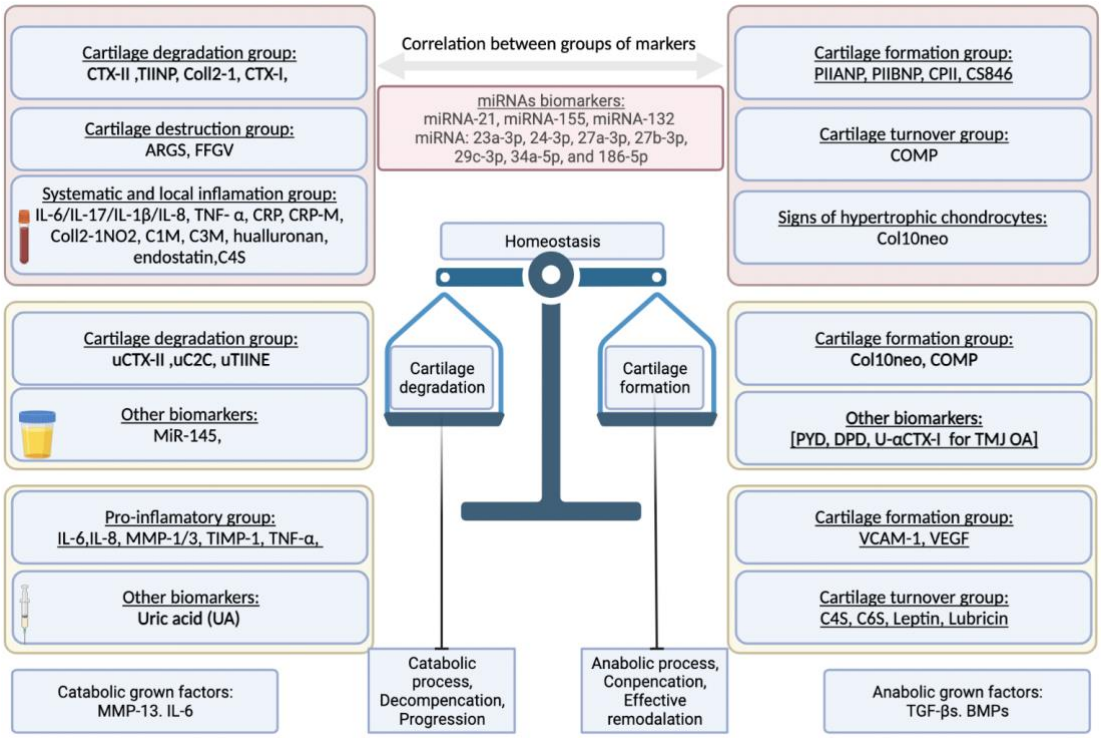

Groups of OA identified biomarkers for multi-etiological disease. Biomarkers are divided into metabolic process-related groups and body fluids where they can be detected.

Markers detectable *in urine* have limitations. Their concentration is further limited by the patient's kidney condition as well as by the stability of the molecule. (Rasmussen et al. 2019). urinary collagen type-II C-terminal cleavage neoepitope (uC2C) (Waluyo et al. 2021; Kuhi et al. 2021)gen type-II crosslinked C-telopeptide fragments (uCTX-II)(Wang et al. 2021)

The analysis of *synovial fluid* using quantitative measurement of biochemical markers can potentially assess the intensity of the pathological process. For example, in the Jian-lan Ding et. al. study, the paragraphs analyzed patients with meniscus trauma and with osteoarthritis, VEGF and IL-6 levels, and lower levels of IL-10 than those with meniscus tarsus. (Boffa et al. 2020) It is the pattern of changes in several biomarkers or groups of markers that can help in the differential diagnosis of orthopedic diseases.

According to Lotz et al.7, SF biomarkers may be divided into 4 types depending on their nature and molecular origin: (1) Biomarkers connected to the metabolism of type II collagen or type I collagen in subchondral bone; (2) Biomarkers connected to the metabolism of aggrecan in cartilage; and (3) Biomarkers connected to a variety of non-collagenous proteins that play a part in other metabolic pathways in the joint, such as glycoproteins, proteoglycans, metalloproteinases, and (4)advanced glycation end-products, as well as

hyaluronan, Additionally, all SF biomarkers were categorized into the 6 BIPEDs categories, and each of them was briefly discussed in its own paragraph and chart. (Lotz et al. 2013)

The most promising in SF: C4S, IL-6, IL-8, Leptin, MMP-1/3, TIMP-1, TNF-α, and VEGF. (Boffa et al. 2020)

Important for differential diagnosing: Uric acid (UA) (Krasnokutsky et al. 2017)

In the case of the arthrosis of the smaller joints, their influence on systematic markers will be significant dut to the constant usage and non-possibility of their immobilization of them., One of the TMJ's significant anatomical characteristics is the presence of the intraarticular disc, which is largely composed of type 1 collagen. This condition allows the selection of additional markers that may be less noticeable or atypical for knee osteoarthritis, along with imaging grades and cytokine levels in the synovial fluid.

Specific markers in body fluids: *Biomarkers in the peripheric bloodstream:*(Henrotin et al. 2012, 2016; Attur et al. 2015; McIlwraith et al. 2018; Kumavat et al. 2021)

Diagnosing from Saliva (VE-cadherin in saliva and headaches, PAI-1 in saliva and headaches, PAI-1 in saliva and range of mouth opening without pain, energy, Haralick correlation, entropy and interactions of TGF-β1 in saliva and headaches, VE-cadherin in serum and angiogenin in saliva.)(Bianchi et al. 2020a) (Ford and Solomon 2019)

1.5.4. Composite diagnostics to harmonize influencing factors.

The combination of groups of biomarkers depending on the selected reference value could serve as a monitoring marker and surrogate endpoint function.

The Ahlbäck classification and Tomihisa Koshino's scoring system were less often used scales. Kellgren-Lawrence classification was the most widely used reference criteria for radiographic severity. Additionally, the Outerbridge classification or the International Cartilage Repair Society classification was used in several papers to assess the severity of arthroscopy procedures. Finally, the extent of the knee OA was assessed by scintigraphy imaging, ultrasonographic findings, macroscopy, and histology, in that order. Joint space narrowing. The WOMAC (Western Ontario and McMaster Universities Osteoarthritis Index) scale is the most used reference parameter for clinical severity; other less frequently used parameters included VAS (visual analog scale) in 7 articles, followed by Numeric Rating Scale (NRS), NPQ (Neurophysiology of Pain Questionnaire) scale, KSS (Karolinska Sleepiness Scale), and Watanabe's pain score.

The The levels of the measured markers can vary throughout the day.(McIlwraith et al. 2018; Waluyo et al. 2021; Östlind et al. 2022) One of the unobvious influencing factors is

the novel selection of inflammatory cytokines, as far as rheumatological diseases are concerned, in which these markers play a significant role(Sierakowski and Cutolo 2011).

Individual characteristics should also be considered among the influencing factors on the development of osteoarthritis, especially the influence of work-related influencing factors and comorbid conditions and teratogenic factors.(van der Molen et al. 2021) In measuring stability biomarkers of musculoskeletal tissues, specifically of articular cartilage, it is necessary to consider the relationship between changes in serum levels of tissue and inflammatory biomarkers of cartilage tissue in connection with an acute response to its functional use such as running and jumping or different regular use(Maren et al. 2022). This relationship has already been determined in a study in healthy men, and it is expected that the changes in patients with tissue damage will be more dramatic and will undoubtedly affect the accuracy of the diagnosis.

For quantitative tests, it is also necessary to consider and correct for the association between age, sex, menopause and biomarker concentrations. For instance, serum COMP concentration and age are directly correlated.(Poole 2003)

1.5.5. Combinations with imaging diagnostic and therapeutic methods

The main methods used include Radiography, Magnetic Resonance Imaging, many of its modifications and the use of Artificial Intelligence in evaluating studies, Computed Tomography and Ultrasonography(Roemer et al. 2021). K-L score, MRI Osteoarthritis Knee Score (MOAKS), High-resolution cone beam tomography (HR-CBCT) is widely used in the field of research, with image resolution reaching sub-millimeter dimensions comparable to micro-CT but with an expressively lower radiation dose. It is also beginning to be widely used by clinicians. (Bianchi et al. 2020b) Although imaging methods are evolving and significantly improving, they are still limited.

Visualization methods such as X-rays, CT, and MRI, Ultrasound also include the influence of the human factor. In contrast, more accurate diagnostic procedures are based on objective criteria resulting from collagen structure.

New technologies allow us to overcome the way from passive to active Tissue/cell-specific targeting technologies. For example, the research used Anti-Coll. 2 labeled niosomes for active target drug delivery to the destructed cartilage tissue in rat models. Some diagnostic methods can be applied as a therapeutic, ultrasound, Radioterapz Gamma knife, and even MRI. The idea of theragnostics brings up a new point of view on the managing of regular diagnoses.

In the field of arthritis, the most promising diagnostic markers are microRNA and genetic studies in people with a genetic predisposition. The most promising diagnostic markers are microRNA and genetic studies in people with a genetic predisposition (Pérez-García et al. 2021) Forty OA patients showed that the gene expression levels of microRNA-21 and microRNA-155 in patients receiving crocin were significantly decreased and increased, respectively.(Mohebbi et al. 2022) miRNAs are very promising tools for diagnosing and targeting treatment fields (Coradduzza et al. 2022a) *miRNA*s important for OA: miRNA-21, miRNA-155, miRNA-132 (Li et al. 2016) miRNA: 23a-3p, 24-3p, 27a-3p, 27b-3p, 29c-3p, 34a-5p, and 186-5p (Munjal et al. 2019)

1.6. Functionalization for Modern Drug delivery systems

In modern medicine, drug delivery systems play an essential role in ensuring the efficient and effective delivery of therapeutic agents to target sites within the body. The development and optimization of these systems are paramount in enhancing therapeutic outcomes, particularly in the treatment of complex diseases such as cancer and arthritis.

Bioactive molecules can be linked to the fiber surface through **non-covalent interactions** (such as Van der Waals forces and hydrogen bonding) or by more **controlled chemical modifications**. Techniques like oxidation, hydrolysis, aminolysis, and surface coating introduce functional groups that improve bonding and biological compatibility. More advanced methods, such as **cold plasma treatment** or **sputtering**, can alter the fiber surface at the molecular level—adding reactive groups or coating the surface with thin films to enhance chemical reactivity. These techniques are especially important in applications like biosensing, where detecting low concentrations of biomarkers requires highly specific and stable molecular interactions on the fiber surface.

Drug molecules can be incorporated into nanofibers either **on the surface** or **within the core** of the fiber. Surface modification allows for external binding, while **encapsulation** during the electrospinning process offers protection for sensitive substances, extending their biological activity. Two main methods are used:

1. **Coaxial electrospinning** employs a dual-syringe setup, where one syringe delivers the polymer and the other delivers the drug solution, forming **core-shell fibers**.
2. **Blending**, where the drug is mixed directly with the polymer before spinning. However, this method may not be suitable for all drugs, especially those that are unstable or poorly soluble in the polymer matrix.

Core-shell nanofibers have shown great potential in **controlled drug release**, particularly for wound care. An ideal wound dressing would release a high dose of the drug

immediately to reduce pain or infection risk, followed by a slower, sustained release to support healing over time. One example demonstrated this approach using **Naproxen-loaded liposomes** embedded in nanofibers, which released the drug rapidly in the first 8 hours and continued releasing it steadily over 12 days. Another example combined **polycaprolactone/gelatin fibers with cationic liposomes**, resulting in strong antibacterial effects.

Beyond medical use, similar techniques are now being adapted for **active food packaging**, where liposome-encapsulated essential oils—such as basil oil—ar used for their antimicrobial properties. Thanks to the protective and functional properties of the liposomes, these electrospun nanofibers maintain structural integrity while providing sustained antimicrobial activity.

Finally, **coaxial electrospinning of liposome-loaded core-shell nanofibers** has gained attention in **tissue engineering**. This technique ensures that proteins and other sensitive molecules maintain their biological activity during fabrication, making these systems ideal for delivering therapeutic agents while supporting tissue regeneration.

Nanomaterials can be administered through various routes, with oral administration being the most convenient method. This process involves several stages:

Oral administration involves several stages that nanomaterials must navigate for effective drug delivery. Initially, they encounter the complex environment of the oral cavity, rich in proteins and bacteria. In the stomach, they face a highly acidic environment, before transitioning to the intestines, where they must overcome digestive enzymes, mucus layers, and tight junctions. Upon breaching the endothelial barrier, nanomaterials enter the bloodstream, where they can be taken up by cells non-specifically or specifically by target cells. The main target sites for drug delivery include the cytoplasm, nucleus, mitochondria, and lysosomes.

Oral administration facing challenges like proteins, acids, enzymes, and barriers. Once in the bloodstream, they can be taken up by cells, either nonspecifically or specifically, targeting various sites within the cell.

Figure 10. Schematic of a conventional electrospinning setup and methods for preparing stimuli-responsive electrospun nanofibers.

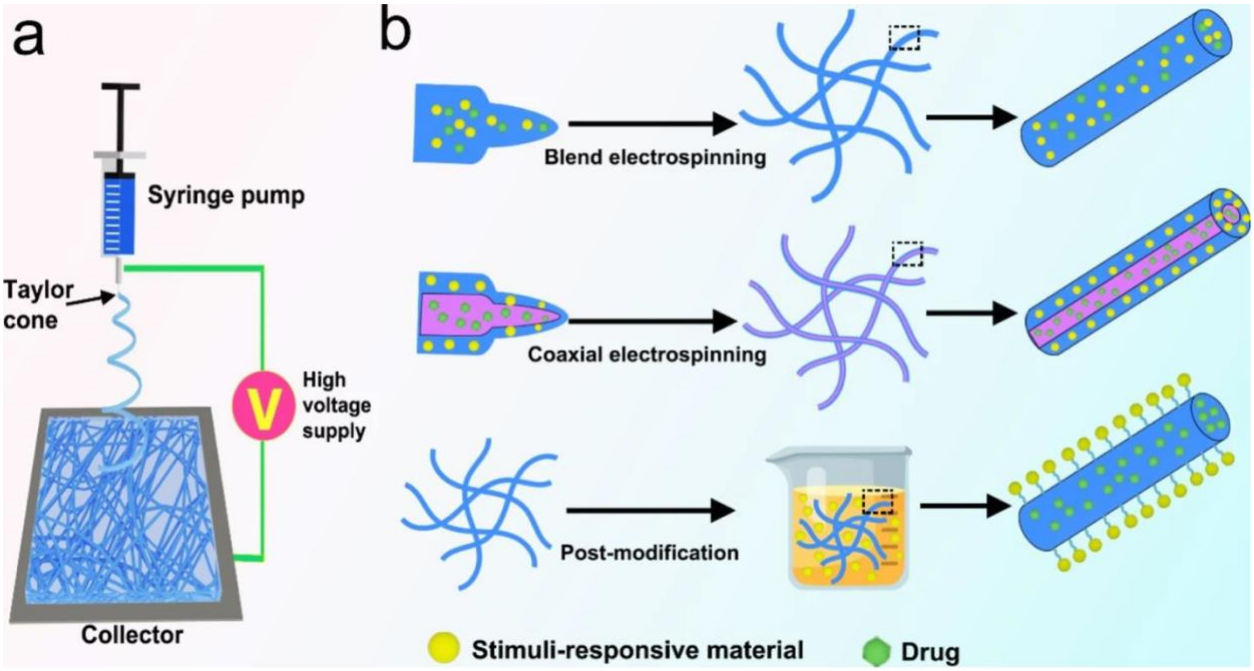

Attribution: Chen, K., Li, Y., Li, Y., et al. (2023). Schematic of a conventional electrospinning setup and methods for preparing stimuli-responsive electrospun nanofibers. Journal of Nanobiotechnology, 21, 237. https://doi.org/10.1186/s12951-023-01987-z. Licensed under CC BY 4.0. (Chen et al. 2023a)

Targeted delivery systems can be effectively developed by functionalizing nanofibers with ligands that specifically bind to receptors overexpressed on cancer cells. For instance, folic acid-conjugated nanofibers may selectively transport chemotherapeutic agents to cancer cells with elevated folate receptor levels. This targeted strategy guarantees a higher concentration of the drug at the tumor site while reducing exposure to healthy tissues.

Different cell types offer viable targets for drug delivery, thus improving treatment efficacy with nanomaterials. Recent innovations in drug delivery technologies have produced various platforms aimed at enhancing the precision and effectiveness of therapeutic agents. Among these innovations are active targeting systems that employ ligands to bind specifically to receptors on target cells. This mechanism ensures that drugs are precisely delivered to the locations where they are most needed. As a result, this targeted method reduces side effects and enhances the therapeutic index of the administered drugs.

Figure 11. Illustration of stimuli-responsive electrospun nanofibers as intelligent drug delivery platforms in biomedicine.

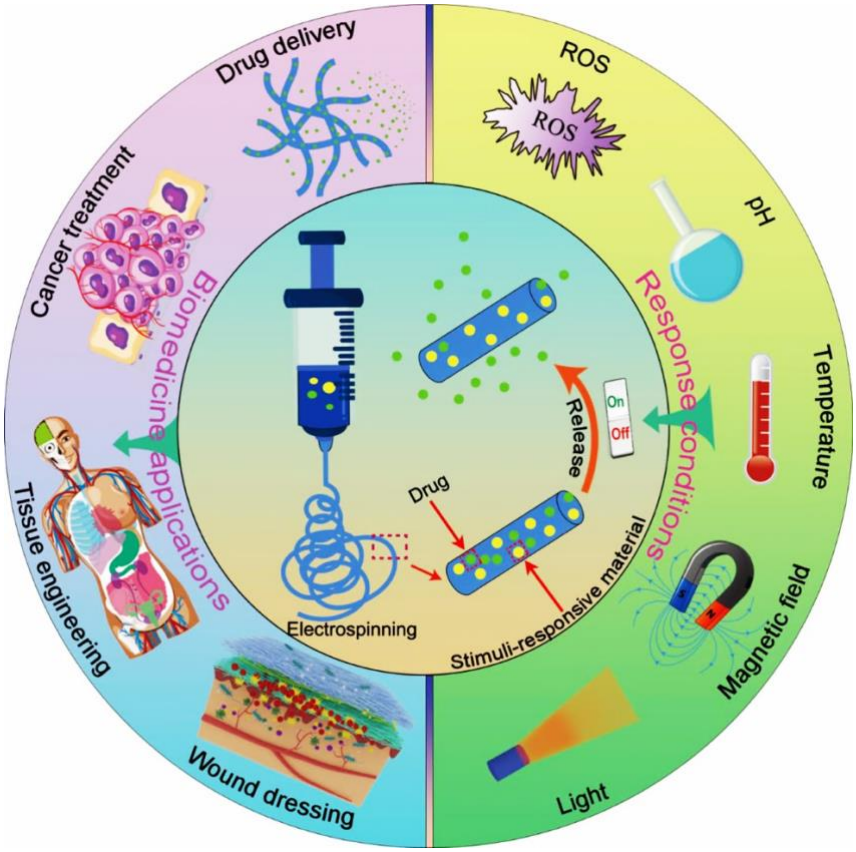

Attribution: Chen, K., Li, Y., Li, Y., et al. (2023). Illustration of stimuli-responsive electrospun nanofibers as intelligent drug delivery platforms in biomedicine. Journal of Nanobiotechnology, 21, 237. https://doi.org/10.1186/s12951-023-01987-z. Licensed under CC BY 4.0.(Akbarzadeh et al. 2013; Chen et al. 2023a)

Modern drug delivery systems frequently employ biodegradable scaffolds and carriers, facilitating the controlled release of medications over extended durations. These systems play a crucial role in managing chronic conditions that necessitate sustained drug levels to ensure therapeutic effectiveness. Prominent examples include polymeric nanoparticles, liposomes, and dendrimers, each presenting distinct advantages in drug encapsulation, stability, and release kinetics.

Functionalized nanofibers enable precise control over drug release via several mechanisms:

- **Diffusion-Controlled Release**:Drugs migrate through the fiber matrix over time.
- **Degradation-Controlled Release**:Biodegradable polymers decompose, gradually liberating the drug.
- **Stimuli-Responsive Release**: External stimuli such as pH, temperature, or enzymatic activity initiate drug release.

The domain of drug delivery systems is now a central focus in modern biomedical research, motivated by the aim of achieving controlled and targeted delivery of therapeutic agents. (Wang et al. 2019a; Chen et al. 2023)These systems are engineered to modulate the pharmacokinetic and pharmacodynamic profiles of drugs, optimizing their therapeutic effectiveness while minimizing potential adverse effects. The complex mechanisms governing drug release from these systems are shaped by an intricate interplay of factors associated with the drug, the delivery system, and the physiological environment.

A fundamental mechanism for drug release from nanofibers is diffusion, which transpires due to the concentration gradient between the interior of the delivery system and the external environment. Drug molecules move from regions of higher concentration to regions of lower concentration until equilibrium is established. Various parameters influence the diffusion rate, including porosity, tortuosity, and the existence of rate-limiting barriers. Particularly significant is the small diameter of nanofibers, which contributes to considerable surface tension.

Degradation serves as another vital mechanism that aids drug release by gradually eroding or breaking down the delivery system's matrix over time. The degradation half-life can be managed by modifying the degree of crosslinking, which impacts the solubility of the microcontainer envelope—such as fractionalized nanofibers with encapsulated drugs—in the surrounding aqueous environment. This degradation can proceed through multiple pathways, including hydrolysis, enzymatic degradation, or biodegradation. Consequently, the release rate of the drug is directly related to the degradation rate of the matrix, which may be influenced by factors such as the chemical composition and structural properties of the delivery system.

1.6.1. Active Drug delivery: therapeutic API, targeting, labeling.

MicroRNAs (miRNAs) have emerged as promising tools for enhancing drug delivery systems due to their ability to regulate gene expression and cellular processes. In the context of active drug delivery, miRNAs can be utilized to label and guide therapeutic agents to specific cells or tissues. This approach holds particular significance in diseases where precision is paramount, such as in targeting cancer cells while minimizing damage to normal tissues.

Figure 12. Avidin-PEG Linker for Antibody Functionalization

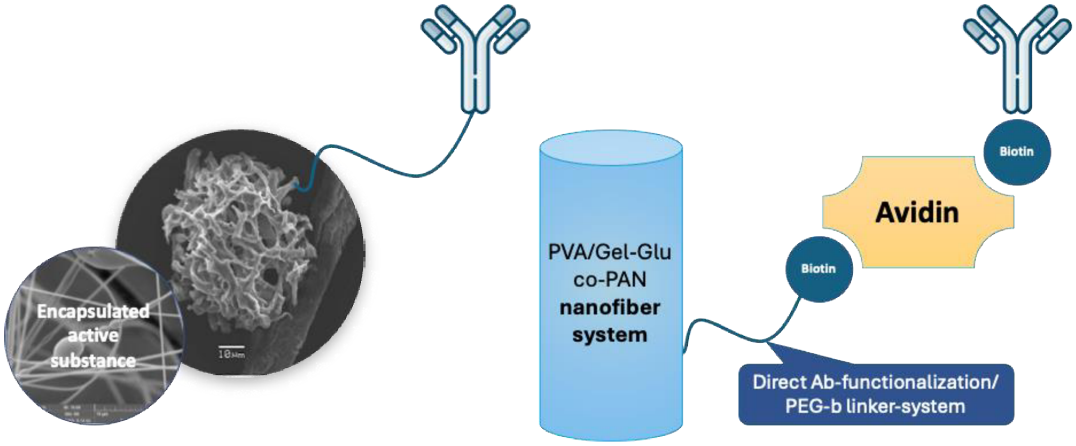

The employment of miRNA as a labeling agent in drug delivery systems presents the potential to enhance the specificity and minimize the occurrence of off-target effects of therapeutic agents. By incorporating miRNA-based labels into drugs, these systems can leverage the inherent regulatory functions of miRNAs to ensure targeted delivery to the desired sites, thereby augmenting the overall efficacy of the treatment.

Therapeutic biomarkers serve as pivotal elements in personalized medicine, providing insights into the biological processes of diseases and the effects of therapeutic interventions. In oncology and arthritis, identifying and integrating these biomarkers into drug delivery systems can significantly improve the precision and efficacy of treatments.

In oncology, the expression of specific biomarkers can guide the selection and dosage of targeted therapies, thereby maximizing therapeutic efficacy while minimizing adverse effects. For instance, HER2 is a well-known biomarker used in breast cancer to identify patients who would benefit from HER2-targeted therapies, such as trastuzumab. As well as patients with cancer, including specific surface protein GPC-3, can benefit from drugs, based on monoclonal antibodies, against this protein or from drug delivery systems, which will release the needed drugs directly around cells near the malignant mutated cells. This technology will decrease effective concentration multiple times and can prolong the release of the drug at the point of application. Incorporating such biomarkers into drug delivery systems ensures that the therapeutic agents are directed precisely to cancer cells, sparing healthy tissues and reducing systemic toxicity.

In arthritis, biomarkers can help stratify patients based on disease activity and response to therapy. For instance, specific inflammatory cytokines can be used to tailor anti-inflammatory treatments, ensuring that patients receive the most appropriate therapy based

on their individual biomarker profiles. This approach not only improves patient outcomes but also helps manage disease progression better.

Traditional chemotherapy is frequently associated with significant systemic toxicity and limited specificity, leading to adverse side effects and reduced therapeutic efficacy. To address these challenges, functionalized nanofibers have emerged as a promising alternative, offering targeted drug delivery with minimized side effects. These nanofibers can be engineered with tumor-specific ligands or antibodies for precise tumor detection and can encapsulate therapeutic agents within their core for effective treatment.

delivery mechanisms.

1.6.2. Role of Oriented/Balk Water in Nanocarrier Delivery

The effectiveness of micro- or nano-carriers is significantly influenced by their targeted delivery into the oriented water region adjacent to cell membranes. This region exhibits distinct properties compared to bulk water. Water molecules, being highly polar, form clusters in bulk; however, near surfaces with strong intermolecular interactions, such as cell membranes, water molecules adhere more strongly, leading to a restructured water layer known as oriented water. This layer is a few nanometers thick and is characterized by altered diffusion coefficients, with lateral diffusion being significantly higher than vertical diffusion. This anisotropy is crucial for cellular functions, such as ATP production in mitochondria, where efficient lateral proton movement is essential.

For drug delivery systems, overcoming the diffusion barrier posed by the oriented water layer is vital. This can be achieved through specific binding to membrane proteins protruding into the oriented water or by utilizing nanocarriers designed to interact favorably with this water layer. Such strategies ensure that therapeutic agents effectively reach the cytoplasm, enhancing treatment efficacy. These advancements underscore the potential of functionalized nanofibers and nanocarriers in improving the specificity and effectiveness of cancer therapies through targeted delivery mechanisms.

1.6.3. miRNA-145, 148, and 185 and Stem Cells in Prostate Cancer.

MiRNAs, MicroRNAs (miRNAs) have emerged as crucial regulators in prostate cancer (PCa) progression, with particular interest in miRNA-145, miRNA-148, and miRNA-185 due to their dysregulated expression in both plasma and tissue samples. These miRNAs are associated with the distinction between benign prostatic hyperplasia (BPH), precancerous lesions (PL), and prostate cancer, positioning them as potential biomarkers for disease diagnosis and prognosis. Additionally, prostate cancer stem cells (PCSCs) play a

fundamental role in tumor initiation, metastasis, and resistance to therapy, making them an essential target for improving treatment outcomes.

MiRNA-145 has been widely studied in prostate cancer due to its significant downregulation in PCa patients compared to those with BPH. Reduced expression of miR-145 correlates with higher Gleason scores, advanced tumor stages, increased tumor size, and elevated prostate-specific antigen (PSA) levels. Functionally, miR-145 modulates apoptosis and suppresses cancer cell migration, invasion, and metastasis by targeting phospholipase D5 (PLD5), making it a promising therapeutic target. Furthermore, an inverse correlation between miR-145 and androgen receptor (AR) expression has been observed, particularly in patients with high Gleason scores, suggesting its role in androgen deprivation therapy (ADT) response. Additionally, miR-145 interacts with inositol 1,4,5-trisphosphate receptor type 2 (ITPR2), which is implicated in epidermal growth factor receptor (EGFR) signaling regulation, particularly in African American prostate cancer patients.

In the context of castration-resistant prostate cancer (CRPC), miR-145 is significantly downregulated in CRPC cell lines, where it directly targets c-MYC and cyclin-dependent kinase inhibitor 1A (CDKN1A), implicating it in apoptosis rather than cell cycle arrest. Loss of miR-145 expression in metastatic CRPC enhances AR activity and cell proliferation, contributing to disease progression. Additionally, miR-145 has been detected in endothelial and stromal tissue, and receiver operating characteristic (ROC) analysis has identified it as a potential biomarker for distinguishing malignant from non-malignant prostate tissue. MiR-148b-3p and miR-148a-3p exhibit upregulation in prostate cancer tissues and plasma, further suggesting their role as biomarkers for PCa detection. In contrast, miR-185 is frequently downregulated in prostate cancer tissues and cell lines, with its suppression leading to the upregulation of anti-apoptotic genes and increased tumor cell survival. While some studies support miR-185 as a prognostic marker, others report its upregulation, highlighting the complexity of miRNA regulation in prostate cancer and the need for further investigation to clarify its precise role. MiR-185-5p has been specifically associated with aggressive prostate cancer phenotypes and poor patient prognosis. However, its role as an oncogene or tumor suppressor appears to be context-dependent, with conflicting findings across different experimental models.

Prostate cancer stem cells (PCSCs) contribute significantly to treatment resistance and tumor metastasis due to their capacity for self-renewal and differentiation. Dysregulated miRNA expression has been linked to the maintenance of PCSC populations, influencing tumor progression and therapeutic resistance. The prostate gland comprises various differentiated cell types, including basal, luminal, and neuroendocrine cells, as well as a pool of undifferentiated stem cells responsible for cellular turnover and morphogenesis. MiRNAs such as miR-148b, miR-148a-3p, and miR-185 have been implicated in regulating PCSCs by targeting oncogenes and stemness-associated factors. These miRNAs suppress tumorigenicity, inhibit cancer cell proliferation, and reduce migration and invasion, suggesting their potential as therapeutic targets for preventing prostate cancer bone metastases.

Overall, miRNAs play an integral role in prostate cancer development and progression, with miR-145, miR-148, and miR-185 emerging as critical regulators of tumor growth and stem cell maintenance. Their potential as biomarkers and therapeutic targets highlights the need for continued research to translate these findings into clinical applications, particularly in developing targeted therapies to improve patient outcomes.

1.6.4. Local: Transdermal and mucosal drug delivery

Wound healing is a multifaceted biological process that necessitates a careful equilibrium between cellular and molecular interactions. Although conventional wound dressings offer fundamental protection, they frequently lack active promotion of the healing process. In contrast, functionalized nanofibers have emerged as a sophisticated solution by delivering antimicrobial agents, growth factors, and regenerative compounds precisely to the wound site.

Electrospinning techniques facilitate the fabrication of nanofiber-based dressings that replicate the extracellular matrix, thereby enhancing cell adhesion and proliferation. Research indicates that the incorporation of silver nanoparticles or antibiotics into these nanofiber dressings effectively prevents infections and promotes tissue regeneration. Furthermore, loading nanofibers with bioactive molecules, such as epidermal growth factor or vascular endothelial growth factor, can significantly accelerate healing by stimulating cell migration and angiogenesis.

Smart skin covers exemplify a groundbreaking progression in the biomedical applications of electrospun polymers. They mimic natural skin properties, ensuring protection while enhancing functionality. Their high porosity and adaptability create ideal conditions for wound healing by maintaining moisture, facilitating gas exchange, and

directly delivering therapeutic agents to the injury site. In addition, these covers can integrate sensors to continuously monitor skin conditions, providing essential insights into the healing process and enabling timely medical interventions.

Figure 13 Liposome structure

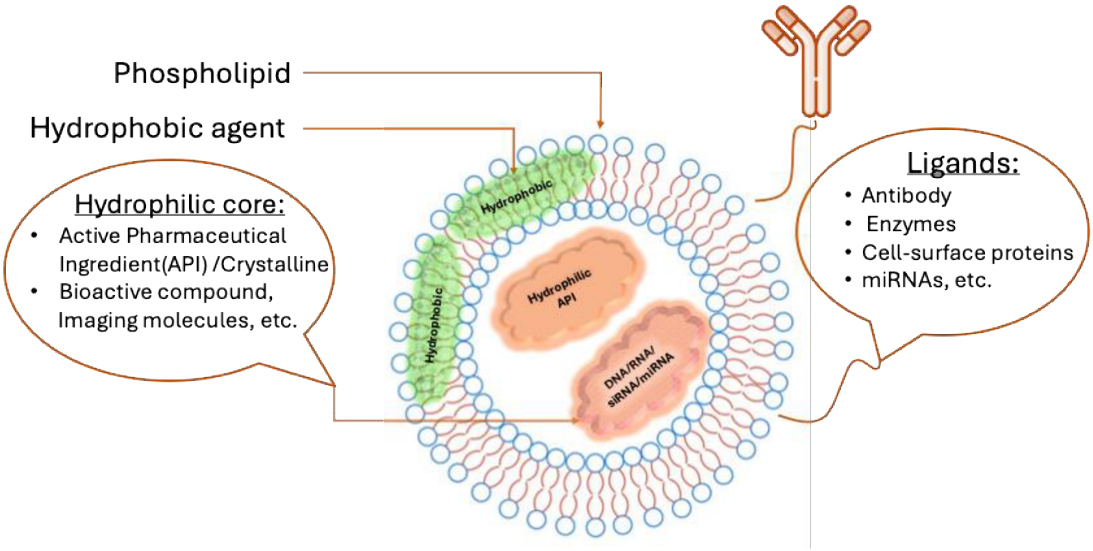

There are various scaffolding systems for drug delivery; one is liposomes, spherical vesicles with lipid bilayers, which are involved in passive and active-targeted drug delivery systems, but due to their physical properties, especially lower resistance to the osmotic pressure, cannot be taken as a unified platform for the drug delivery with decreased side effects. Another scaffolding system for drugs can be represented by electrospinning core-shell combinations of polymer and active compounds in the core layer, which found their applications in the field of smart skin wounds and regenerative medicine where sophisticated multi-polymer systems allow to release of certain drug components with the regulated time, and even observe changes in wound environment such as pH of diverse excaudate biomarkers, characterizing the healing process.

Figure 14. Electrospun Nanofibers for Smart Skin Wounds

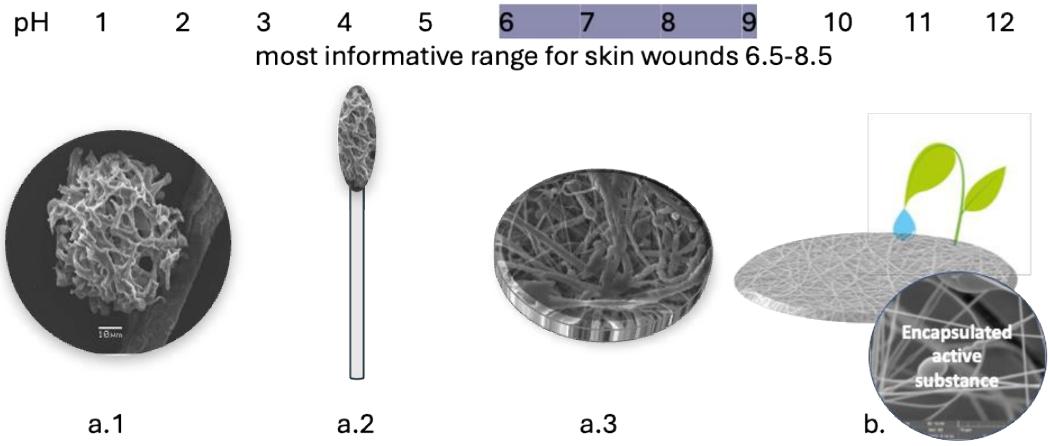

a. ***pH-sesetive electrospun (1) nanoParticles, (2)nanoSwabs, (3) nanoMembranes*** *for colorimetric pH sensing in skin wounds.*
b. ***Nanofibers-based skin wounds:*** *Synergy of modern nanotechnology and ancient Mediterranean medicine. This interdisciplinary exploration showcases the potential for synergistic advancements in wound care by leveraging both modern scientific advancements and ancient therapeutic knowledge. Through the integration of liposome-functionalized nanofibers, this system promises targeted and efficient administration of therapeutic agents, marking a significant advancement in personalized medicine.* ***Nanothergnostics*** *concept introduces a groundbreaking technology platform designed for theragnostic applications, with a particular focus on precise drug delivery.*

The skin, recognized as the largest organ of the human body, demonstrates a remarkable capacity for self-healing. Nevertheless, significant injuries such as burns or chronic wounds frequently necessitate advanced therapies to facilitate regeneration. Nanofiber-based scaffolds have emerged as a promising solution to enhance skin regeneration by creating an optimal environment that promotes cell proliferation and differentiation.

Recent investigations reveal that electrospun nanofibers, particularly when enriched with natural products like Helichrysum italicum extract, significantly enhance collagen deposition and accelerate the wound healing process. These bioactive components possess anti-inflammatory and antioxidant properties that mitigate oxidative stress and inflammation at the wound site. The sustained release of these natural agents from the nanofiber scaffold ensures a prolonged therapeutic effect, which is crucial for effective wound healing.

Additionally, the structural characteristics of nanofibers, including their diameter and porosity, can be tailored to modify cell behavior. Studies indicate that smaller fiber diameters correlate with enhanced adhesion and proliferation of keratinocytes, which are vital for the re-epithelialization process. Moreover, the integration of antimicrobial agents into nanofibers can assist in preventing infections—a prevalent complication in wound care.

Nanofibers also offer an efficient method for transdermal drug delivery through the skin barrier. By incorporating penetration enhancers into nanofiber mats, drug permeation can be

optimized, promoting effective systemic absorption. Transdermal patches manufactured from nanofibers have been successfully developed for the release of analgesics, hormones, and anti-inflammatory agents, providing a convenient and painless alternative to injections.

One significant research breakthrough in this area is the NanoPCL-M skin cover, a nanodevice designed to deliver myrtle extracts. These extracts positively impact the proliferation of skin stem cells (SSCs) and dermal fibroblasts while counteracting UV-induced senescence. This indicates that NanoPCL-M may aid in preserving SSC characteristics and collagen supplies, potentially supporting a youthful appearance of the skin.

Electrospun polymers have revolutionized “on-tissue” and post-surgical healing processes by using functionalized dead space fillers. These fillers are meticulously engineered to fill the voids left behind after surgical procedures, such as tumor removals, to prevent fluid accumulation and infection. These fillers promote a safe and effective healing environment by ingeniously incorporating antimicrobial agents and growth factors. The remarkable customizability of electrospun polymers enables the development of fillers that not only conform to the physical space but also release therapeutic agents in a controlled manner. This controlled release enhances tissue regeneration and integration, ultimately promoting a successful healing outcome.

Moreover, modern materials provide novel functions and tools in already established areas, which is obvious in material science and implant compositions. Nanofibers, particularly fractionalized chitosan nanofibers, show promise in accelerating the healing of intestinal anastomoses. These nanofibers stimulate collagen production, increasing mechanical strength and improving tissue formation compared to nanofiber membranes. A composite scaffold of polypropylene mesh and poly-ε-caprolactone (PCL) nanofibers was tested in a minipig model for incisional hernia repair. While the nanofibers promoted tissue overgrowth and improved scar flexibility, the composite scaffold showed reduced resistance to distracting forces. The study suggests PCL nanofibers alone could be viable for hernia repair.

2. OBJECTIVES

The primary objective of this thesis is to explore and develop innovative strategies for bionanosensors targeted at early-stage detection. Additionally, it focuses on the development of nanotheragnostics—a field that combines diagnostics with targeted therapies. This research aims to leverage nanotechnology and biomarkers to create advanced molecular diagnostic tools while improving drug delivery mechanisms in personalized medicine.

The specific objectives of this thesis are as follows:

a. **Development of specifically functionalized Nanofiber-Based Bionanosensors for Detection of Biomarkers**: The aim is to design nanofiber membranes that function as ultrasensitive bionanosensors.

b. **Development of Electrospun Nanomaterials–Based Drug Delivery Systems**. The aim is to create and optimize electrospun nanoparticles to facilitate drug delivery.

d. **Improvement of Technological Transfer**: novel applications of nanomaterials for personalized, regenerative medicine and theragnostics.

d. **Exploration of Biomarkers for early-stage diagnosing applications:** This component will include a comprehensive literature review on recent advancements in biomarkers and bionanosensors and their therapeutic applications in modern medicine. It will also address current challenges in early diagnosis and explore the role of nanotechnology in improving molecular diagnostics and drug delivery systems, focusing on clinical applications for degenerative diseases and cancer.

3. MATERIALS AND METHODS

The thesis is prepared in extenso, grounded on the results of seven original scientific papers, accompanied by three comprehensive review articles, and supported by findings presented in four international conference contributions. It provides a thorough analysis of the fundamental methodologies utilized in these research activities.

- This section systematically consolidates and delineates the experimental frameworks, fabrication techniques—including electrospinning methods and their characterization, and biological evaluation processes employed throughout the studies.
- This structured approach enhances accessibility and clarity, delivering a cohesive overview of the research methodology. Furthermore, it aids navigation while emphasizing the technical consistency and innovative strategies implemented during various phases of material synthesis, functionalization, and application testing.
- Additional details regarding the methodology can be found in the attached manuscripts.

3.4. For Biosensing applications

3.4.1. For Bacteria trapping

The polyacrylonitrile (PAN) nanofibers of different area densities were obtained from Nanoprogress, s.r.o (Pardubice, Czech Republic), and visualized by scanning electron microscopy (SEM) Vega3 SB TESCAN a.s. (Brno, Czech Republic). Before sample visualization, samples were sputtered (Sputter Coater Q150R, Quorum Technologies Ltd, Lewes, UK) by a conductive 10 ± 2 nm layer of golden nanoparticles to prevent the samples' charging during SEM visualization. Images were analyzed by ImageJ software (NIH, Bethesda, USA) from five different areas of each sample.

Nanofiber diameter distribution was automatically generated by the software OriginPro based on manual measurement performed at SEM images with use of ImageJ software. Measurements of nanofiber diameter were performed at five different SEM images from different areas of PAN nanofiber sample. Analyzed SEM images were created at a working distance of 8 mm and a view field 92,3 μm.

Surface zeta potential was measured on PAN nanofiber samples by Zetasizer nano ZS (Malvern Panalytical Ltd, Malvern, UK) with use of Universal Dip cell (ZEN1002) accessories to measure surface zeta potential at five different distances from the PAN nanofiber sample surface. Final surface zeta potential was evaluated automatically by Malvern software using linear regression to calculate the final surface zeta potential at the distance 625 μm from the PAN nanofiber sample surface.

3.4.1.1. Visualization of Nanofibers and Diameter Determination

Scanning electron microscopy (SEM) was used to visualize the structure of the PAN nanofiber membrane for filtration experiments, utilizing the Vega3 SB SEM (TESCAN a.s. Brno, Czech Republic). Before visualization, samples were coated with a conductive 10 ± 2 nm layer of gold nanoparticles to prevent charging during SEM analysis, using Sputter Coater Q150R (Quorum Technologies Ltd, Lewes, UK). Images were analyzed with ImageJ software (NIH, Bethesda, USA) across five different areas of each sample. Nanofiber diameter distribution was automatically generated by OriginPro software based on manual measurements from SEM images using ImageJ software(Schneider, Rasband & Eliceiri, 2012).("Origin, OriginLab Corporation" 2003) Measurements were performed on five different SEM images from distinct areas of the PAN nanofiber sample. Imaging was performed with a VEGA 3 SBU electron microscope (Tescan, Brno, Czech Republic) at magnifications ranging from 500× to 5000×. A secondary electron (SE) detector and an accelerating voltage of 10 kV were employed to capture detailed surface morphology.

Multiple SEM images were captured at different magnifications to ensure a statistically significant dataset for diameter estimation. The software's measurement tools were employed to assess fiber uniformity, distribution, and potential variations in thickness. To enhance accuracy, at least 100 individual fibers were measured across multiple regions of the samples, minimizing localized deviations and providing a more representative average diameter value.

This approach enables a comprehensive assessment of nanofiber morphology, which is crucial for optimizing the electrospinning process and tailoring fiber properties for specific applications, such as biomedical scaffolds, filtration membranes, and biosensing platforms.

3.4.2. Evaluation of surface modification and used chemicals

All chemicals and reagents used in the experiments were of analytical grade, ensuring precision and accuracy in the results. The study was designed to implement methods that could be quickly deployed and scaled up for future use, aligning with the goal of developing practical diagnostic tools for clinical or research settings.

The reagents utilized in this study include biotin (B4501, Sigma-Aldrich, CAS: 58-85-5) and biotin-fluorescein (Pierce™ Biotin-Fluorescein Conjugate, Thermo Scientific™, CAS: 2420-94-2). Both are commonly employed in biological applications for fluorescence-based detection methodologies. Additionally, phosphate-buffered saline (PBS) with Tween, a widely used buffer system incorporating a surfactant, was incorporated. This combination proves highly effective in sample washing and dilution, minimizing non-specific binding, thereby enhancing the accuracy and sensitivity of the detection method. In this study, MilliQ water was employed for the preparation of all aqueous solutions, ensuring a high level of purity and reliability (Milli-Q® IQ 7005 Water Purification System, Millipore, Billerica, MA, USA). All chemicals and reagents utilized in the experiments were of analytical grade, ensuring precision and accuracy in the obtained results. The study was meticulously designed to facilitate the rapid deployment and scalability of methods for future utilization, in accordance with the objective of developing practical diagnostic tools for clinical or research settings. The selection of methods was guided by the behavior of the analyte or detection substances, aiming for optimal interaction and binding with sensor materials. By prioritizing scalable and straightforward methods, and employing high-grade reagents and PBS with Tween, the study was conducted.

3.4.3. Cultivation of Escherichia coli

The Gram-negative bacteria *Escherichia coli* was used as a model organism for the detection. The reference bacterial strains were provided from the bacterial collection of the University of Chemistry and Technology, Prague. The cultivation of bacterial colonies was performed on an agar medium. Chemicals used to prepare the agar medium (NaCl, peptone, agar, and yeast extract) were obtained from Sigma Aldrich (St. Louis, USA).

3.4.4. Measurement of optical density and data evaluation

The measurement itself was carried out deploying standard filtration technique, with the detection of passed bacteria *Escherichia coli* by measuring O.D. at 600 nm nm (Mandelstam et al. 1982). The data were processed using the log-linear regression, implemented in the open-source statistical software R (R Core Team, Vienna, Austria).

3.4.5. For biosensing of biomarkers

The methodology for preparing polyacrylonitrile (PAN) nanofibers began with selecting the PAN polymer for its excellent flexibility, water insolubility, reproducibility in production, and electrospinning into nanofiber mesh. PAN was sourced from ProNanoTech, s.r.o (Czech Republic). Post-production handling, including the surface modification—reduction, aimed to obtain suitable functional groups (−NH), which act as chemical bonds. The nanomaterial functionalization, avidin-linking processing, was held by EBAS Nano s.r.o. (Czech Republic), the design of material function is represented in Figure 1.

Figure 1: Schematic design of the functionalized material.

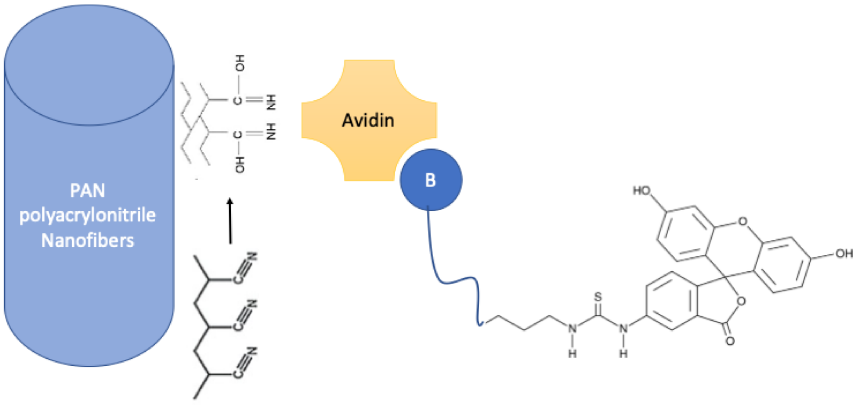

PAN nanofiber surface was chemically modified, typically with amino groups, before membrane functionalization with an avidin linker. This functionalized nanofiber membrane is ready for a highly specific binding of fluorescently labeled biotin.

Filtration setup

A filtration setup was designed for PAN nanofiber-based membranes using 3D-printed custom-printed holders. The holders were specifically tailored to fit plastic tubes to hold membranes at the same distance and let all volumes of the analyzed solution pass the membrane. The membranes were positioned securely within the holders and integrated into the plastic tubes. These tubes were connected to a collector for analyte collection.

Figure 2: Filtration setup.

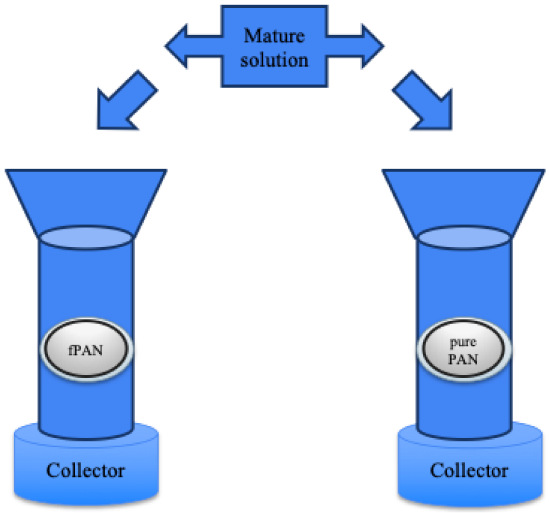

Specific binding has been determined as a difference between binding on functionalized (fPAN) and non-functionalized (pure PAN) membranes.

The solution containing the model biomarker(biotin-FITC) passed through the membrane under the influence of gravity alone without applying any external force. The same setup was used for testing both unmodified and functionalized membranes(fPAN). The stock solution was analyzed both before filtration and immediately after passing through each membrane type to evaluate retention and functionality. This approach was also applied to multi-step filtration tests to assess the effectiveness of washing out non-specific binding. These tests helped ensure the reliability and specificity of the functionalized membranes in detecting biomarkers at low concentrations.

Fluorescence Detection

The Fluoromax4 HJY spectrometer measured the fluorescence intensity (IF(λ)) of the samples. with excitation and emission slits set to 2 nm. The system set the excitation wavelength to 490 nm and recorded emission over a wavelength range of 505 nm to 600 nm. Each measurement took approx. 40 seconds, and the procedure measured each sample three times to obtain a mean fluorescence intensity value (IFm(λ)). The same procedure measured the fluorescence intensity of the buffer (IFb(λ)).

The software exported the collected data during the measurements. The calculation corrected the fluorescence intensities for both the sample (IFs(λ)) and the buffer (IFb(λ)) using the equation:

$$IF(\lambda)cor = IF(\lambda) * Q(\lambda)$$

, where Q(λ) represents the detector's quantum sensitivity at the respective wavelength. The analysis subtracted the mature solution background and device calibration from the results

for both pure PAN membranes and functionalized fPAN membranes to evaluate their binding properties and sensor functionality.

To calculate the final corrected fluorescence intensity for the sample (IFs(λ)), the formula subtracted the buffer fluorescence intensity (IFb(λ)) from the mean sample fluorescence intensity (IFm(λ)) and multiplied the result by the detector's quantum sensitivity: $IFs(\lambda) = [IFm(\lambda) - IFb(\lambda)] * Q(\lambda)$.

The processing software generated the fluorescence data, including graphs and illustrations, using OriginPro software.("Origin" 2003). The Bezier smoothing method in Gnuplot 5.4 displayed and compared fluorescence intensity maximums. ("Gnuplot: An Interactive Plotting Program")

3.5.Drug. Delivery applications

3.5.1. Production of nanomaterials for Drug Delivery applications

Nanofibers were prepared by the electrospinning method. Poly (vinyl alcohol) (PVA) (5 and 40 KDa, 90% hydrolyzed, Merck) was dissolved in distilled water under 70°C. 10% w/w aqueous solution of PVA was used for electrospinning with the addition of phosphoric acid to lower pH and glyoxal as a PVA crosslinker. Electrospinning was performed by a spinner (NanoSpider, Elmarco) with a wire electrode, a wire collector covered with polypropylene nonwoven textile, and an electrical field intensity of 25 kV/cm. The PVA nanofibers were crosslinked by glyoxal 72 hours at temperature 60°C to prevent the dissolution of nanofibers in a wet environment.

Polycaprolactone (PCL) nanofibers were also prepared by electrospinning using a Nanospider Elmarco NS 500 spinner. Polycaprolactone (Mn 45,000, Aldrich) was dissolved in chloroform at 23 ° C. A 24% w / w solution was used for spinning. The fibers adhered to the nonwoven fabric throughout the spinning process.

3.5.2. Fractionalization of nanofibers

PVA and PCL fibers were ground into small pieces with scissors. They were then divided into two parts. Each working cycle included 10 grinding (1 min) and re-cooling periods (1 min). The applied impact frequency was 10 Hz. Nanofibers were ground in liquid nitrogen using a cryogenic grinder (Freezer/Mill 6870, SPEX SamplePrep) with small vials.

3.5.3. Visualization of nanofibers and diameter determination

Nanofibers Morphology of PCL and PVA nanofibers as well fractionalized fractions were examined by electron microscopy. First, samples were sputtered with a thin gold layer

by a rotatory pumped coater (Q 150R S, Quorum). Magnification of the electron microscope (VEGA 3 SBU, Tescan) varied from 500x to 2000x, and a secondary electron (SE) detector at an accelerating voltage of 10 kV was used. Second, the average fiber diameter was measured for 50 randomly selected fibers using Tescan software.

3.5.4. Gel preparation and its functionalization

The gels were prepared from the tone of the following ingridients: Agar-Agar (powder BioScence – Grade, ROTH), Standard agarose (powder, ROTH).

The mixture was put into the heating nest (Heating Nest LTHS for 1 000 mL), which was heated to 150 degrees, and the gels were taken out when boiling. The gels were then poured into plastic Petri dishes about average 3,5 cm, slowly cool down to the laboratory temperature in a humid atmosphere, and placed into 5 ° C.

Agar and agarose concentrations were selected based on the standard concentration for agar and agarose medium preparation. Other agarose concentrations (1% and 3%) were also generated to the initial desired concentration (1.5%).

Agarose (0.15 g + PCL 0.15 g) / 10 ml distilled water, (0.15 g + PCL 0.015 g) / 10 ml distilled water and Agarose (0.15 g + PVA 0.15 g) / 10 ml distilled water, (0.15 g + PVA 0.015 g) / 10 ml distilled water - agarose gel was done in the same way as above. The only difference was in addition (0.15 g of fibers per 10 ml of gel) of fibers, which were added to the gel after cooling to approximately 60 ° C. The reason for the reduced temperature is that the nanofibers were not damaged at this temperature rate and fulfilled their function.

3.5.5. Determination of Young's modulus

Young's modulus of elasticity has been determined on Vertical Thermomechanical Analyzer TMA PT600. The relative deformation $\varepsilon = \Delta l/l$ of the tested material exposed to compression 50 mN/ 12,56 mm2 has been detected, and Young's modulus of elasticity has been calculated as:

$$E = \frac{F/S}{\Delta l/l} = \frac{Fl}{S\Delta l}$$

E - Young's modulus, pressure units,

F - is the standard component of the force,

S - is the surface area over which the action of the force is distributed,

l - is the length of the deformable bar,

Δ l (Delta l) - change in the length of the bar as a result of elastic deformation.

Ɛ - relative deformation

These values of Young's modulus of elasticity can be considered approximate since the thickness of the gel (approximately 0.004m) changes over time, and this value was recalculated from the initial measurement parameters and the measured delta l, points were selected in the 1st minute of measurement when the sample was exposed to the initial force of 0,05N. The pressure area in the material was 0.00001256 m2.

3.5.6. Degradation of PVA nanofibers

Polyvinyl alcohol (PVA) nanofibers were produced from a 10% PVA stock polyvinyl alcohol solution. For fluorescent labeling, solution of polyvinyl alcohol 40-88 and 5-88 (Merck) at 1: 1 v/v ratio, was mixed with 0.042% Fluorescein Isothiocyanate-Dextran (Sigma-Aldrich) (FSC). Non-crosslinked nanofibers were prepared by electrospinning from a stock solution without any further treatment. Crosslinked nanofibers were prepared from the stock solution mixed with 0.6% H_3PO_4 and 0.4% Glyoxal (Sigma-Aldrich) and crosslinking was induced by 82 h incubation at 60 ° C and 15% relative humidity. Nanofiber degradation was observed by disolving of fluorescent labeled nanofiber scaffold in 0,9 % NaCl aqueous solution. Six identical fluorescent labeled samples of weight of 0,280 g ± 0,003 g were put into glass bottles with 177 ml of 0,9 % NaCl aqueous solution. The bottles with samples were located in to the shaking incubator with shaking frequency 60 Hz and temperature 37 °C. The aqueous solution samples of 100 µl from each glass bottle were taken in defined time intervals and analysed by SYNERGY H1 (BioTeK) on emission frequency 520 nm and with excitation with 490 nm. Degradation of the functionalized PVA loaded with FSC was statistically evaluated according to calibration curve prepared by dissolving of 0,007 g, 0,014g, 0,028 g, 0,056 g, 0,084 g, 0,112 g, 0,14 g, 0,0168 g, 0,196 g, 0,224 g, 0,252 g, 0,28 g of noncrosslinked fluorescent labeled samples loaded in 177 ml of 0,9 % NaCl aqueous solution.

3.5.6.1.Colonization by eukaryotic cells

Colonization of gels by eukaryotic cells were performed as in vitro experiments on immortalized BALB/3T3 mouse fibroblasts cell line obtained from the American Type Culture Collection (ATCC, USA). Mouse embryo fibroblast BALB/3T3 clone A31 cells (ATCC CCL-163) were cultured as adherent monolayers in plastic Petri dishes Nunc™ (Fisher Scientific) in Dulbecco's modified eagle medium (4 mM L-glutamine, 4500 mg/L glucose, 1 mM sodium pyruvate, and 1500 mg/L sodium bicarbonate, Sigma-Aldrich) supplemented with 10 % (v/v) fetal bovine serum (Sigma-Aldrich) and antibiotic-antimycotic solution (Sigma-Aldrich).

Cell concentrations were determined by microscopy using a Burker chamber. On the 1st, 3rd and 7th day of the experiment samples were visualized using phase contrast microscopy (Optika). Cells were seeded in Petri dish with gel at a density of 3,000 cells/cm2. The cells were cultivated under normal cell culture conditions (37 °C; 5% CO2; 95% humidity). After 72 hours of cultivation, cells on gels were stained by The LIVE/DEAD® Viability/Cytotoxicity Kit (L3224, Thermo Fisher] following protocol [Cell Viability Assays for Neural Stem Cells | Thermo Fisher Scientific - CZ] and analyzed under a fluorescence microscope (Olympus).

3.5.6.2.Cell proliferation analysis

The MTS test was used to evaluate influence of gels on cells proliferation. 2 mL of growth media (DMEM with FBS and ATB) was incubated 48 hours on tested gels. 3T3 cells were seeded in 96-well culture plates at a density of 3,000 cells/cm2. To each well 20 µL of MTS substrate (Promega) and 100 µl of growth media was added. The cells were cultivated for 1 hour under normal cell culture conditions (37 °C; 5% CO2; 95% humidity). Then absorbance was spectrophotometrically measured (100 µl of product media at wavelength 490 nm), reference wavelength 690 nm. Cells cultivated in a culture medium without incubation on gels were used as a negative control. Proliferation was measured on the 1st, 3rd and 7th day of the experiment.

3.5.6.3.Testing invasion by prokaryotic cells

Bacillus subtilis microbiological cultures were inoculated into 50 mL of liquid culture medium (10 g yeast extract, 10 g peptone, 5 g NaCl per 1 L dH2O) in Erlenmayer flask and placed overnight on a shaker (18 hours, 80 RPM, 30°C). The grown culture were diluted to concentrations of 10-9 and 20 µL was inoculated on sterile Petri dish with gels with nanofibres. The samples were cultivated for 24 hours in an incubator (30°C,90% humidity) and then subtracted by the number of colonies.

3.6.Nanofiber production and functionalization for theragnostics

Povidone-iodine (1-ethenyl-2-pyrrolidone, BETADINE) has been used for functionalization of Poly(vinyl alcohol) (PVA) nanofibers (Fig. 1).

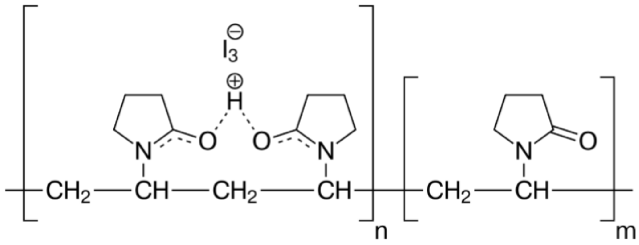

Figure 1. Structure of Povidone-iodine

PVA 5-88 (MERCK) and PVA 40-88 (MERCK) in ration 1:1 was dissolved in 10 % povidone-iodine solution to create 6.2 % PVA spinning solution with povidone-iodine. Final iodine concentration in nanofibers was 10 mg/mL. Dissolving of PVA in povidone-iodine was provided during continual stirring and heating of the solution to 60° C. PVA functionalized nanofiber scaffold was prepared by AC electrospinning method by supplying voltage of 40 kV to spinning electrode. Grammage of the prepared PVA functionalized scaffold was 1 g/m^2.

3.6.1. Nanofiber Visualization.

Functionalized nanofiber scaffold visualization was provided by scanning electron microscope (SEM) Vega3 SB (TESCAN a.s.). To remove electric charge induced in the scaffold during the scaffold imaging, the nanofiber scaffold was coated by golden conductive layer sputtered by coater Q150R (Quorum) in thickness of 8-12 nm.

Degradation of the functionalized nanofiber scaffold during wearing of the face mask with the functionalized nanofiber scaffold membrane was visualized by SEM images.

3.6.2. Determination of Nanofiber Degradation.

Nanofiber degradation was observed in distilled water, by releasing of Fluorescein Isothiocyanate-Dextran (Sigma-Aldrich) (FSC) from the scaffold into distilled water. For the degradation observation were created samples according to method described in Nanofiber production and functionalization, wherein into PVA spinning solution was added 0.042 % FSCfluorescent dye.

Six identical functionalized PVA samples loaded with FSC of weight of 0.280 g ± 0.003 g were put into glass bottles with 177 ml of distilled water. The bottles with samples were located into the shaking incubator with shaking frequency 60 Hz and temperature 37° C. The water samples of 100 µl from each glass bottle were taken in defined time intervals and analyzed by SYNERGY H1 (BioTeK) on emission frequency 520 nm and with excitation with 490 nm. Degradation of the functionalized PVA loaded with FSC was

statistically evaluated according to calibration curve prepared by dissolving of 0.007 g, 0.014g, 0,028 g, 0.056 g, 0.084 g, 0.112 g, 0.14 g, 0.0168 g, 0.196 g, 0.224 g, 0.252 g, 0.28 g of fun1ctionalized PVA samples loaded with FSC in 177 ml of distilled water.

3.6.3. Clinical trial and Statistics.

207 adults (40.6 ± 9.7 years old) indicated as SARS-CoV-2 positive by PCR method have been involved into the clinical observation trial in April and May 2021. All subjects have agreed with participation in the study including all conditions. The participants applied an active nanofiber membrane with incorporated povidone-iodine into their regular face mask and breathed over the active filter active filter from four to eight hours daily for from one to four days, starting immediately after their positive PCR test. The participants have answered questionnaires with 11 questions (see the Appendix 1) three weeks after their positive PCR test. The data have been analysed and compared with the ÚZIS data (IHIS CR - Institute of Health Information and Statistics of the Czech Republic) as a reference group. Instead of reference group we used the above-mentioned state collected epidemiological data, following the "WMA Declaration of Helsinki – Ethical Principles for Medical Research Involving Human Subjects – 2013" . For statistical analyses the R program with package survey was use. The results were stratified using the age structure of the county.

4. RESULTS

Main achieved goals of the thesis

1. **Specifically Functionalized membranes have been proven for the specific detection of bacteria**
    a. Functionalized nanofiber membranes were successfully designed and validated for the specific detection of bacteria.
2. **Specifically Functionalized membranes are effective for the detection of picomolar concentrations in model fluids:**
    a. Fluorescent Bionanosensor has been tested for Picomolar detection of Biomarkers in fluids
    b. Electrical and Optical methods of memembrane evaluation were represented in the study entitled - Nanotechnology for distance diagnostics.
    c. Ability of sensitive sample collection described in paper - Contactless collection of impurities on ultrasensitive nanofiber membrane
3. **Functioned filters for theragnostic (prophylactic and treatment application)**
    a. Test of protective membranes represented in work: Povidone-iodine functionalized nanofibers are prophylactic and protect against the dissemination of SARS-CoV-2 infection.
4. **Functionalized gels and nano-membranes for induction of chemotaxis and support of cell proliferation**

A gel-based drug delivery system was developed in the framework of the study: Low Concentrated Fractionalized Nanofibers as Suitable Fillers for Optimization of Structural-Functional Parameters of Dead Space Gel Implants after Rectal Extirpation.

Skin cover applications and regenerative uses were described in manuskripts:

a. Hydrolat of Helichrysum italicum promotes tissue regeneration during wound healing.,
b. Nanofibers Encapsulated with Natural Products: A Novel Strategy to Counteract Skin Aging.
c. Effects of nanofibers and essential oil in maintaining skin integrity, cell elasticity, and proliferation

4.1. Specifically Functionalized membranes have been proven for the specific detection of bacteria

4.1.1. *Bacteria trapping effectivity on nanofibre membrane in liquids is exponentially dependent on the surface density*

Protection against water- and air-borne bacteria as well as their detection at very low levels is a big challenge for the health care profession. The study's main goal was to prepare bacterial filters with a tunable trapping effectivity. We revealed that the trapping efficiency of Escherichia coli estimated from the optical density of bacteria passed through the filter exponentially depended on the surface density of the polyacrylonitrile nanofibre membranes. This log/linear regression profile was proven for bacterial trapping efficiency higher than 99.9% which opens a door for easy and tunable constructions of ultrasensitive filters and/or nanosensors as well as for the standardization and quality control of nanofibre membranes.

Preparation of nanofiber sensor

Nanofibers have been prepared from water insoluble polymer since the nanofiber filter application is intended for liquids and humid air. PAN polymer was selected after several preliminary experiments since the PAN nanofibers were characterized with a very good flexibility, water insolubility and production reproducibility. Scanning electron microscopy (SEM) was employed to visualize the structure of PAN nanofiber membrane used for filtration experiments. The samples examined exhibited randomly oriented fibers with submicrometer diameters, and the nanofiber membranes displayed no significant structural defects (Figure 1A). Naturally, variations in surface density were found to influence pore size.

Fig. 1A: The SEM image of PAN nanofiber.

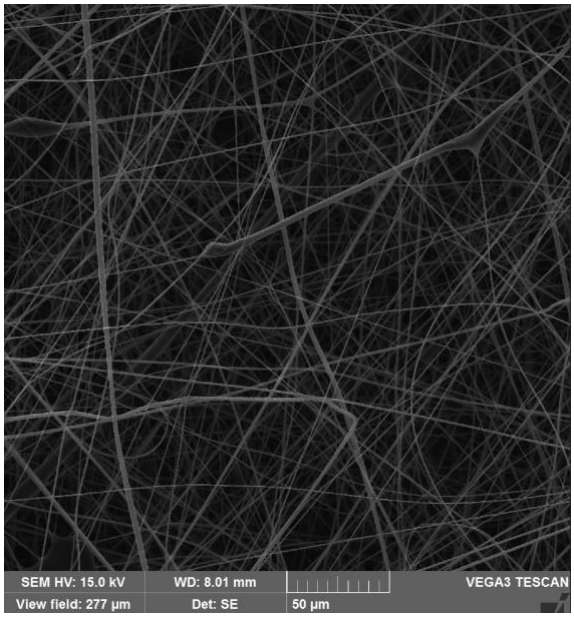

The SEM image (with a scale bar) of PAN nanofiber membrane with a density of 2.68 g/m^2.

Subsequently, the diameter distribution of the nanofibers was quantified from the SEM images according to the technique described Method and visualized in Fig. 2. The data indicated that the diameter of more than 95% of polyacrylonitrile (PAN) fibers was less than 500 nm. Since the number of fibers with a respective diameter range was obtained by a simple counting of these fibers in the SEM picture, we have omitted error bars similarly as in our previous publications. Notably, 58% of fibers fell within the 200 nm to 400 nm range (Figure 2A).

Fig. 2A: PAN nanofiber diameter distribution.

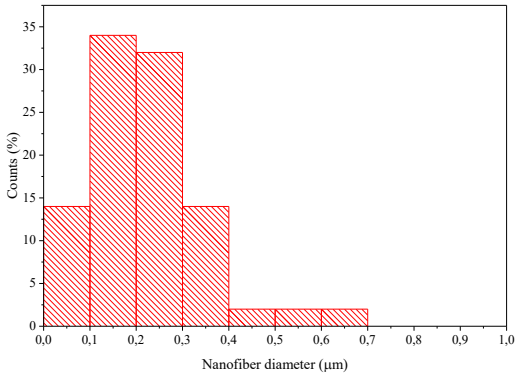

PAN nanofiber diameter distribution was obtained from the SEM picture by the computer analysis as described in Methods.

The nanofiber membrane was further characterized for its surface properties. Clearly, the development of a net surface charge affects the distribution of ions in the surrounding

interfacial region, resulting in an increased concentration of counter ions (ions of opposite charge to that of the particle) close to the surface. The liquid layer surrounding the particle exists in two parts; an inner region called the Stern layer, where the ions are firmly bound, and an outer, diffuse area where they are less firmly attached. There is a notional boundary inside within the diffuse layer, there which the ions and particles form a stable entity. When a particle moves (e.g. due to an electric field or gravity), ions within the boundary move with it, but any ions beyond the boundary do not travel with the particle. The respective potential is called a zeta potential and indicates the amount of charged particles to be adhered to the nanofiber surface.

Fig. 3A: Surface zeta potential of PAN nanofibers.

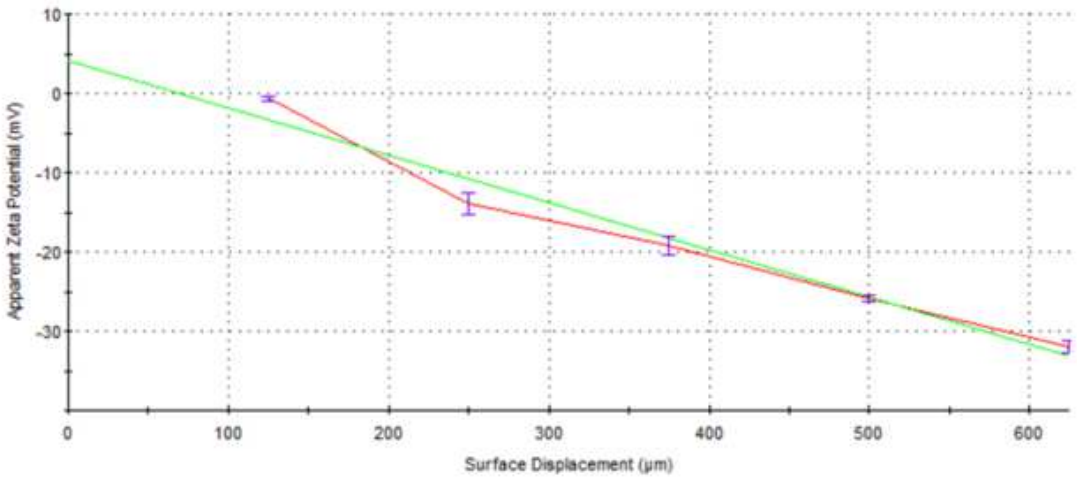

The average values and standard deviations were obtained from 15 determinations. Surface zeta potential of PAN nanofibers (-34.7 mV ± 2.8 mV).

The zeta potential of PAN nanofibers was measured as shown in Figure 3. Model particles (polystyrene latex particles) were used for determination of the affinity to the PAN nanofiber sample. Measurement of surface zeta potential with the use of model particles suggests the suitability of PAN nanofiber membrane for construction of sensors highly sensitive to bacterial contamination. The surface zeta potential of PAN nanofiber membrane at a distance 625 µm from the sample surface was measured as -34.7 mV ± 2.8 mV indicating the strong affinity of bacteria surface to PAN nanofiber membranee and its suitability for biosensor.

Our structural analysis confirms that the samples meet the established criteria for nanofibers and that the uniformity of the PAN nanofibers is sufficient for the subsequent fabrication of sensors.

Characterization of the PAN nanofiber-based sensor for Escherichia coli detection of in liquids

The experimental procedure is described in details in the Methods. Suspensions of Escherichia coli (1.12×10^9 cells/mL) were filtered through PAN nanofiber filters with varying surface densities (1.34 to 6.82 g/m^2). Each trial was replicated three times. Bacterial counts in solutions were quantified by optical density (OD) measurements at 600 nm wavelengths optimal for *E. coli* (Figure 4A). Standard errors were negligible and, thus, are not shown in the Fig. 4A.

A logarithmic decrease of OD was observed with increasing surface density of PAN nanofiber membranes, This linearity was observed for all test densities, excluding the control (0 g/m^2 surface density). This control represented the bacterial count prior to filtration. The log-linear decrease was analysed by regression methods described in the Methods section. The equation used was log(OD) = -5.93×(surface density) - 5.90

From these results, we calculated the bacterial trapping efficiency as outlined in the Methods. It was determined that a 99.9% efficiency in bacterial trapping could be achieved at a PAN nanofiber surface density of 6.46±0.14 g/m^2 for OD at 600 nm.

Figure 4A: Dependence of O.D. (600 nm) of *Escherichia coli* at the filtrate on the surface density of the nanofiber filter.

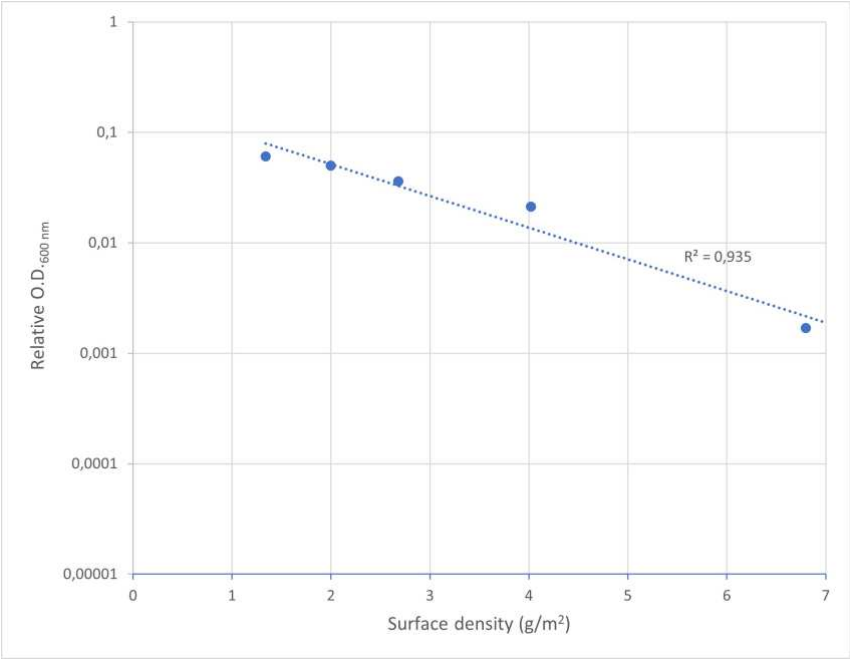

*The Y-axis is logarithmic, and the lines denote the results of log-linear regression. The Pearson regression coefficient was 0.93.*Specifically Functionalized membranes are effective for the detection of picomolar concentrations in urine.

4.1.2. Bionanosensors for Early Detection of Low-Conc. Diagnostic Biomarkers

Characterization of Fractionalized Nanofibers

Nanofibers were fabricated using electrospinning method from polyacrylonitrile (PAN). A fragment of the PAN nanofiber membrane was preserved as a reference, while the PAN nanofiber surface underwent further processing and functionalization with avidin for the sample preparation, as outlined in the Methods section. The surface morphology of both sample and reference was examined using scanning electron microscopy (Fig. 3B). Both samples exhibited a very similar submicroscopic fibrous structure indicating that the functionalization had only a negligible effect on nanofiber membrane morphology.

To quantify the morphological structure, the diameters of at least 50 individual fibers were measured from each image, and the data were analyzed to characterize the structural properties of the nanofiber mesh. The average diameter of the polyacrylonitrile (PAN) nanofibers was determined through detailed analysis of SEM images. As Fig. 4B shows, more than 95% of fiber diameter fall within at the interval between 400 nm, and 1μm combines an optimal structural characteristic for filtration with low obstacles for medical applications. Clearly, the diameter distribution provifes key information for the including of the potential biosensor among nanomaterials from a medical device perspective. Consequently, the functionalized PAN nanofiber membrane is an optimal system with a high retention due to a small nanofiber diameter with a high membrane porosity, but still sufficiently well above the diameter of 100 nm fiber size decisive for insertion of the potential biosensor among nanomaterials.

Figure 3B. Scanning electron microscopy (SEM) of polyacrylonitrile (PAN) nanofibers.

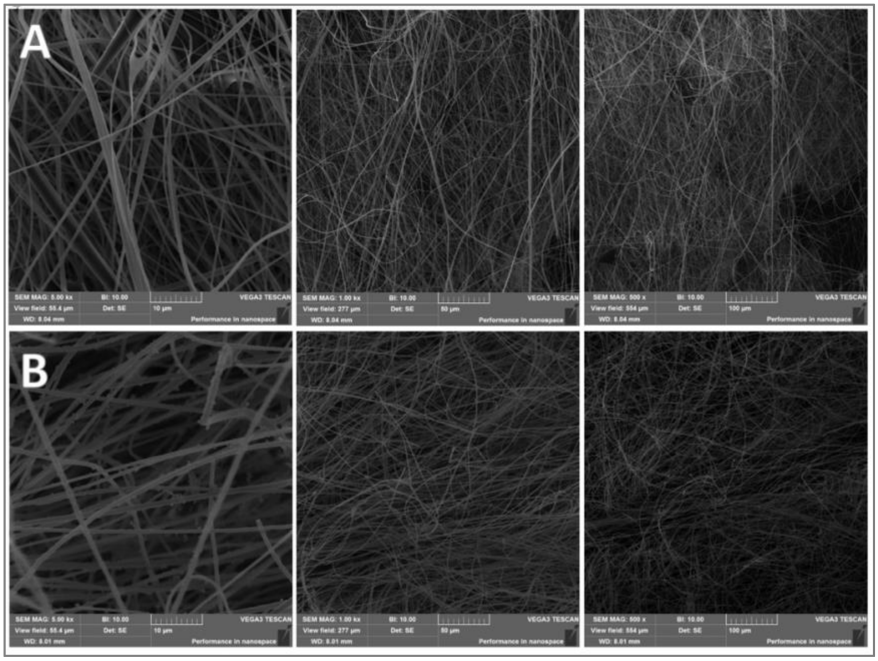

Visualization of nanofiber membranes. The diameter distribution analysis is in Fig. 4B.

A. Pure PAN (non-functionalized) on Magnification 5000×, 1000×, 500×.

B. *fPAN(functionalized) SEM on Magnification 5000×, 1000×, 500×.*

Figure 4B. The average diameter of the PAN nanofibers.

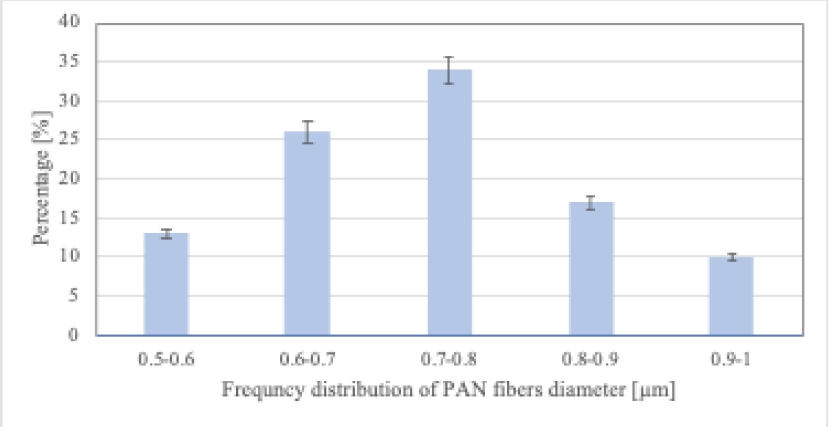

Diameter distribution analysis based on SEM pictures in Fig. 3B. Functionalization has no significant effect on diameter distribution.

The sensitivity test

Linearly dependent fluorescence intensity on concentration of fluorophores with a higher quantum yield which is well detected by most fluorometers, was reliably observed at the nanomolar concentration range. However, biomarkers in urine and other body fluids typically exist in much lower than nanomolar concentrations. . To overcome this obstacle, nanofiber filters can be used to specifically retain biomarkers and measure them at lower volumes, where they become detectable at higher concentrations. This tool helps to prepeare

a secondary (more concentrated) solution in a lower volume. Clearly, knowledge of the trustworthy concentration range for fluorescence measurement is a key step towards construction of bionanosensors and it is essential for preparation and optimization of nanofiber membrane for application in microfluidic sensors.

The sensitivity test of functionalized PAN nanofiber membrane was performed with a model fluid with a fluorescein moiety. A solution of 10μM biotin-FITC in PBS-Tween was prepared and titrated, then fluorescence intensity was measured as described in Methods. As shown in Fig. 5B, the fluorescence intensity increased linearly throughout the whole titration starting already at the lowest concentration measured (1 ng/mL). This indicates a sufficient sensitivity of the method for the determination of biomarkers of the highest interest, which is supposed to be around dozens of nanomoles and hundreds of picomoles in non-pathological states. This indicates sufficient sensitivity of the method for determination of several most important biomarkers (see below in Discussion).

The Biotin-FITC molar mass is 732.80 g/mol), thus, the concentration of 1 ng/mL corresponds to 1.4×10^{-9} M and 2.5 ng/mL to 3.41×10^{-9} M. Clearly, fluorescence intensity increased linearly with concentration within this nanomolar range, just in concentration range relevant for prostate-specific antigen (PSA) molar concentration for healthy man.

Fig. 5B. Linear dependence of fluorescent intensity on Biotin-FITC concentration

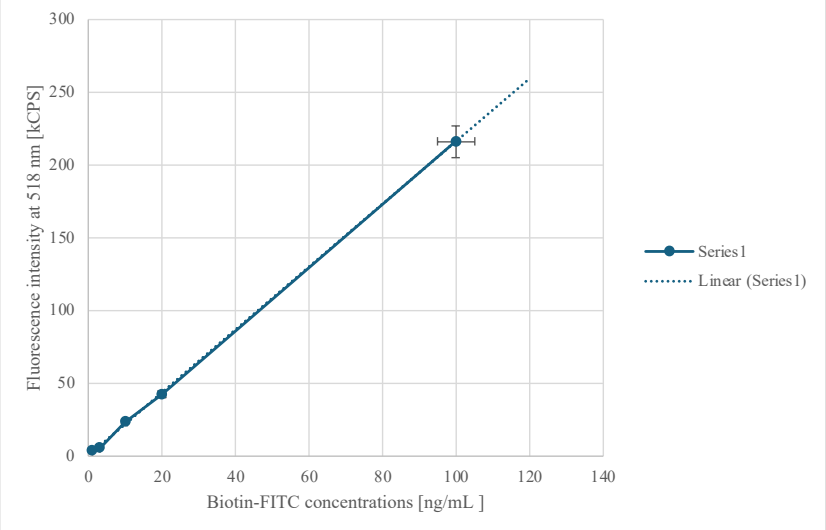

Fluorescent intensity has been measured at λ=518 nm (λ_{ex}=490 nm).

kCPS – kilo counts per second

Binding Capacity of Functionalized PAN Membranes

After proving the fluorescence detection system as sufficiently sensitive, the next step was determining and optimizing the specific binding capacity of bionanosensors, another key step toward developing nanosensors. To observe the specific binding and also a difference between the specific and non-specific binding, filtration of Biotin- FITC

throughout the PAN nanofiber membrane with and without functionalization by avidin, respectively, was performed and compared with fluorescence of the stock solution (without any filtration). The fluorescence spectra of the FITC-biotin solution were first measured before filtration (purple line in Fig.6B). This solution was was then filtered through the PAN nanofiber membrane with and without the avidin modification, respectively, and the fluorescence spectra of the filtrate were collected for both samples (green and blue lines, respectively, in Fig. 6B).

The fluorescence analysis of the functionalized PAN (fPAN) membranes revealed a maximum fluorescence intensity at around λ = 518 nm, which corresponds well with the literature values for the fluorescence of biotin and biotin-fluorescein. Naturally, fluorescence intensity decreased after filtration as a reflection of non-specific and total (specific and non-specific) binding. As Fig. 6B clearly demonstrates, there were significant differences among all three samples. For the pure PAN membranes, the absence of avidin on the membrane surface allowed only non-specific interactions, while the surface-bound avidin caused a stronger binding since beside of a non-specific binding, a significant specific binding was detected.

The results indicate that the selected membrane functionalization efficiently captured the biomarker, which proved the fPAN membranes' sufficiently high sensitivity for low-concentrated biomarkers. Notably, the surface modification by avidin was also found to be optimal for reliable resolution between specific and non-specific binding.

Fig. 6B. Fluorescence emission spectra of Biotin-FITC bound to PAN nanofibers.

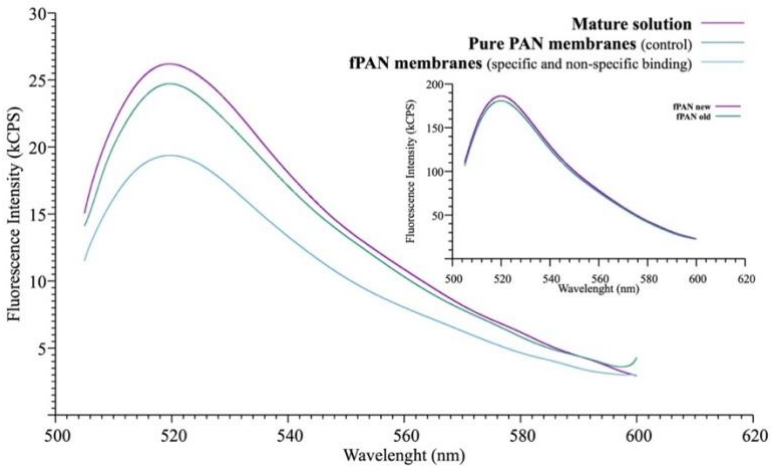

Spectra were taken after filtration through the membrane.

The green spectrum of biotin FITC represents non-specific binding, which is significantly higher than specific binding (blue line). The purple line represents a control sample that has not been filtered. Fluorescent intensity has been measured at λ=518 nm (λex=490 nm), kCPS – kilo counts per second.

The functionalized membranes were also tested on their shelf life. The fluorescence intensity was measured after three months of storage. The inset of Fig.6 clearly shows that pure PAN and fPAN membranes after filtration reveal that membrane maturation does not significantly impact the binding capacity. This indicates that once the functionalization process has been completed, the sensor maintains its high level of specificity and efficiency over at least three months. However, future studies should explore the longer-term stability of the functionalized PAN membranes to ensure their reliability in real-world applications.

To test the efficiency of filtration, multi-filtration experiments were performed to observe how many times filtration should be repeated to reach saturation with fPAN membranes.

Figure 7B. Dependence of saturation capacity on filtration sequence number

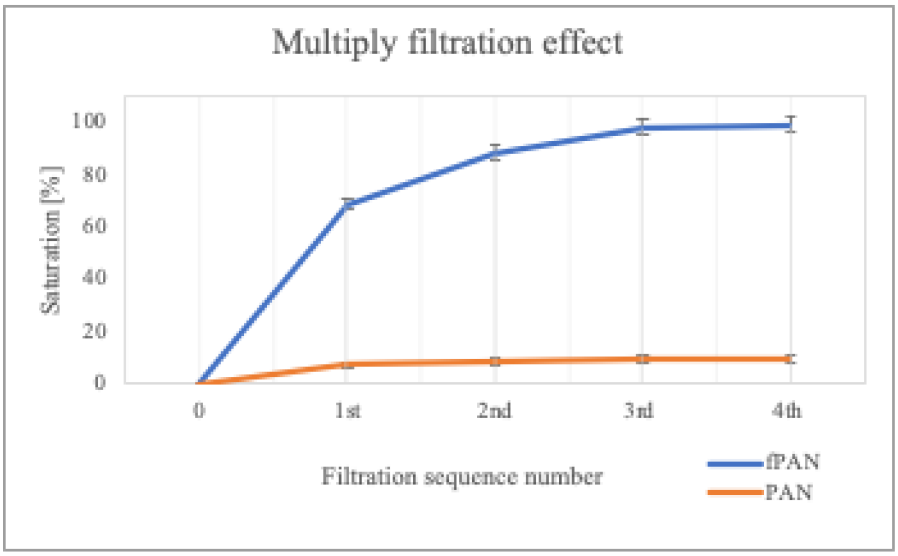

Filtration through fPAN membranes was repeated, demonstrating that more than 99% of saturation of the membrane's specific binding capacity occurred after the third re-filtration (Fig.7B). However, the results suggest that while the single re-filtration could serve for a quick orientation test, two filtrations were already sufficient for reliable results.

Our fluorescence analysis and multi-filtration experiments highlight the strong specific binding affinity of functionalized PAN membranes for biotin-fluorescein and suggest that these sensors could be promising for early disease detection and biomarker monitoring.

4.1.3. Nanotechnology for distance diagnostics.

The aim of the research was to developed membrane frames for the measurement, which hold the membrane, protect it, and help ensure good repeatability. Subsequently, the measuring test beds were adapted to this membrane attachment system, and a small ecosystem was thus created to evaluate nanomembranes.

Electrical impedance results

In the experimental setup with the horizontal bed (a), several challenges were encountered, which were systematically identified and addressed through the refinement and modification of the test bed. Despite these challenges, the impedance behavior was successfully captured and analyzed. In contrast, the liquid chamber (b) produced more reliable results. The theoretical impedance behavior of distilled water was verified, providing a crucial baseline. The "water plateau" and consistent impedance curve were successfully identified during these measurements.

horizontal bed (a)

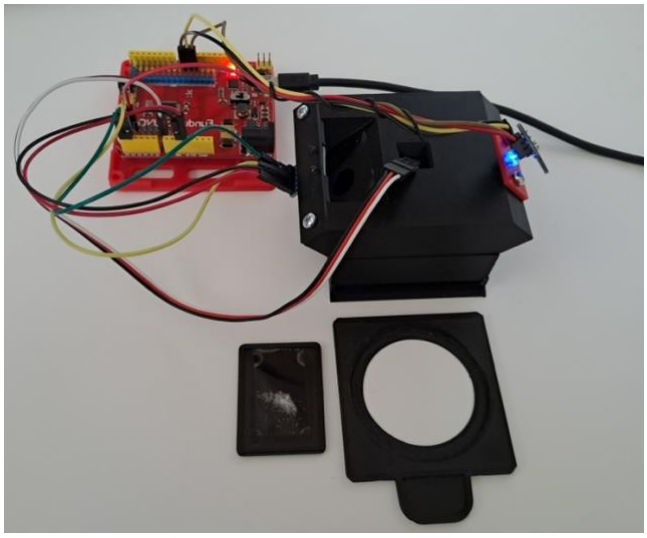

liquid chamber (b),

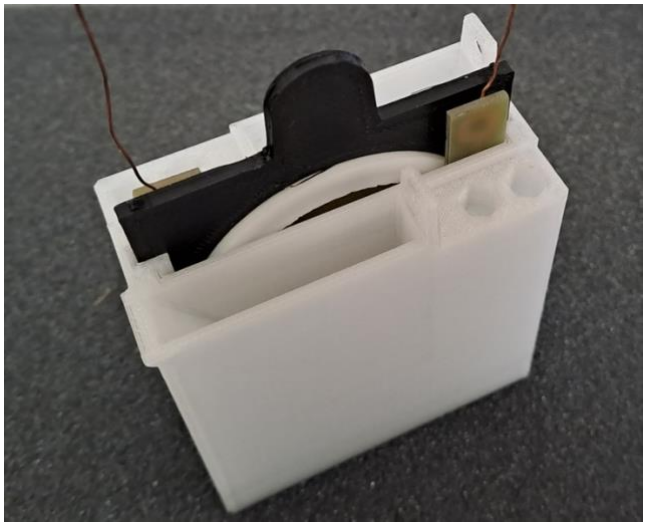

Subsequent measurements with the samples mainly exhibited a capacitive component, which further validated the system's ability to detect and measure impedance accurately. The use of a thin copper-gold (Cu+Au) electrode surface, initially expected to cause variability due to ion escape, can be improved by using a complete noble metal

electrode or a thicker layer of noble metal. This modification would likely stabilize the measurements. Further analysis, including electron microscopy, is planned to inspect the electrode surface.

Additionally, impedance data were collected for both the horizontal bed (a) and liquid chamber (b) setups. The frequency and Nyquist plots revealed different impedance models for each setup. Notably, the liquid chamber setup also exhibited characteristics of a Wartburg impedance component, which will be further analyzed in future experiments. Upcoming tests will focus on creating a more stable environment, refining the electrolyte solution, and exploring improved electrode configurations.

Optical spectral response results

Experiments were conducted in the optical chamber, beginning with a dark experiment to assess the noise level in the system. A sample-free test with excitation followed, to determine the amount of radiation entering the optical sensor. The final set of experiments involved varying concentrations (µg, mg) of luminophores and luminescent substances to monitor the sensor's response.

An additional experiment with CaF2(Eu) was performed, allowing the fluorescence to be evaluated over time. This experiment provided further insights into the behavior of the optical system and its sensitivity to changes in fluorescence. Fluorescence intensity measurements were carried out using a fluorospectrometer, with the excitation wavelength set to 491 nm and the emission wavelength set to 505 nm, using a slit size of 2 nm. The resulting fluorescence intensities are shown in **Graph 1C**, where the intensities of different concentrations of Biotin-FITC are represented.

A scattered plot in **Graph 2C** illustrates the fluorescence intensities at 518 nm, which correlate with varying concentrations of Biotin-FITC. The results were processed using second-order polynomial interpolation, yielding a curve with an excellent fit ($R^2 = 0.99$), demonstrating the reliability and accuracy of the measurements.

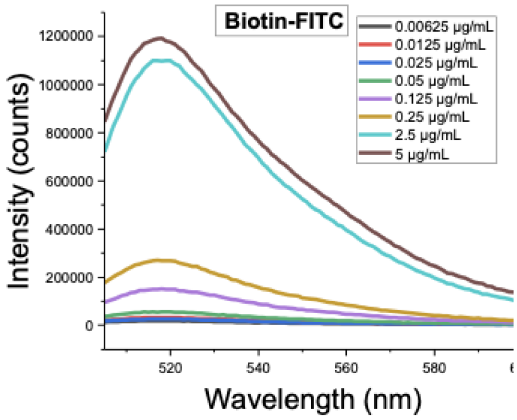

Graph 1C Fluorescent Intensities of different concentrations of Biotin-FITC.

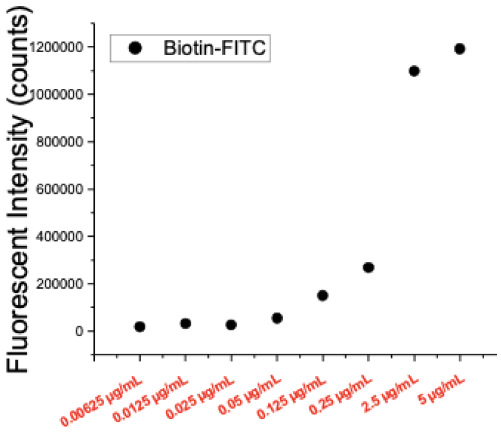

Graph 2C Scattered Plot showing the fluorescent intensities (at 518 nm) related to the different concentrations of Biotin-FITC concentrations

4.1.4. Contactless collection of impurities on ultrasensitive nanofiber membrane

Collection of microscopic particles

The main goal of the experiment was to prove that the nanofiber filter in our experimental set-up is able to collect microscopic and submicroscopic particles. Thus, to collect the particles we have used our above mentioned home-made apparatus in suckling mode, i.e. we have yielded a single tube producing negative pressure only. All the air, therefore, has been sucked for 60 sec. and filtered through the nanofiber membrane attached inside the filter holder. We have tested the nanofiber membrane ability both for microscopic and submicroscopic particles.

First, wheat flour has been chosen to test the nanofiber ability to collect the wheat flour that has been poured in the heavy textile material. Suckling has been subsequently carried out for 60 sec. and the visualization has been performed by SEM.

Collection of wheat flour

In Figure 4D (SEM image) particles are shown of wheat flour on PVA nanofiber filter after 60 sec. filtration.

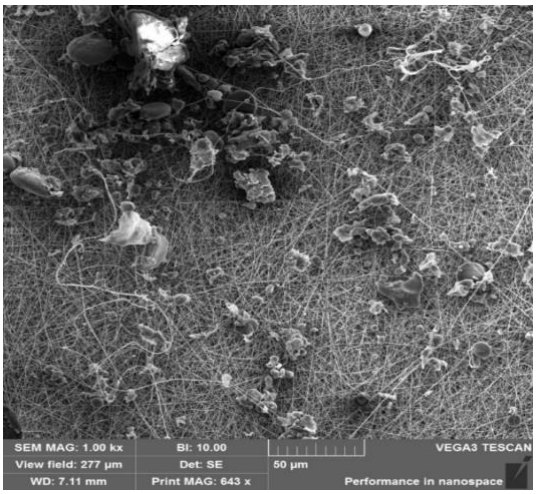

Figure 4D. Particles of wheat flour on PVA nanofiber filter after 60 sec filtration. Magnification 10.000x

Collection of air dust

The PVA nanofiber filter has been used, successively, to collect air dust as an example of smaller particles (see Figures 5D and 6D).

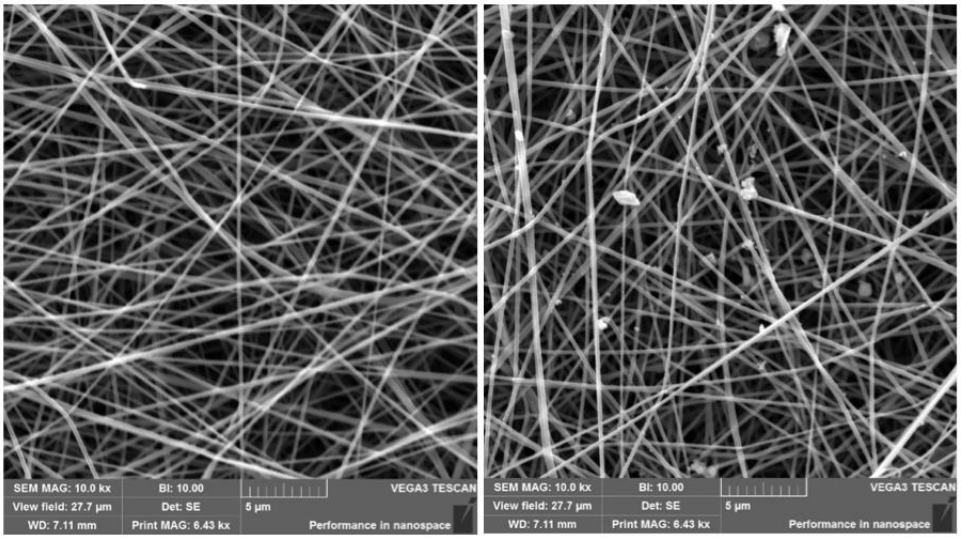

Figure 5D. PVA nanofiber filter: clean filter (left); filter after 60 sec. of filtration of laboratory air. Magnification 10.000x

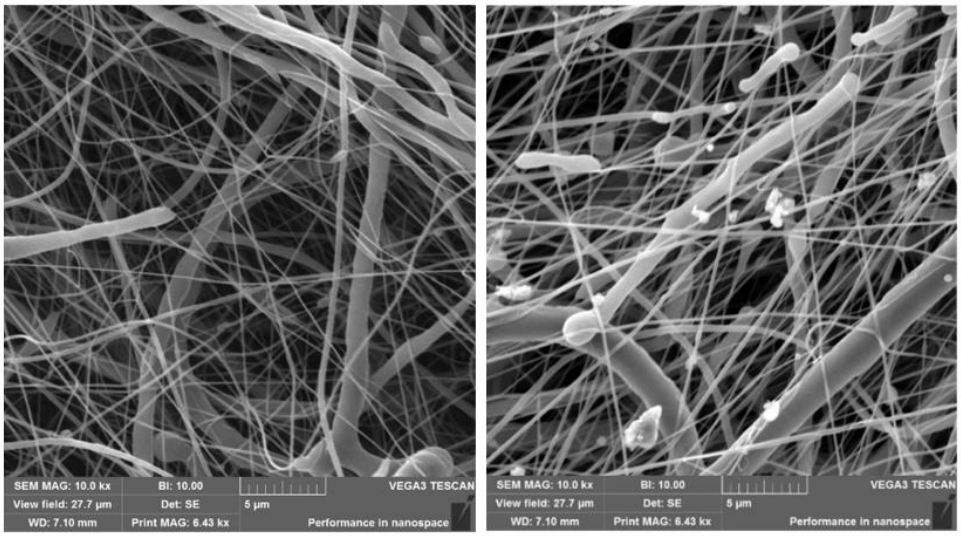

Figure 6D. PCL nanofiber filter: clean filter (left); filter after 60 sec. of filtration of laboratory air. Magnification 10.000x

Collection of bacteria Escherichia coli

We have tested the system, successively, to collect bacteria Escherichia coli. In all cases, there was absorption and capture of bacteria, which was verified by placing the filter on a solid nutrient medium, with subsequent cultivation in an incubator (24 hours, 37 °C, 5% CO_2, Humidity 90%). The bacterial strain Escherichia Coli (gram-negative rod) was selected for testing. Colony growth on filter plates was high, beyond countable range. Figure 7D shows the detected bacteria.

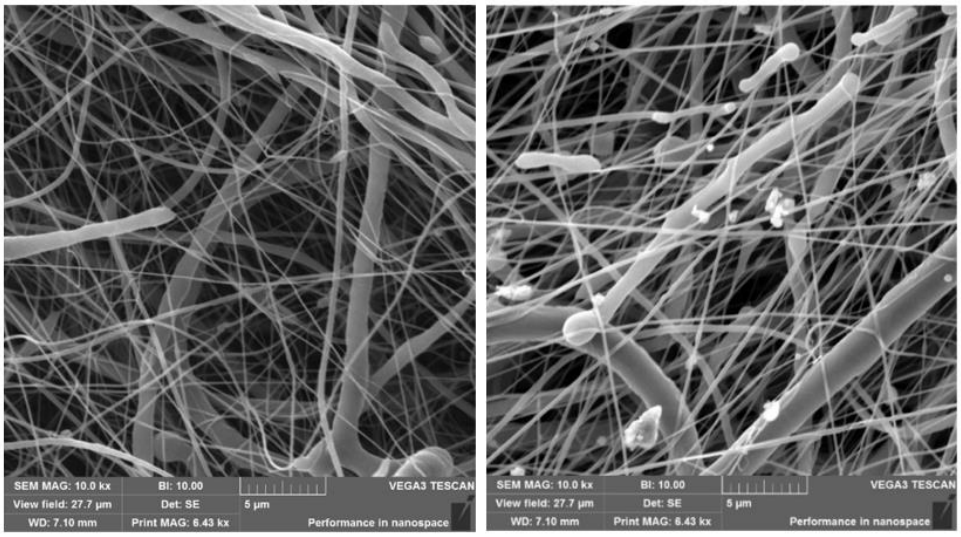

Figure 7D. Bacterial presence on the nanofiber membrane

Trapping of submicroscopic particles

To test the trapping of submicroscopic particles, cat panleukopenia viruses have been selected. In this experimental setup, just a filtration of the viral solution throughout the nanofiber membrane has been performed. A sterile glass table (2×2 cm) has been covered

with the nanofiber membrane and 105 viral particles (in 10µl suspension) have been applied. The membrane has been removed after 5 min. and the viral particles penetrated throughout the nanofiber membrane have been washed out into 10 µl sterile PBS. The virus presence in the solution has been determined by qPCR. Two types of membrane have been employed, i.e. without and with 10% povidone iodine. As Table 1D clearly shows, the concentration of penetrated viral particles has been lower than 1%. In addition, povidone iodine inactivated another ~90% of all viral particles penetrated throughout the nanofiber membrane.

Table 1D. Example of the table spread over the width of the document

Sample	Number of viral particles	Coefficient of impermeability
Control	**4,27E5**	
PVA nanomembrane	**2,95E3**	**144**
PVA nanomembrane with povidone iodine ions	**4,95E2**	**862**

4.2. Functioned filters for theragnostic (prophylactic and treatment application)

4.2.1. Povidone-iodine functionalized nanofibers are prophylactic and protect against dissemination of SARS-CoV-2 infection.

SARS-CoV-2 pandemic is a huge medical problem creating, in addition to medical complications, vast social challenges. Vaccination and/or an illness recovery are currently the most promising tools and weapons fighting spreading epidemy by generating antibodies in patients. However, an antibody level, necessary for efficient protection against illness, and half-time of their disappearance is highly volatile and unpredictable. Despite of undoubtedly overweighting positive effects of vaccination, neither vaccination nor recovery do not fully guarantees protection against illness. Application of disinfection of airways mucosa, thus, emerges as a highly desirable supplement or alternative.

Iodine is known for a long time as a bactericide substance, moreover active against viruses, yeasts, moulds, fungi, viruses, and protozoa, as well. Among disadvantages of free iodine, however, belonged namely tissue irritation of its aqueous solvents. This drawback has been overcome by discovery of povidone-iodine, a bound iodine complex, decreasing drastically a free iodine concentration. Clinical studies and already a long-lasting practice

clearly proved superiority of the povidone-iodine complex compared to all other iodine preparations with the sensitization dropping to 0.7 % only. Povidone-iodine is usually applied in 3-10 % w/w concentrations in solutions, sprays or tampons and is available without medical prescription . Free iodine from the complex is slowly released which minimize side effects. Reportedly, low povidone-iodine concentrations could be superior to more concentrated solution. Nano-structures could lead to extremely large surface compared to volume which could further contribute to increasing the effectivity of iodine molecules and, thus, decreasing of the used concentration. In addition, nanovesicles or fractionalized nanofibers have been reported as highly efficient system for influencing of not only external interactions of nanovesicles with cells but also for modification of cell functions. We can expect a similar phenomenon also for interaction of nanodroplets of povidone-iodin with viruses.

We encapsulated 10% povidone-iodine solution into nanofibers from polyvinyl alcohol (PVA) in 1:10 ratio w/w. (Fig. 2E) Consequently, the final povidone-iodine concentration in nanofiber mesh was 1% w/w.

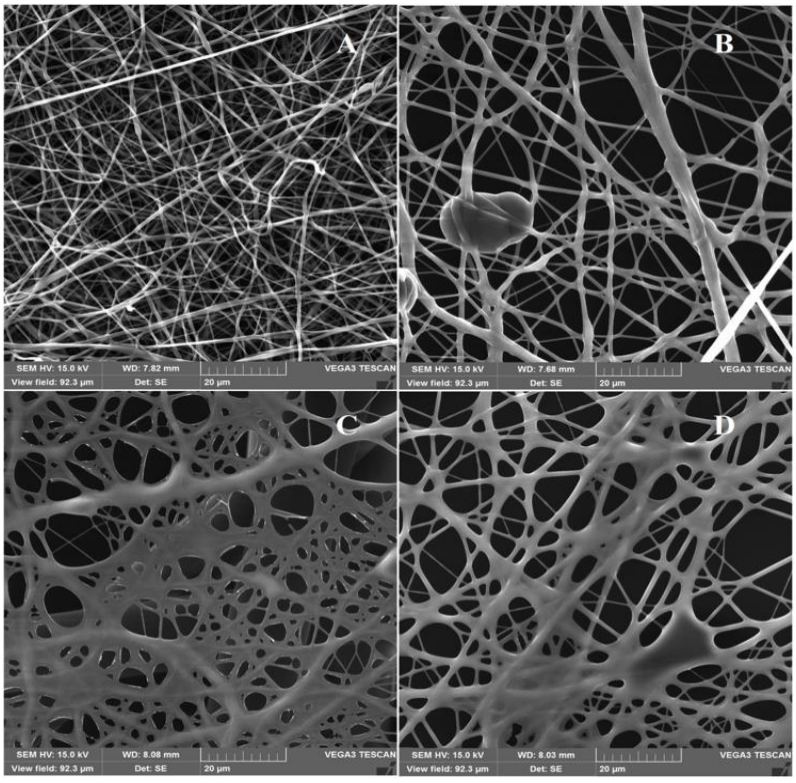

Figure 2E. Electron microscopy image of the PVA Povidone-iodine functionalized nanofibers
A) PVA Povidone-iodine functionalized nanofibers at the beginning of the test,
B) 1.5 hours of breathing through the PVA Povidone-iodine functionalized nanofibers,
C) 3 hours of breathing through the PVA Povidone-iodine functionalized nanofibers,
D) 6 hours of breathing through the PVA Povidone-iodine functionalized nanofibers.

The nanofiber membrane (with the basis weight about 1 g/m^2) was formed (Fig. 3E). This nanofiber mesh was very tiny but sufficiently solid for further processing. The mesh was subsequently cut into 100 cm^2 filters, folded and the functionalized filters slipped into an ordinary face mask.

Figure 3E. Macroscopic image of Povidone-iodine functionalized nanofibers

Such an ordinary face mask was equipped with low-density nanofiber mesh functionalized with encapsulated PVPI. Such a PPE was found as a very comfortable for application (wearing). First, this relatively low nanofiber density allowed a very comfortable breathing since the filter´s flow resistance was low. This is important since classical nanofiber filters (often used in PPE) can protect against virus penetration in laboratory conditions. Their effect in PPE, nevertheless, is highly questionable. Clearly, a higher basis weight (density) naturally protects more efficiently against virus penetration since the average pore diameters decreases. Simultaneously, however, the smaller pores also significantly increase air flow resistance. Consequently, major part of breathing air flows into nose via unprotected space instead of through the nanofiber filter. Highest filter porosity of the novel PPE increased the amount of air flowing through the filter due to the overall lower filter air resistance. On the other hand, PVPI functionalization of nanofibers created an active barrier and viruses were not only mechanically trapped, but also inactivated due to the interaction of the virus with the PVPI which is explicitly recommended by WHO as disinfection against SARS-CoV-2. This additional function more than compensated the lower efficiency of mechanical filtration. Naturally, this function works not only for air inhalation but also for air exhalation. Consequently, the novel PPE can protect neighbourhoods of infected persons.

Figure 4E. Degradation of PVA povidone-iodine. The red line is the spline connection for easier orientation.

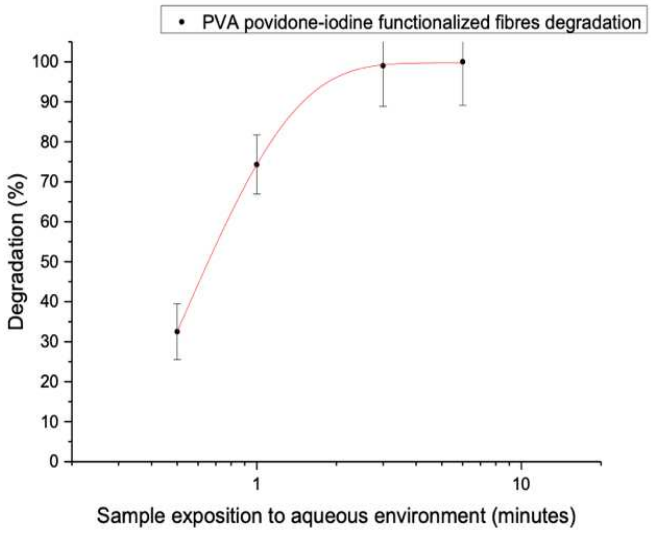

Another important property of the nanofiber filter was its controlled degradation and very slow release of iodine molecules due to that a low amount of iodine is released for disinfection of airways. Mixture of povidone-iodine with PVA results in nanofibers with further slowing down of iodine release from povidone-iodine complex. Notably, the release half-time strongly depends on air humidity and it can also be regulated (Fig. 4E).

We have adjusted nanofiber mesh functionalized with povidone-iodine with majority of its degradation after 8 hours of breathing under normal physical activities in offices or households. We have simply calculated the amount of iodine from nanofibers mass with encapsulated PVPI (1% PVPI solution and 1g/m^2 nanofiber weight) as 100µg iodine in the filter (size100 cm^2). The total amount of iodine in the filter is 0.4×10^{-7} mol (0.01 g nanofibers/0.1 iodine concentration in nanofibers/ 257 g per mol – molar mass of iodine). Supposing 16 breath-in and 16 breath-out per minute, each of 2L, the consumed molar gas volume is about 1.378 mol per 8 h (or 689 mol per 4 h), the resulting ratio is 0.00028 ppm in case of 8 hours .This is 33 times less than the permissible exposure limit (PEL) 0.0095 ppm. Moreover, the Maximum Allowable Concentration (NPK-P in Czech legislative) is 1 ppm, which cannot be exceed under these conditions. Despite of this extremely low amount, the filter was effective as the study shows (see below). We hypothesize that this is a way how the active filter minimizes the health consequences and why the patients undertook only a mild course of the illness. The nanofiber scaffold can filter particles of nanometric scale, wherein SEM image (fig. 5E) illustrates restrain capability of

the scaffold for the particles of size from 70 nm because of nanofiber surface chemistry and high fiber density.

Figure 5E. Electron microscopic image of dust on nanofibers

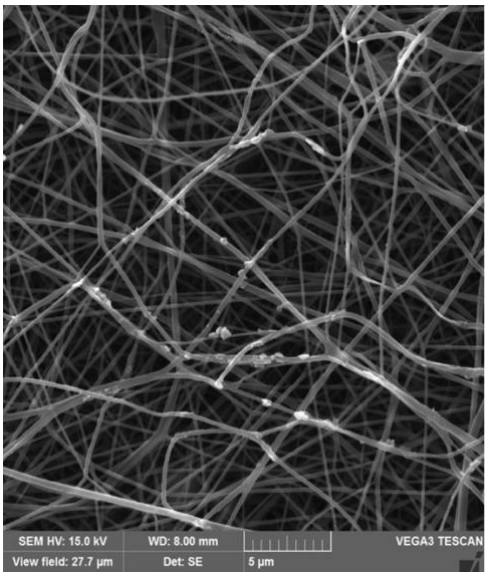

The face mask equipped with the functionalized filter was used for the clinical observation study. This filter, however, is characterized with a typical odour and there was easy to recognize it. Consequently, employment of the reference group equipped with a filter without povidone iodine, was fully impropriate and against good practice. Instead of reference group the Czech state collected epidemiological data have been used as a reference group. Altogether, 207 adults indicated as SARS-CoV-2 positive by PCR method have been involved into the clinical observation trial in April and May 2021. The participants applied an active nanofiber membrane with incorporated povidone-iodine into their regular face mask and breathed over the active filter minimum 4 hours, maximally 8 hours daily for a period from one to four days. We have found a clear positive epidemiologic effect since:

We have found that the reproduction number R0 was about 1.1 on the day two and three (Table 1E). This fits very well with the number R0 at the Czech Republic in April and May 2021. However, the reproduction number R0 significantly decreased on the day four and five. Notably, respondents of our observational study haven't infected any other person since the 4. day from the beginning of application of the povidone-iodine filter and, consequently, the study the reproduction number R0 decreased to zero (Table 1E). This clearly reflects a significant virus transmission in connection with application of the active filter. Importantly, there was neither mortality nor even one hospitalization. In addition, all patients declared only minor symptoms of the disease.

Interestingly, we have not observed dependence on the length of application, which indicated that already 4 h exposition is sufficient for protection.

4.3. Functionalized gels for induction of chemotaxis and cell proliferation

4.3.1 Low Concentrated Fractionalized Nanofibers as Suitable Fillers for Optimization of Structural-Functional Parameters of Dead Space Gel Implants after Rectal Extirpation.

Gel Maturation Is a Key Step for Biomechanical Parameters

Agar and agarose gels were selected in this study as a basis for the preparation of 3D implants. All gels were prepared as described in the methods section. Importantly, maturation was found to be an essential step towards implant biomechanical property formation. We compared two freshly prepared samples of agar and agarose with maturated samples kept for one week at 5 °C under 100% humidity. The relative deformation ε at temperatures ranging between 31 °C and 45 °C was measured. A phase transition between 30 °C and 37 °C was identified in the agar sample (Table 1F). This indicated that the material at the body temperature was too soft for an optimal implant. Agarose gel, however, showed much better characteristics, and a significantly broader phase transition makes it favorable for a clinical application. Clearly, such a gradual transition makes the implant more stable in case of temperature variation around 37 °C. In addition, we found that one-week-lasting maturation at 5 °C resulted in further broadening of the phase transition (Table 1F), which makes the artificial implant even more biomimetic. Thus, we can apply maturation as a method for controlling biomechanical parameters.

Table 1F. Dependence-relative deformation on gel maturation.

Gel Composition Heated to 37 °C	**ε =Δl/l (%)**
Agarose 1.5% matured	14 ± 1
Agarose 1.5% fresh	18 ± 2
Agar-Agar 1.5%	24 ± 2

3.2. Characterization of Fractionalized Nanofibers

Nanofibers from PVA and PCL were prepared by electrospinning as described in the methods section, and their structure was visualized by scanning electron microscopy (Figure 3D a, b). SEM analysis of materials proved the fibrous morphology of both samples. Diameters of at least 50 different filaments were measured for each image and the resulting data were processed to yield the structural characteristics of the nanofiber mesh (Figure 4F).

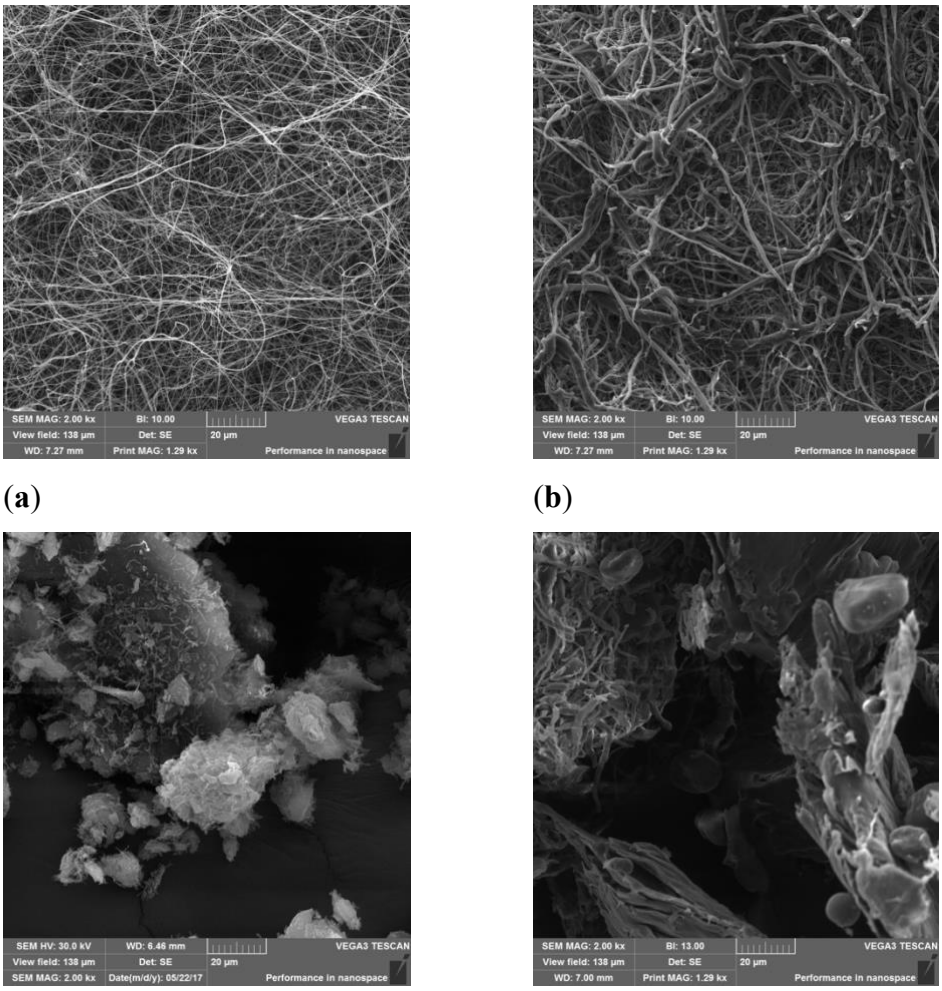

(**a**) (**b**)

(**c**) (**d**)

Figure 3F. Scanning electron microscopy images of nanofibers. SEM of whole PVA (**a**) and PCL nanofibers (**b**); ground PVA (**c**) and ground PCL (**d**) nanofibers. Magnification 2000×.

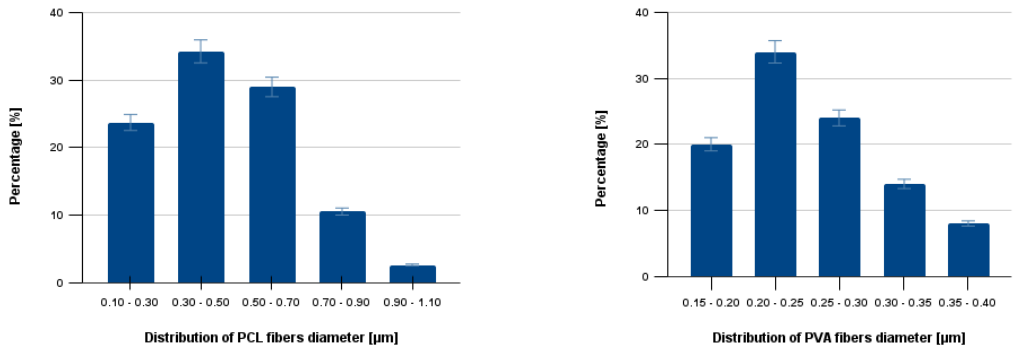

(**a**) (**b**)

Figure 4F. The average diameter of the PCL and PVA nanofibers. Subfigure (a) shows the average distribution of PCL nanofibers, and subfigure (b) describes the average distribution of PVS nanofibers.

Clearly, the diameter distribution showed significantly different structural characteristics for each nanofiber mesh. Different structural characteristics of nanofibers were observed for different polymers and for different physical parameters employed during the electrospinning process. Consequently, determination of structural characteristics belongs among the key parameters for reproducible production of the nanofiber-based drug delivery system. The average diameters of the PCL and PVA were determined immediately after electrospinning (Figure 4F) and remained constant even after NaOH treatment.

Nanofiber meshes prepared as described above are 2D-like materials due to their minimal thickness. This is hardly acceptable for filling large 3D lesions. To solve this problem, we prepared nanofibrous materials suitable for dispersion in liquids or gels. First, nanofiber mesh was fractionalized on micro-sized particles at a temperature below the gel phase transition. It was then mixed with a suitable gel. Such a 3D system maintained all the advantages of nanofibers, as fractionalization at liquid nitrogen temperatures yielded a fine powder with preserved nanofiber internal substructure (Figure 3F c, d).

The average diameter of the PCL and PVA nanofibers was determined from scanning electron microscopy images by TESCAN software. The average diameter of the PVA nanofibers was smaller than the average diameter of the PCL nanofibers because, with used fabrication technology, the higher viscosity of the used PCL solution limits the stretching of the jet during formation and therefore affects the diameter.

Fractionalized Nanofibers at Low Concentration Stiffen the Agarose Gels

Gel functionalization was performed with fractionalized nanofibers to develop a novel generation of smart scaffolds with modifiable biomechanical and chemical properties. First, we tested the effect of fractionalized nanofibers on gel structural properties. The optimal description of biomechanical properties is a stress–strain diagram reflecting properties over a wide range of applied stress. We determined the stress–strain diagram for the agarose gel enriched with either PCL or PVA nanofibers (Figure 5F). We proved that the addition of nanofibers (both PCL and PVA) significantly modified the stress–strain diagram, with PVA having a more profound effect. Tests were performed to determine the ultimate load capacity of the gels. The graph shows that the admixture of nanofibers significantly affects the yield strength and relative elongation. In the case of PVA, the yield strength increased by about 80% and allows the use of up to 10 mmHg of operating pressure, unlike agarose itself, which is destroyed at 6 mmHg. In the case of PCL, the increase is not as significant (50%), which corresponds to a destruction pressure of about 8 mmHg. In addition to an increase in the yield strength, nanofibers allow greater relative compression and elongation of the material from 0.29 to 0.37, an increase of about 25%.

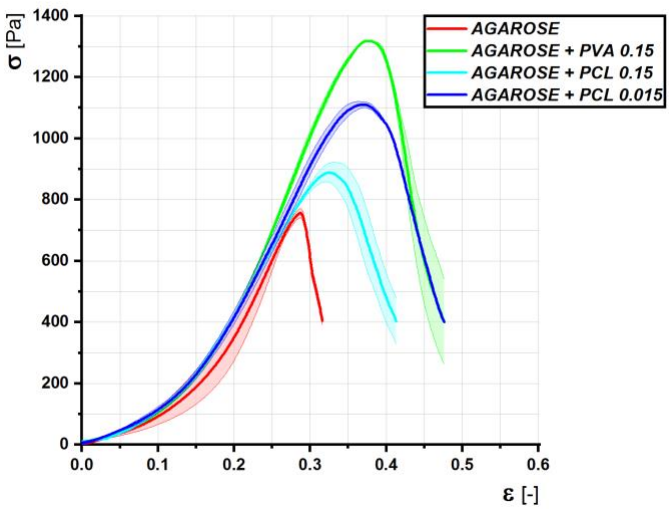

Figure 5F. Dependence of the internal stress on the relative deformation under the loading of the gel by simple pressure. The thick line indicates the average of the measurements, the field standard deviation. The samples were compressed at a rate of 0.5 mm/s.

Nevertheless, owing to the relatively narrow intervals of temperature and stress values to which the ideal implant should be exposed, the determination of the Youngś modulus of elasticity (i.e., at a single point of the stress-strain diagram) was chosen to be a sufficient experimental approximation. Gel deformation as a stress reaction was measured at 23 °C and 43 °C, and the Youngś modulus of elasticity was calculated. Figure 6 shows an almost linear dependence of Youngś modulus on agarose concentration at 23 °C. The same dependence was observed when the material was heated to 43 °C, leading to slightly reduced values of the Youngś modulus.

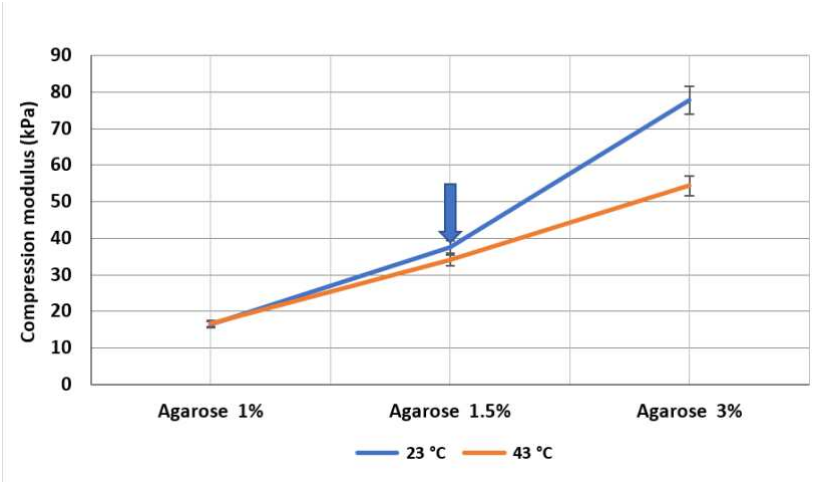

Figure 6F. Dependence of the Young's modulus of elasticity on agarose concentration.

Implant structure should resist at least the pressure applied during laparoscopic surgery. A set of gels withstanding the recommended pressure was prepared, and their biomimetic parameters were evaluated by surgeons. Based on the surgeons' experience, the gel with Youngś modulus of elasticity characteristic for the 1.5% agarose was also identified as the most biomimetic gel resembling the native tissue macroscopically, as indicated by a blue arrow in Figure 6. Thus, we considered the pressure range affecting the optimal abdominal implant ranging from 10 mmHg to 14 mmHg, i.e., 1.3–1.9 kPa, and the gels with adequate rigidity were prepared and tested (Figure 6F).

Biomechanical gel properties belong indisputably among the key parameters of the optimal implant. The effect of fractionalized nanofibers on gel rigidity was considered as potentially significant and, thus, was carefully studied.

The thick line indicates the average of the measurements, the field standard deviation. The samples were loaded with a constant force; the internal stress was calculated according to the instantaneous average cross section of the samples. The tests were performed in order to obtain the rheological properties of the gels, the modulus of elasticity, and the viscosity. These quantities were calculated using the Kelvin rheological model. From the graph and the calculated values, it can be deduced that the admixture of nanofibers causes a reduction in the modulus of elasticity and viscosity, more significantly in the case of PCL. The added gels will therefore be softer, more fluid, and at the same time withstand higher loads and deformations.

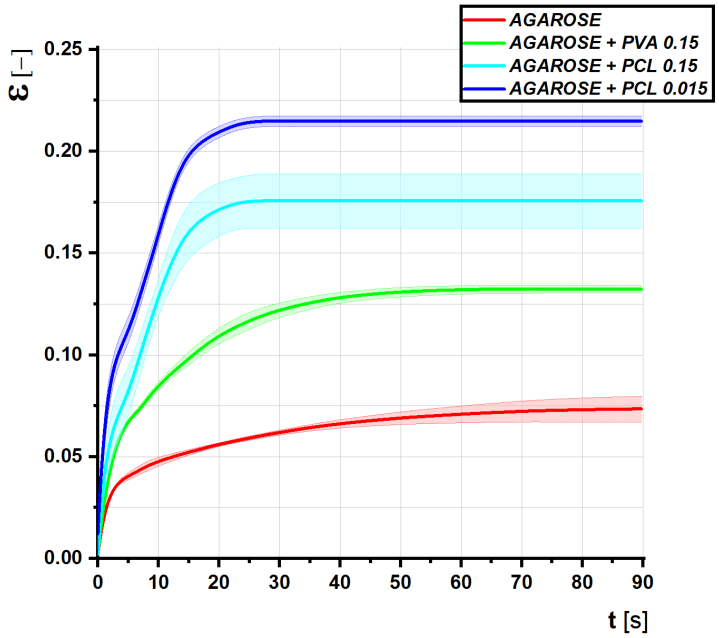

Figure 7F. Graph of relative elongation versus time at constant internal stress for individual types of gel (creep).

Clearly, the presence of the fractionalized nanofibers significantly influenced the Youngś modulus of elasticity even at very low concentrations. The PCL nanofibers affected the relative elongation of gels more than the PVA (Figure 7F). Both PVA and PCL fractionalized nanofibers, however, increased the Youngś modulus of elasticity at about 1.5% concentration. However, their effect was clearly observed already at a ten-times-lower scale, i.e., about 1.5‰ fractionalized gels.

Fractionalized Nanofibers Serve as a System for a Controlled Drug Delivery

First, fractionalized nanofibers were found as essential for gel rigidification. However, gel functionalization by degradable nanofibers could also open the door for the development of gels with the controlled release of encapsulated bioactive substances. Thus, the effect of nanofibers with a controlled degradation was examined and PVA nanofibers were used as a model system. Clearly, PVA as a hydrophilic substance is easily degradable in an aqueous environment. However, controlled crosslinking can prolong their degradation half-life in water.

PVA nanofibers have been produced from polymers of different degrees of crosslinking, and their degradation was measured in distilled deionized water at a temperature of 36 °C on a vibrating heated platform with a vibrational frequency of 51 Hz. Fluorescein Isothiocyanate-Dextran was used as a marker for determination of the degradation half-time and nanofiber labeling was performed and analyzed as described in the methods section. Measured data clearly show that crosslinking can significantly prolong the degradation half-time (Figure 4F). While the PVA nanofibers have been characterized with a degradation halftime shorter than 1 min, crosslinking prolonged this half-time by several orders. Noticeably, only 8% of the weight of samples with crosslinking modification were dissolved in 0.9% NaCl aqueous solution during 12 h. Thus, the system allows regulation of the degradation process on a very broad time window, as the half-time of degradation of our partially crosslinked sample clearly demonstrated (Figure 8F).

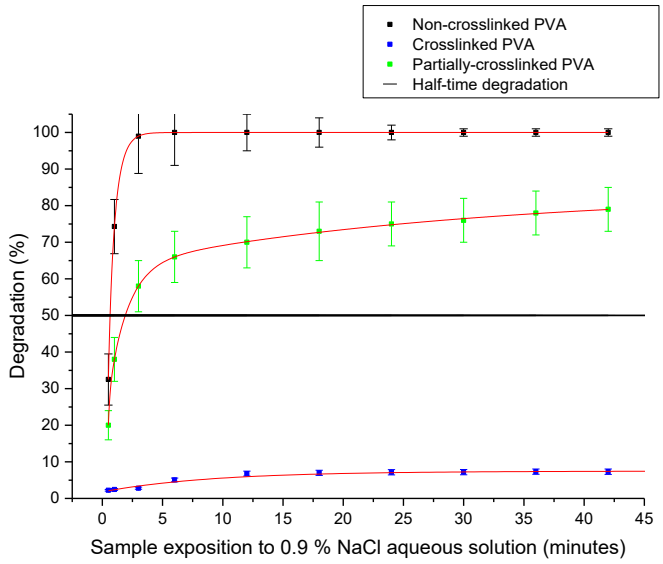

Figure 8F. Degradation of crosslinked PVA nanofibers and noncrosslinked PVA nanofibers.

Biocompatibility Testing

Cell proliferation was used for testing of the fractionalized nanofibers' biocompatibility. Both PCL and PVA fractionalized nanofibers were tested, and cells cultivated in a culture medium without incubation on gels were used as a negative control.

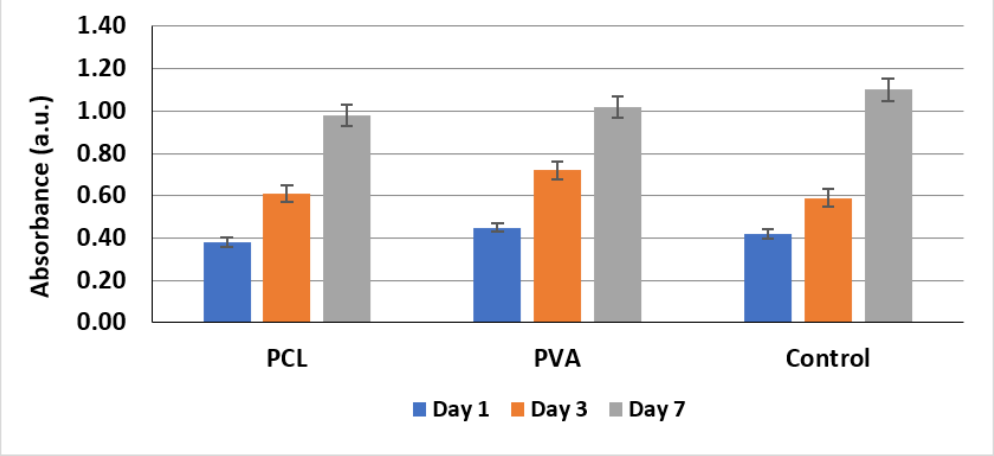

Figure 9F. Cell proliferation analysis.

The cell cytotoxicity test did not show significant differences between the standard culture medium used for cell culture experiments, PCL-conditioned medium, and PVA-conditioned medium (Figure 9F). Therefore, gels with PVA or PCL nanofibers were considered noncytotoxic and subsequently used for other cell culture testing. High cell viability was found on both gels' material, more than 95% by the LIVE/DEAD® Viability/Cytotoxicity Kit.

4.3.2. Hydrolat of Helichrysum italicum promotes tissue regeneration during wound healing.

Hydrolat of *H. italicum* is reach in phytochemicals

As previously reported, the characterization of the phenolic compounds was performed by HPLC-DAD analysis. A screening approach by selecting multiple wavelengths in a diode array detector allowed us to determine the presence of some hydrophilic phenols. Compounds identification, obtained by chromatographic comparison of their UV spectrum with analytical standards, was followed by quantitative analysis using external standard method. The UV analysis highlighted the presence on HH of two main phytochemicals groups related to caffeoylquinic acid derivatives and naringenin derivatives (Table 1G). Due to the absence of commercial standards, caffeoylquinic acid derivatives were expressed as chlorogenic acid, and naringenin derivatives were expressed as naringenin. Caffeoylquinic acid derivatives were the most abundant compounds in samples analyzed whit a

concentration of 421 ± 20 mg/L followed by naringenin derivatives that showed a concentration of 27 ± 1 mg/L (Table 1).

Phenolic compounds	HH mg/L ± DS
Caffeoylquinic acid derivatives (£)	421 ± 20
Naringenin derivatives 9(ø)	27 ± 1

Table 1G. Phenolic compounds quantified in HH.
Results are expressed as mean ± standard deviation.
(£) Caffeoylquinic acid derivatives were expressed as chlorogenic acid.
(ø) Naringenin glycoside derivatives were expressed as naringenin.

Hydrolat of *H. italicum* stimulate cell viability

MTT assay was performed on HFF1 and SSCs to evaluate the toxicity at different concentrations and timepoints (Figure 2G). The assay was performed after 24h or 48h of culturing under the above described conditions, showing a low toxicity of the treatment at concentrations tested. In the presence of extract, cell viability of SSCs for all the concentration tested was similar to control, represented by untreated cells, after 24h and 48h (Figure 2, panels b and d). On the other hand, a significant decrease in cell viability could be observed only in fibroblasts treated with 40% HH for 24h or 48h (Figure 2G, panels a and c) . Such as SSCs, no cytotoxic effects were detected when HFF1 were cultured with the other concentrations ((Figure 2G, panels a and c). Figure 2 also shows that HH was not toxic for both HFF1 and SSCs for all the concentrations under 30% tested.

Hydrolat of *H. italicum* induces cell proliferation

The BrdU assay was performed to analyse cell proliferation (Figure 3G). The test revealed that the treatment with HH does not affect the proliferation of the cell populations analyzed, not undergoing wound. Figure 3 shows that these cells reached a proliferation rate similar to that observed for the control sample (Figure 3, panels a and b). On the other hand, after scratch test, a significant increase in cell proliferation for both fibroblasts and stem cells could be observed (Figure 3, panels c and d). Both cell types show a significant proliferation

increase when cultured with 30% HH for 24h (Figure 3G, panels c and d). While SSCs show a significant increase even after culturing with 20% HH for 24 h (Figure 3, panel d).

Hydrolat of *H. italicum* promotes cell migration

The ability of HH to stimulate fibroblast and stem cells proliferation and/or migration was detected by the scratch assay. Figure 4 shows fibroblasts treated with the different concentrations of HH (40%,30%,20% and 10%). The figures 4 and 5 show the migration of cells after scratch for different time point (day 0, 24h and 48h). Figure 4 revealed that fibroblasts treated with 20% and 30% HH for 24 h increased the number of migrating cells detectable in the wound site compared to control cells (untreated samples). After 48 hours, samples treated with the other concentrations of HH selected (30% and 20%) reached confluence. Figure 4 show that both samples treated with 30% and 20% of HH showed an increased number of migrating cells detectable in the wound site as compared to control untreated cells. In contrast, in the untreated control, the wound site was not healed. On the other hand, cells treated with 10% of HH showed reduced migration and proliferation activity, compared to cells treated with 20% or 30%. However, fibroblasts treated with 40% HH were not committed to migration (Figure 4G). Figure 5 shows SSCs migration and proliferation were induced as early as 24h by 20% and 10% HH concentrations. After 48h, also the cells treated with 30% HH showed complete confluence of the wound site (Figure 5). Results were also analysed comparing wound clousure area after 24h and 48h of HH treatment to untreated cells, and measured in percentage considering as 0 % the wound area at T0 (moment of wound creation) and 100% the full confluence of cells in wound area (Figure 4, panel a and Figure 5, panel b).

Hydrolat of *H. italicum* induce a molecular program of skin regeneration

Figure 6 Shows HFF1 cultured in the presence of different concentrations of HH. Results show a modulation of the expression of the TNF-α gene, involved in acute inflammation. In particular, we detected also a significant increase of TNF-α gene expression for samples cultured with 40% HH, while the concentration of 30% HH induced a downregulation as compared to control sample (Figure 6G, panel a). Moreover, all treatments induced increased expression of CASP8 and HAS2 genes, (Figure 6, panels b and c), being particularly evident for cells cultured in the presence of 20-30% of HH. Figure 7 shows gene expression analysis of SSCs. Cells show a significant increase in SOX2 (Figure 7G,panel a), Oct-4 (Figure 7G, panel b) and NANOG (Figure 7G, panel c) expression, when cultured in the presence of 10%,20% and 30% HH respectively, as compared to control cells.

Nanofibers Encapsulated with Natural Products: A Novel Strategy to Counteract Skin Aging.

2.1. Essential oil composition

The GC-MS analysis- highlighted 35 distinct compounds, comprising five monoterpenes, nine oxygenated monoterpenes, fourteen sesquiterpenes and five oxygenated sesquiterpenes (Table 1).

Table 1G. Results by GC- MS analysis show the groups of compounds present in *HO.*

Monoterpens	**α-pinene, α-fenchene, β-pinene, Limonene, γ-terpinene**
Oxygenate Monoterpens	Linalool 1,8-Cineolo, Neryl propionate, Neryl isobutanoato, Ner isovalerato, Nerol, Nerolidol, Nerol oxide, Neryl acetato, Geraniol
Sesquiterpens	Italicene, Iso- Italicene, Caryofillene, γ-Curcumene, Ar-Curcumer cis-β-Guaiene, cis-α-Guaiene, trans-β-Guaiene, γ-Cadinene, δ-Cadiner α-Cadinene, α-cis-Bergamotene, α-trans-Bergamotene, Alloaromandre
Oxigenate Sesquiterpens	τ-Cadinolo, Guaiol, β-Eudesmol, α-Eudesmol, Eudesm-5-en-11-ol

2.2. Nanofibers Features

All samples were studied with scanning electron microscope (SEM) (Device Vega 3 from Tescan, CZ Czech Republic) after spinning thanks to sputtering tiny samples by thin film of gold (Quorum Q150R S). Figure 1G (panel a and b) and figure 2G (panel a and b) shows the morphology of fibers. Figure 3 shows histograms of diameters of each sample. Electrospinning is a self-organized procedure, so the orientation of fibers is random. The fibers of sample 1 (figure 1G, panel a) are uniform in diameter with an average of 365,5 nm with a standard deviation of 95 nm. Sample 2 (figure 1G, panel b) has more ribbon like fibers with higher average of 709 nm, sd 479,5 nm. Layer density of all samples was about 10 gsm.

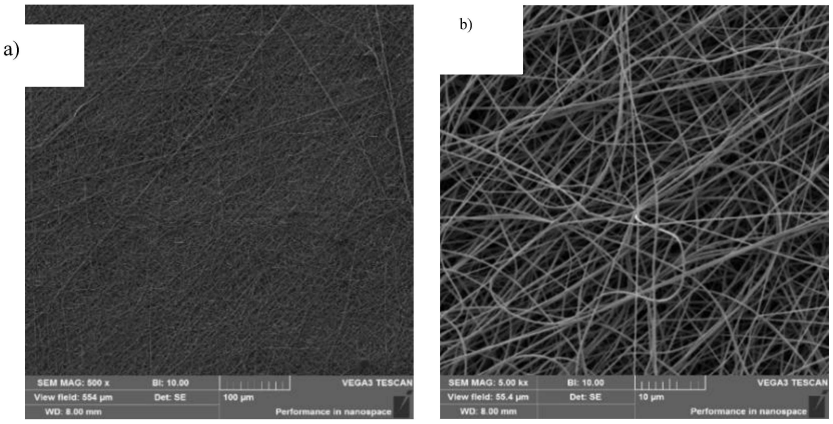

Figure 1G. Images acquired with SEM microscope showing PVA 1% (sample 1) nanofiber structure. Panel a) shows nanofiber at 500 x magnification and panel b) shows nanofiber at 5000 x magnification.

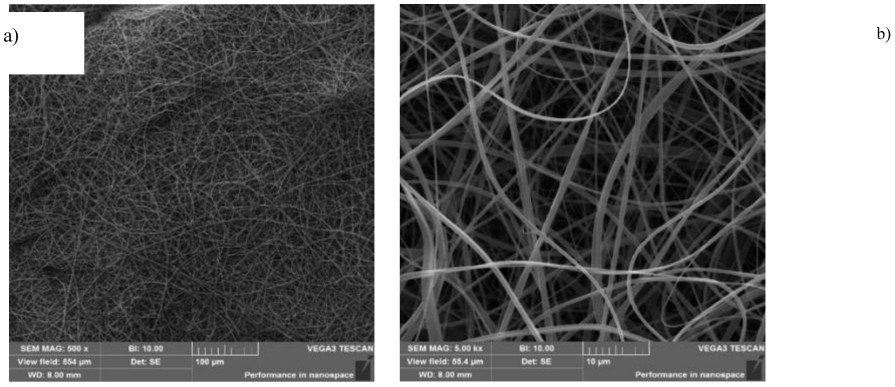

Figure 2G. Images acquired with SEM microscope showing PVP with 1% oil (sample 2) nanofiber structure. Panel a) shows nanofiber at 500 x magnificent and panel b) shows nanofiber at 5000 x magnification.

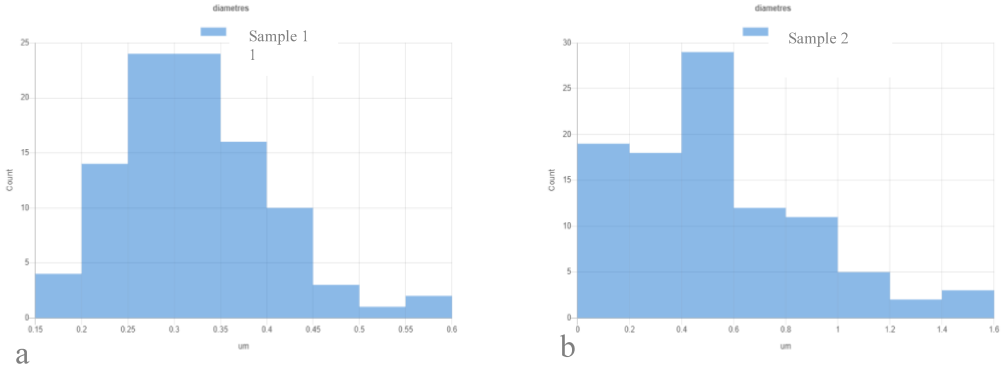

Figure 3G. Images show histograms of fibers´ diameters. Panel a) sample 1 (PVA1%) and panel b) sample 2 (PVP1%).

2.3. PVA and PVP pretreatment maintain cell viability under UV stress

SSCs cultured with PVA1% or PVP1% for 2 hours show an increase in viability (Figure 4G, panel a) as compared to the untreated control (Ctrl), being statistically significant only for PVA1%-treated cells. Pretreatment of SSCs (Figure 4G, panel b) with PVA1% and PVP1% before UV-stress, induced a significant increase in cell viability, as compared to the positive control (UV). On the other hand, when SSCs were treated with PVP1% (Figure 4G, panel a), they showed only a faint proliferation rate increase compared to untreated control (Ctrl). BJ fibroblasts cultured in the presence of both PVA1% and PVP1% show a significant increase in viability as compared to the untreated control (Figure 4G, panel c). Interestingly BJ fibroblasts pre-treatment with both PVA1% and PVP1% before UV exposure was able

to induce a significant increase in cell viability, as compared to control stressed cells (Figure 4G, panel d).

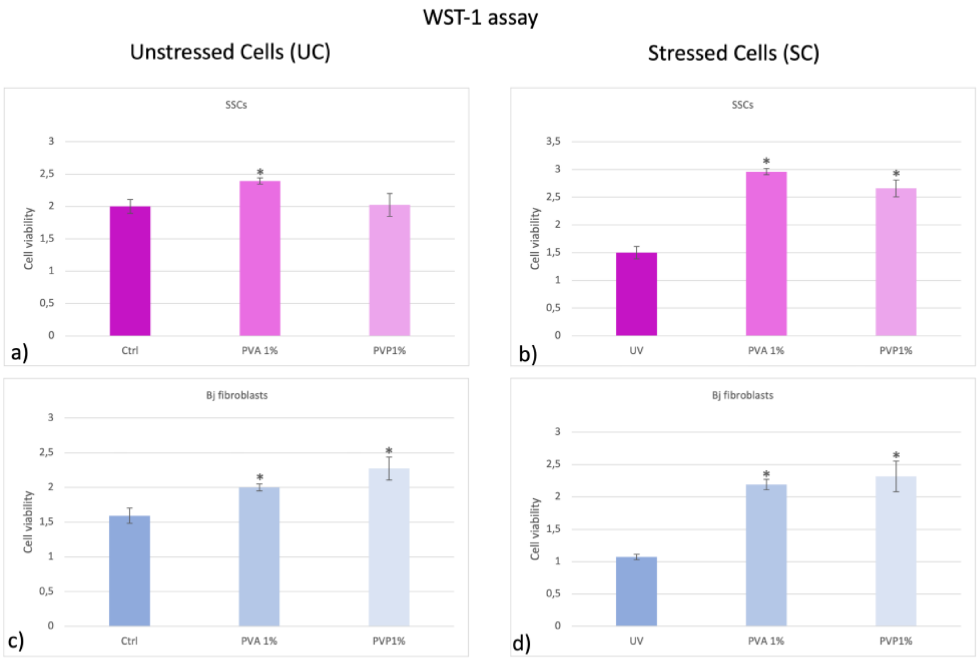

Figure 4G. WST1 assay in SSCs and BJ Fibroblasts after 2h of treatment with PVA 1% and PVP 1% nanofibers. Panel a) and c) show cells cultured for 2h with sample 1 (PVA 1%) and sample 2 (PVP1%) and not exposed to UV (UC). Panel b) and d) show pretreated cells for 2h with sample 1 (PVA1%) and sample 2 (PVP 1%) and then exposed to UV (SC). Error bars represent standard deviation. * p value ≤ 0.05.

2.4. PVA1% and PVP1% protect cells from UV-induced senescence.

β -galactosidase colorimetric assay shows that the number of blue positive cells was reduced when they were pre-treated with nanofiber, both PVA and PVP, encapsulated with 1% *HO*, before exposure to UV light, as compared to positive controls (UV) (panel a). No particular differences were observed in the absence of UV exposure, although it can be observed that the number of positive cells is slightly lower than untreated controls (UC) for both treatments (PVA and PVP) (panel b).

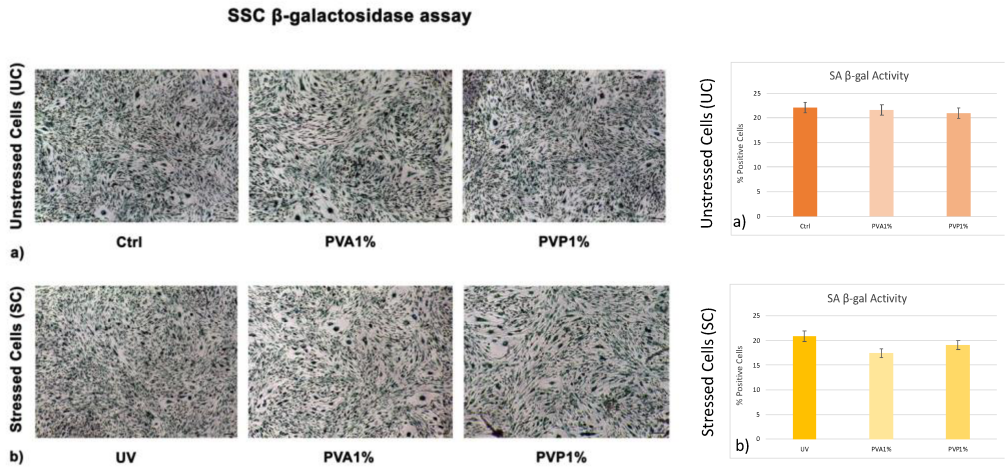

Figure 5G. Senescence-associated β-galactosidase activity was evaluated after 2h of culturing with PVA 1% and PVP 1% nanofibers in SSCs and eventually exposed to UV. Scale bar=100 µm. The numbers of positive (blue) cells for each condition was calculated as the number of positive cells divided by the total number of cells counted using an image software analysis (ImageJ). Data are expressed as mean± SD referring to the control.

2.5. PVA1% and PVP1% pretreatment promote a molecular program of youngness

Real-time qPCR reveals that pretreatment with PVA1% and PVP1% before UV exposure was able to prevent the UV-induced downregulation of TERT and Bmi1 gene expression on skin stem cells (Figure 6, panels c and d). Concomitantly, the same pretreatment inhibited the appearance of the senescence-regulating genes p16 and p19 (Figure 7, panels c and d). Moreover, the expression of the stemness genes Oct-4, Sox2, and NANOG was significantly increased on skin stem cells pretreated with both PVA1% and PVP1% and then exposed to UV (Figure 8 panel d, e, and f).

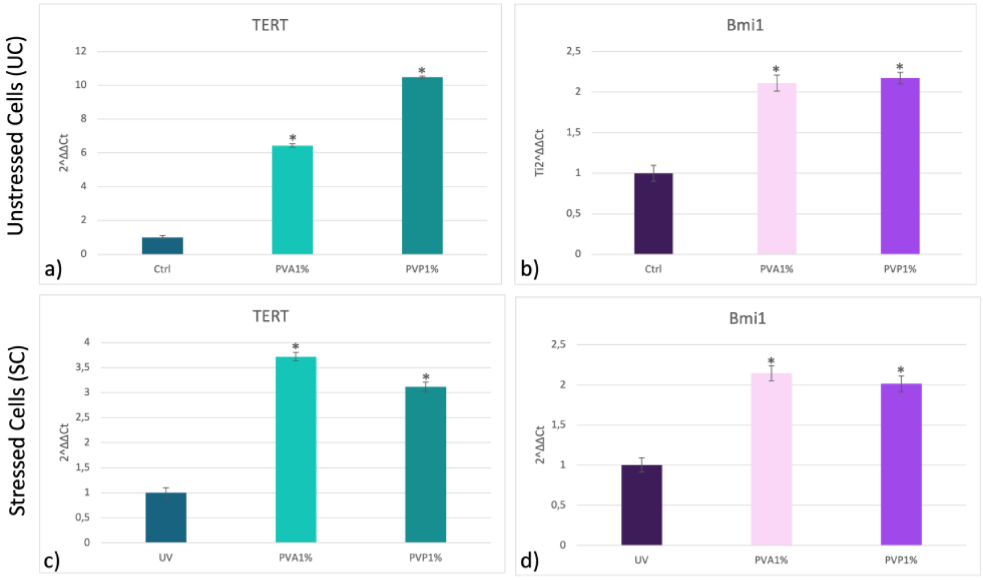

Figure 6G. Effect of PVA1% and PVP1% treatment on the expression of TERT (**a,c**) and Bmi1 (**b,d**) in SSCs. SSCs were exposed for 2 hours with PVA1% and PVP1% and then stressed (panel c and d) or not (panel a and b) with UV. The amount of mRNA was normalized to GAPDH and was plotted as fold change ($2^{-\Delta\Delta CT}$) as compared to controls. * p value ≤ 0.05.

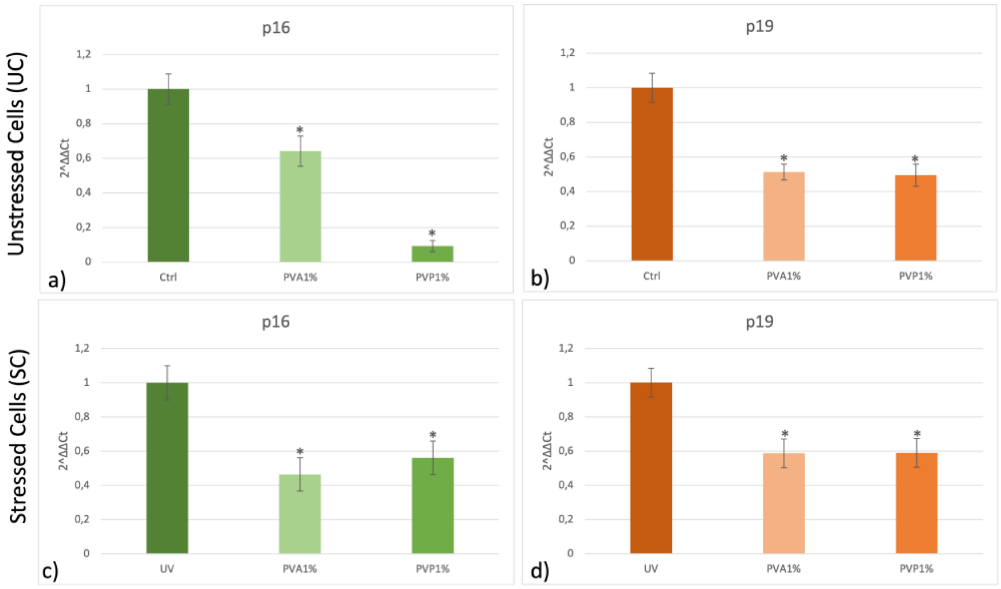

Figure 7G. Effect of PVA1% and PVP1% treatment on the expression of p16 (panel a and c), p19 (panel b and d) on SSCs. SSCs were exposed for 2 hours with PVA1% and PVP1% and then stressed (panel c and d) or not (panel a and b) by UV. The amount of mRNA was normalized to GAPDH and was plotted as fold change ($2^{-\Delta\Delta CT}$) as compared to controls. * p value ≤ 0.05.

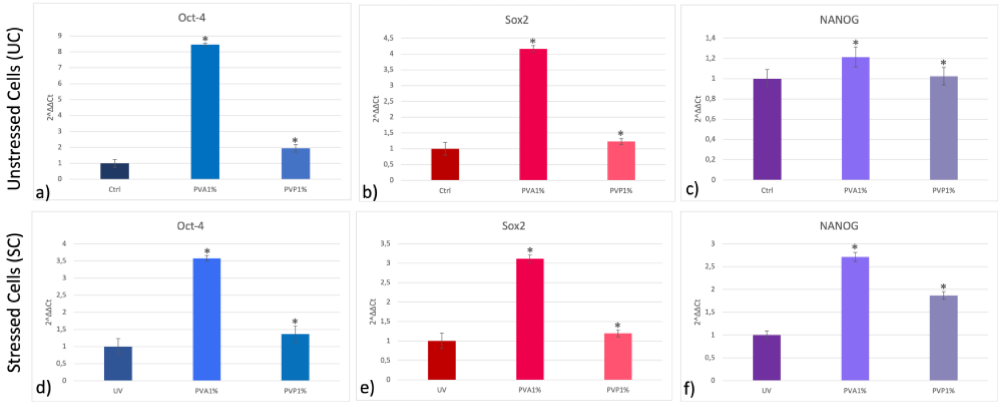

Figure 8G. Effect of PVA1% and PVP1% treatment on the expression of Oct-4 (a,d), Sox2 (b,e) and NANOG (c,f) on SSCs. SSCs were exposed for 2 hours with PVA1% and PVP1% and then stressed (panel d, e and f) or not (panel a,b and c) by UV. The amount of mRNA was normalized to GAPDH and was plotted as fold change ($2^{-\Delta\Delta CT}$) as compared to controls. * p value ≤ 0.05.

4.3.3 PVA and PVP nanofibers combined with Helichrysum italicum oil preserve skin cell interactions, elasticity and proliferation

PVA1% and PVP1% stimulate cell viability and cell proliferation after scratch assay

Human skin keratinocytes (HaCaT) cultured for 24 h after scratch with PVA1% or PVP1%, based on previously tested condition (Supplementary Fig. S1) exhibit an increase in viability (Fig. 1, panel a) as compared to cells. cultured for 24 h after scratch without any treatment (untreated control CTRL) (Fig. 1, panel a). At the same time, the BrdU assay was performed to analyze proliferation of HaCaT (Fig. 1, panel b) cultured under the condition described above. The results revealed that treatment with PVP1%, after scratch test, significantly increased cell proliferation, as compared to the untreated control (CTRL), (Fig. 1H, panel b). On the other hand, when HaCaT were treated with PVA1%, they showed only a faint proliferation rate increase, as compared to the untreated control (CTRL) (Fig. 1H, panel b).

PVA1% and PVP1% promote cells migration after scratch

The capability of PVA1% and PVP1% to enhance HaCaT migration was detected by the scratch assay. Figures 2 and 3 show the healing process at two magnifications (4× and 10×, respectively) under an optical microscopy (Leica, Nussloch, Ger-many) and quantified by ImageJ Software (Supplementary Fig. S2H). Figures 2 and 3 shows HaCaT treated with PVA1% or PVP1% and the migration of cells after scratch at two different time point (day 0 and 24 h). Figures revealed that both treatments increased the number of migrating cells detectable in the wound site as compared to untreated cells (CTRL).

PVA1% and PVP1% induce the expression of Occludin (OCLN)

The expression of Occludin was evaluated in HaCaT treated for 24 h with PVA1% or PVP1% after scratch (Fig. 4H). PVA1% and PVP1% treatment increased the expression of Occludin at nuclear level, as compared to control untreated cells (CTRL). This effect was clearly evident in all the analyzed cells treated with PVA1%, while in cells cultured in the presence of PVP1%, this increased expression could be detected mainly closed to the scratch area (Fig. 4H).

Cell elasticity after treatment

HaCaT showed a different behavior when treated with PVA 1% or PVP 1%, as compared to control untreated cells (CTRL). In particular, we observed in the external layer (Y1) a slight (yet not statistically significant $p=0.08$) decrease in apparent Young's modulus for PVA 1%, as compared to control, while no variations were observed in

PVP 1%. This trend was more evident and statistically significant ($p<0.01$) in the internal layer (Y2) where we observed a significantly decrease in apparent young's modulus for the

PVA 1% while no variation was observed in PVP 1% as compared to controls. This seems to indicate that PVA 1% induced a change in the nuclear and perinuclear regions, causing a significant softening of these regions, while in the cytoskeleton and membrane regions the effect is less evident. On the other hand, it seems that PVP 1% did not affect at the biomechanical properties of cells as compared to control, leaving both layers (internal and external) unaltered.

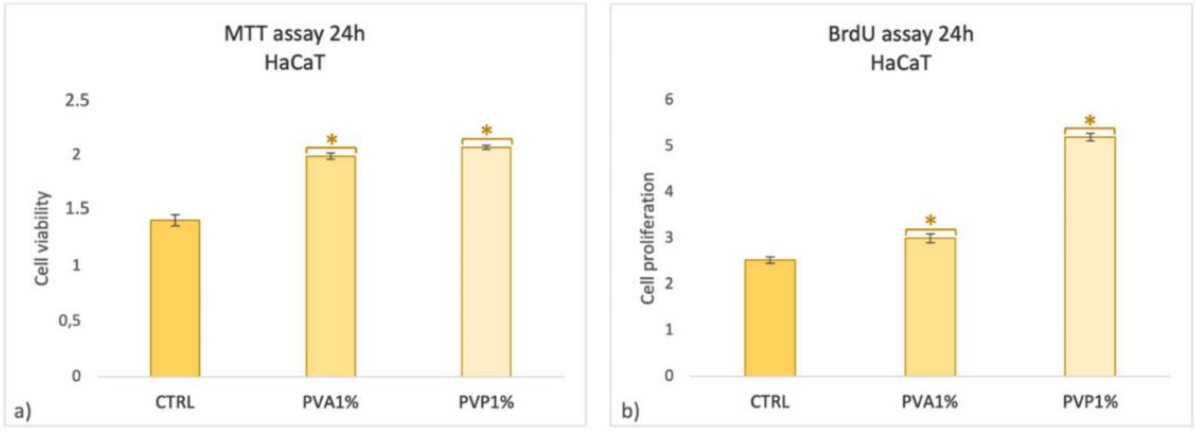

Fig. 1H. MTT assay (panel a) and BrdU assay (b) of HaCaT cultured for 24 h in the presence of PVA1% or PVP1%. Cell viability (panel a) and cell proliferation (panel b) of treated cells (PVA1% and PVP1%) are expressed as mean±SD reffering to the untreated control (CTRL). (*$p<0.05$).

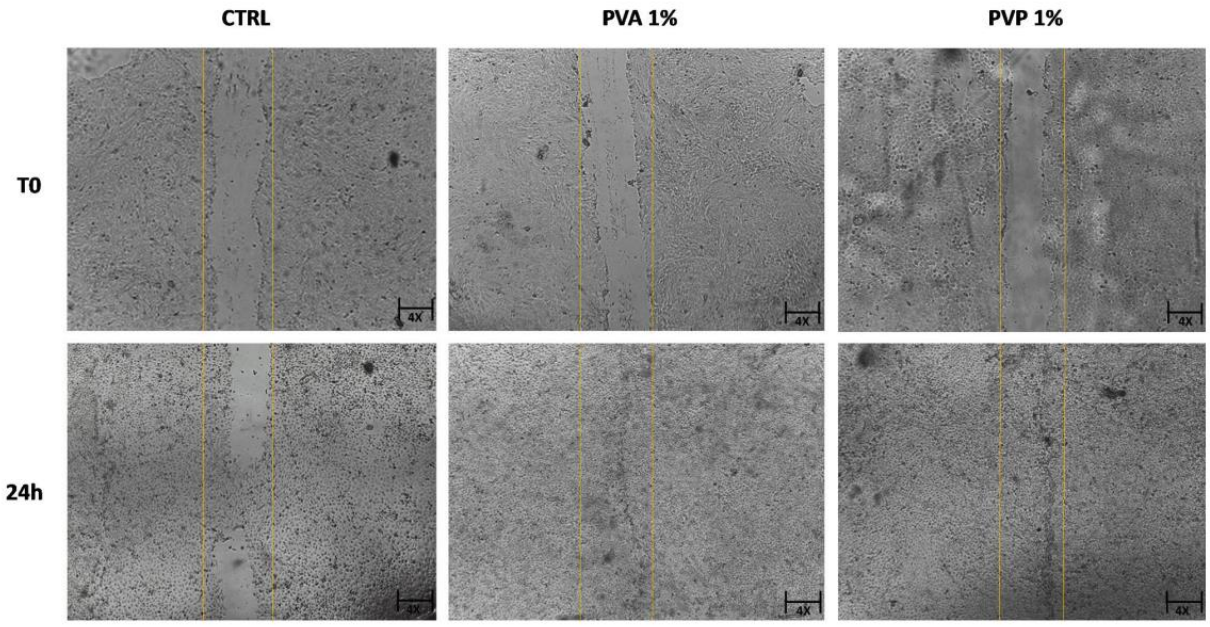

Fig. 2H. Shows migration of HaCaT after scratch and treatment with PVA1% or PVP1%. Images were taken under inverted light microscope at time of cutting (day 0) and after 24 h

of treatment. Treated cells were compared to untreated cells (CTRL). Figure shows HaCaT migration at 4×magnification.

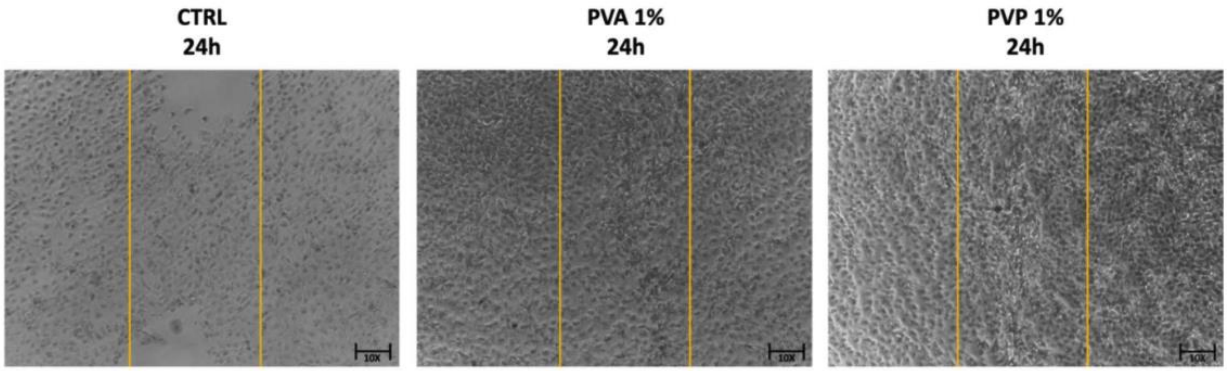

Fig. 3H. Shows migration and/or proliferation of HaCaT after scratch and treatment with PVA1% or PVP1%. Images were taken under inverted light microscope after 24 h of treatment with PVA1% and PVP1%. Treated cells were compared to untreated cells (CTRL). Figure shows HaCaT migration at 10×magnification.

PVA1% and PVP1% modulate inflammatory-related genes

Figure 6 shows the effect of PVA1% and PVP1% on IL-8 and IL-1β gene expression. Gene expression of IL-8 and IL-1β were influenced by both treatments. Figure 6 shows that the mRNA levels of IL-8 (panel a) and IL1β (panel b) were significantly upregulated after 24 h of treatment with PVP1% or PVA1%, as compared to untreated cells (CTRL).

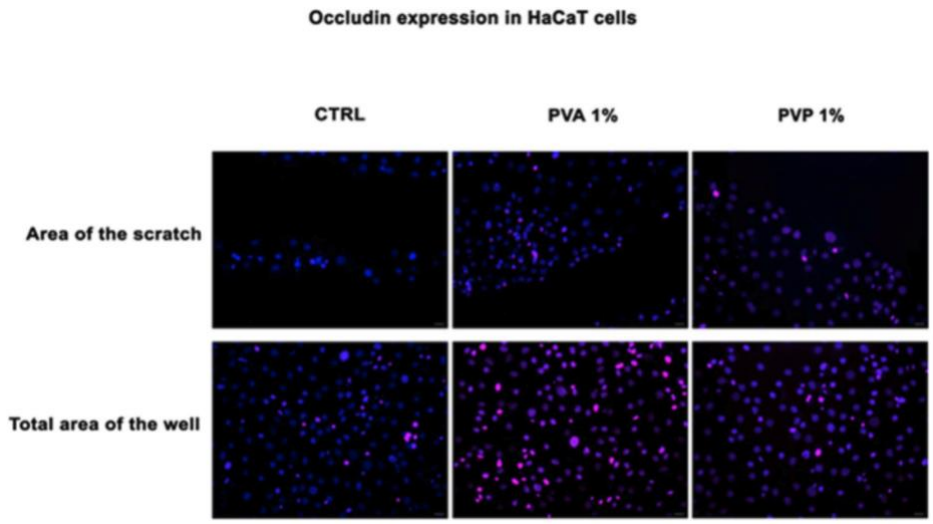

Fig. 4H. Analysis of Occludin expression in HaCaT during wound closure. Immunohistochemical analysis of the expression of Occludin was assessed in HaCaT after scratch and treatment with PVA1% or PVP1% as compared to control cells (CTRL). Nuclei are labelled with 4,6-diamidino-2-pheny

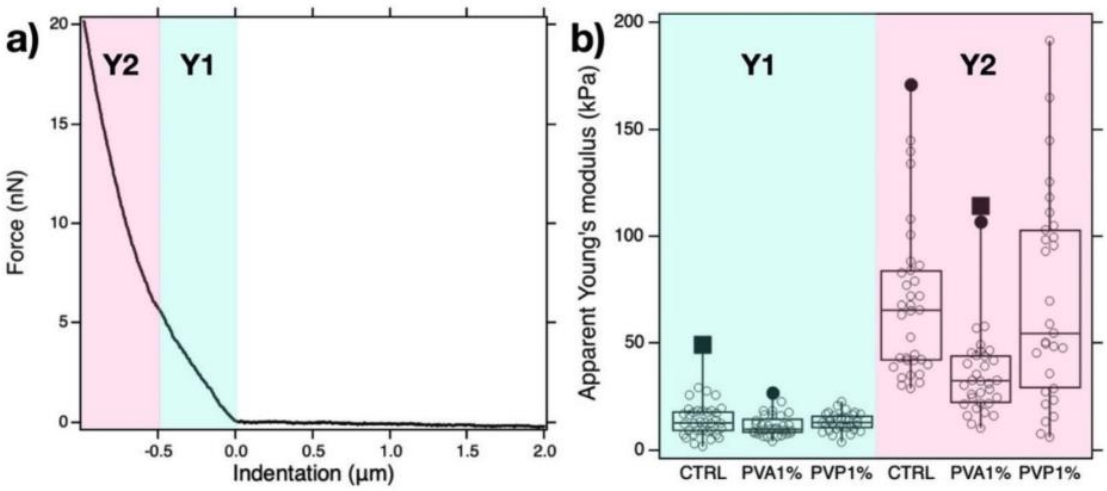

Fig. 5H. Panel (a) Representative AFM force-indentation curve of HaCaT cells, where we highlighted in light blue and light pink the layers used for the fit with the two-slope modified Hertz-Sneddon model; panel (b) boxplots showing the apparent Young's moduli Y1 (external layer) and Y2 (cell body) of the cells, obtained as described in panel (a). The lower and the upper boundaries of the box represent Q1 (25 percentile) and Q3 (75 percentile) of the data, respectively; the horizontal bar inside the box represent the median of the data.

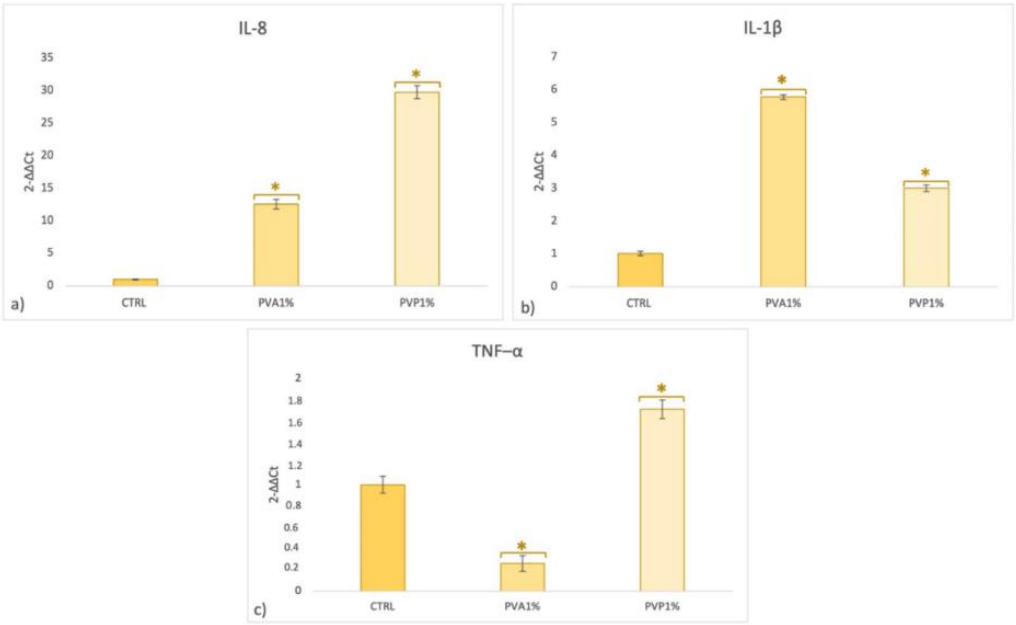

Fig. 6H. Gene expression of proinflammatory cytokines IL-8 and IL-1β. The expression of Interleukin 8 (IL-8) and Interleukin 1 beta (IL-1β) was evaluated in cells treated with PVA1% or PVP1% for 24 h after scratch assay (Figure, panels (a) and (b) respectively). The mRNA levels for each gene was expressed as fold of change (2−ΔΔCt) of mRNA levels observed in untreated HaCaT (CTRL) and normalized to (GAPDH). Data are represented as mean±SD referred to the control (*p≤0.05).

5. DISCUSSION

Modern technology is gradually changing therapeutic and diagnostic capabilities even in well-established and stable areas of medicine field of oncology(Coradduzza et al. 2022b), followed by nanomaterials in surgery(Kralovic et al. 2019) and, of course, in orthopedics (Smith et al. 2018). There is a significant opportunity for applying new technologies in their development.

Nanotechnologies have the potential to revolutionize diagnostics, treatment, and research in Clinical practice. The expectation that nanotechnology will someday play a significant role in clinical treatment is supported by the success of the area in the commercial and public sectors. Nanotechnology has the potential to replace many expensive traditional treatments and offer a wide range of unique uses. They offer more precise therapeutic modalities that could result in implants that are more effective and last longer, have lower infection rates, and have better bone and tendon healing. Numerous unique uses of nanotechnology are available, but one that stands out is the use of nanoparticles as scaffolds to promote a better connection between orthopedic implants and natural bone. Over time, nanomaterials are becoming more and more deeply integrated into clinical practice, appearing in research in various forms and applications . Their applications are very broad, starting with surface patches with the function of regulated drug release to nanobiosensors and targeted drug delivery with the help of designated nanoparticles. The use of nanomaterials brings new possibilities to already mature fields.

Novel insights from the use of nanomaterials can be felt in the field of oncology , followed by nanomaterials in surgery and, of course, in orthopedics . Based on newly-validated biomarkers in various disciplines, portable biosensors and nanobiosensors are being developed to measure a critical marker accurately and rapidly or a set of markers

5.1. The window of opportunities for molecular diagnosing

Several essential aspects cannot be overlooked in diagnosing and treating degenerative joint disease. They involve the heterogeneity of symptoms in the early stages, indirect correlation of diagnostic findings using common imaging techniques with patient complaints and frequent low availability of imaging techniques. (“S84 Abstracts / Osteoarthritis and Cartilage 31 (2023) S74eS419”) This brings us closer to answering the question, why early diagnosis and staging of these diseases is a difficult task? The answer to this question is the multifactorial nature of most degenerative diseases and a significant link between the musculoskeletal system's functionality and the patient's well-being at detecting pathological conditions. Diagnostics based on biomarkers alone is challenging as well. Limitations are

caused by the low availability of knowledge about the concentrations of individual markers in different fluids, their exact origin, and their relationship to the observed pathology, which plays a key role in finding reference values. (Poole 2003). This obstacle can be resolved by a number of additional experiments on animal models, as well as by using advanced laboratory analysis methods such as tests on organ models or by proteomics and cell biology methods. The next key point is the evaluation of disease treatment results, patient care, and comprehensive rehabilitation. In these areas, non-invasive and laboratory methods are imbalanced with invasive, for example, arthroscopy revision. However, it has sufficient medium-term risks to accelerate the development of arthritis (within 10-15 years)). The monitoring of the progression and treatment outcome nowadays could be evaluated by comparison of CT scans. Imaging methods in this application results evaluation have several limitations, such as the standard resolution of CT scans, the multifactorial diseases (not only visual manifestations) and the inaccuracy resulting from the review of scans by different specialists and in other diagnostic units. The laboratory confirmation of the suspected diagnosis is a significant benefit for prescribing a suitable treatment. (Bianchi et al. 2021). After confirming the cure, the next priorities for this area are to assess the monitoring of treatment response and the prevention of recurrences of the condition and achieve a comprehensive rehabilitation, both on a functional and tissue level, if necessary. Modern technologies are gradually changing therapeutic and diagnostic capabilities even in well-established and stable areas of medicine. In orthopedics, there is a wide space for applying new technologies. Early detection of osteoarthritis would allow the "**window of opportunity**" for early diagnosis to be exploited and thus improve the effectiveness of conservative treatment. Also, monitoring relevant markers or groups of markers would allow more accurate identification of trigger events in individual patients and an understanding of the development and key stages of the disease. The potential for early diagnosis and intervention in arthritis is a compelling focus in molecular diagnostics. To capitalize on these opportunities, a comprehensive understanding of the disease's progression and the strategic application of diagnostic tools are crucial. Molecular diagnostics offers a unique window to detect arthritis at its early stages, making early intervention a powerful tool for significantly altering the disease course and enhancing treatment effectiveness. By leveraging this "window of opportunity," healthcare providers can tailor strategies to optimize patient care. The strength of molecular diagnostics lies in its ability to uncover the earliest signs of disease activity. Advanced techniques like biomarker analysis and genetic profiling enable clinicians to pinpoint the onset of arthritis before clinical symptoms appear. This proactive approach

allows for a more targeted treatment plan, focusing on halting disease progression and preserving joint function. Strategic timing in treatment is paramount. The concept of a "timeslot" for treatment emphasizes the significance of early-stage intervention. Various treatments, including lifestyle modifications, pharmacological therapies, and evidence-based recommendations, demonstrate higher efficacy when implemented promptly.

1. Lifestyle Modifications: Altering lifestyle factors such as exercise habits and dietary changes can significantly impact disease progression. Early adoption of these changes enhances patient outcomes and improves overall quality of life.

2. Pharmacological Interventions: Early use of disease-modifying antirheumatic drugs (DMARDs) and biologics can alter the disease trajectory, reducing joint damage and improving long-term functionality. The timely introduction of these therapies is essential to maximize their benefits.

The early-diagnosis application of molecular markers in arthritis management is a groundbreaker in the fiels of prevention of an advanced stages of disease. Early identification and intervention not only offer the best chance for effective treatment but also align with patient-centered care objectives. Ongoing research and technological progress will further refine these strategies, underscoring the significance of early diagnosis and personalized treatment plans in managing arthritis effectively.

5.2. Limitations of Nanomaterials in Biomedicine

Nanotechnology has revolutionized this field by enabling the design of drug carriers at the molecular level, enhancing their ability to navigate biological barriers and reach target tissues. Nanoparticles, for instance, can be engineered to exploit the enhanced permeability and retention (EPR) effect, a phenomenon where they accumulate preferentially in tumor tissues due to their leaky vasculature.

Furthermore, research is ongoing into stimuli-responsive delivery systems that release their payload in response to specific physiological triggers such as pH changes, temperature variations, or enzymatic activity. This approach not only improves the precision of drug release but also reduces systemic toxicity.

Overall, the future of drug delivery is promising. Current research is focused on combining multiple strategies to create smarter, multifunctional systems capable of overcoming the challenges posed by complex diseases. Enhanced imaging techniques and the integration of artificial intelligence in drug delivery design are also paving the way for more personalized and effective treatment regimens.

The application of nano theranostics spans various medical disciplines. In oncology, it offers a powerful tool for the targeted treatment of tumors, allowing for real-time monitoring of drug delivery and therapeutic response. The integration of imaging agents within nano theranostics platforms enables noninvasive tracking of treatment progress. Beyond cancer, nanotheragnostics holds promise for neurological disorders, cardiovascular diseases, and infectious diseases. Its ability to cross biological barriers, such as the blood-brain barrier, opens new avenues for treating complex conditions like Alzheimer's and Parkinson's disease.

Despite its potential, nanotheragnostics faces several challenges. The complexity of designing multifunctional nanoparticles that are safe, effective, and economically viable remains a significant hurdle. Regulatory frameworks need to adapt to evaluate the safety and efficacy of these novel treatments effectively. Research is ongoing to address these challenges, with interdisciplinary collaboration being key to advancing the field. As nanotechnology continues to evolve, the vision of personalized medicine tailored to individual patient needs becomes increasingly attainable.

The use of nanomaterials in the field of biomedicine is a growing area of interest within nanotechnology. The potential of nanomaterials is remarkable, but there are limitations and obstacles to the utility of them in biomedicine. Although some nanomaterials have gained FDA approval for parenteral uses, proving their safety and efficacy, it is essential to evaluate the parameters that limit the wider use of these materials in the realm of biomedicine.

The primary concern regarding nanomaterials in biomedicine is their potential toxicity. The diminutive size of nanomaterials facilitates their interaction with biological systems at a molecular level, potentially leading to toxicological effects that have yet to be elucidated. Furthermore, the classification of nanoparticles and electrospun or force-spinning materials is of paramount importance, as these technologies have found applications beyond traditional domains, including food supplement production. However, the toxicity of certain types of nanomaterials in humans remains poorly understood, particularly in the context of extended exposure. In this regard, we are more focused on nanoparticles synthesized chemically rather than physically. The preparation method and characterization play significantly more crucial roles in complex processes such as testing novel materials, which also encompasses prospective areas for future applications, such as sensing, where we will primarily work with analyte samples collected from patients or on skin applications, where toxicity tests are prevalent. In any case, the implementation of drug delivery systems will require a more extended timeline due to the longer certification process.

The regulatory framework for nanomaterials in the medical domain is still in flux. The absence of standardized protocols for the evaluation of nanomaterials poses a significant challenge for regulatory bodies, such as the FDA, to effectively assess and approve novel nanomaterial-based therapies. This uncertainty can impede the development and approval process for new nanomaterials, thereby limiting their availability and utilization in clinical settings.

Producing nanomaterials with consistent quality and properties is another obstacle. Variations in the manufacturing process can result in differences in the size, shape, and surface properties of nanomaterials, which can impact their behavior within biological systems. Ensuring reproducibility and uniformity in nanomaterial production is paramount for their reliable utilization in biomedical applications.

The utilization of nanomaterials in the medical field also entails ethical and societal concerns. Prominent issues include privacy, consent, and equitable access to nanotechnology-based treatments. Furthermore, there are concerns regarding the environmental impact of nanomaterials, particularly with regard to their disposal and potential accumulation in ecosystems.

Despite nanomaterials' substantial potential for advancing biomedicine, their limitations cannot be disregarded. Comprehensive research, stringent regulatory frameworks, and ethical considerations are indispensable in addressing these challenges. By comprehensively addressing these limitations, the biomedical community can effectively harness nanomaterials' full potential to enhance healthcare outcomes.

6. CONCLUSION

This thesis has successfully achieved its stated research objectives, demonstrating the high potential of functionalized nanofibrous membranes in the field of early-stage theragnostics. The results obtained from both theoretical design and experimental validation confirm the multifunctionality, sensitivity, and practical applicability of the developed materials:

a) The study confirmed that functionalized nanofibrous membranes are suitable for a wide range of theragnostic applications. Their unique physicochemical properties—namely high surface area, tunable porosity, and surface modifiability—make them ideal platforms for combining diagnostic sensing with therapeutic action. Their versatility enables integration into multiple biomedical technologies, including biosensing platforms, smart wound dressings, and targeted drug delivery systems.

b) The research demonstrated that specifically functionalized membranes exhibit excellent sensitivity in detecting extremely low concentrations of analytes, achieving detection limits in the picomolar range, particularly in urine samples. This highlights the effectiveness of surface functionalization strategies, and the stability of biological recognition elements immobilized on nanofiber matrices. Such sensitivity is critical for the early detection of disease biomarkers before clinical symptoms manifest, fulfilling one of the key promises of theragnostic technologies.

c) Furthermore, the study validated that these membranes are capable of selective detection of clinically relevant bacterial species (e.g., E. coli) and specific protein biomarkers, with results supporting the reproducibility and robustness of the sensing system. Due to their straightforward production process, compatibility with scalable fabrication techniques (such as electrospinning), and adaptability to existing detection platforms, these functionalized membranes are now considered ready for technological transfer. The advancement of biosensor technologies, whether bionanosensors, electrochemical, or optical, continues to revolutionize the fields of medical diagnostics and environmental monitoring. These innovations not only provide rapid and accurate detection of diseases and pollutants but also open new avenues for personalized medicine and sustainable environmental practices.

7. SUMMARY

The thesis is grounded in the findings of seven original research articles, supplemented by three comprehensive review papers and four conference presentations. Collectively, these contributions establish a robust framework for enhancing understanding in the realm of functionalized nanofibers and their therapeutic applications.

Functionalized nanofibers have garnered considerable interest across various biomedical domains, particularly in wound healing. Dressings composed of nanofibers are engineered to deliver antimicrobial agents and regenerative biomolecules directly to the site of injury. These constructs replicate the extracellular matrix, thereby facilitating cell adhesion, proliferation, and tissue remodeling.

Moreover, recent developments have broadened these applications to include diagnostics. Microfluidic platforms alongside specially designed nanofiber membranes, which are integrated with specific antibodies, aptamers, or microRNAs (Mahmoudian et al. 2021), demonstrate substantial potential for non-invasive point-of-care diagnostics. These systems are capable of identifying disease biomarkers at extremely low concentrations, even at picomolar levels, in biological samples such as urine or saliva. Their straightforward

design and high sensitivity provide avenues for routine disease screening within general practitioners' offices or even at home, potentially leading to decreased healthcare costs and enhanced access to medical care. In summary, this research advances the next generation of therapeutic solutions by bridging advanced materials science with practical medical applications. The evident promise of nanofiber-based systems in both therapeutic and diagnostic domains open new pathways for personalized medicine, enabling precise interventions that can be administered early, accurately, and efficiently

8. **REFERENCE LIST**

1) Amler E, Abbott A, Ball WJ (1992) Structural dynamics and oligomeric interactions of Na+,K(+)-ATPase as monitored using fluorescence energy transfer. Biophys J 61:553–568. https://doi.org/10.1016/S0006-3495(92)81859-3
2) Anderson J, Caplan L, Yazdany J, et al (2012) Rheumatoid arthritis disease activity measures: American College of Rheumatology recommendations for use in clinical practice. Arthritis Care Res (Hoboken) 64:640–647. https://doi.org/10.1002/ACR.21649
3) Attur M, Krasnokutsky S, Statnikov A, et al (2015) Low-grade inflammation in symptomatic knee osteoarthritis: Prognostic value of inflammatory plasma lipids and peripheral blood leukocyte biomarkers. Arthritis and Rheumatology 67:2905–2915. https://doi.org/10.1002/ART.39279
4) Bauer DC, Hunter DJ, Abramson SB, et al (2006) Classification of osteoarthritis biomarkers: a proposed approach. Osteoarthritis Cartilage 14:723–727. https://doi.org/10.1016/J.JOCA.2006.04.001
5) Bay-Jensen AC, Reker D, Kjelgaard-Petersen CF, et al (2016) Osteoarthritis year in review 2015: soluble biomarkers and the BIPED criteria. Osteoarthritis Cartilage 24:9–20. https://doi.org/10.1016/J.JOCA.2015.10.014
6) Bernotiene E, Bagdonas E, Kirdaite G, et al (2020) Emerging Technologies and Platforms for the Immunodetection of Multiple Biochemical Markers in Osteoarthritis Research and Therapy. Front Med (Lausanne) 7:622. https://doi.org/10.3389/FMED.2020.572977/BIBTEX
7) Bhalla N, Jolly P, Formisano N, Estrela P (2016) Introduction to biosensors. Essays Biochem 60:1. https://doi.org/10.1042/EBC20150001

8) Bianchi J, de Oliveira Ruellas AC, Gonçalves JR, et al (2020a) Osteoarthritis of the Temporomandibular Joint can be diagnosed earlier using biomarkers and machine learning. Sci Rep 10:. https://doi.org/10.1038/S41598-020-64942-0

9) Bianchi J, de Oliveira Ruellas AC, Gonçalves JR, et al (2020b) Osteoarthritis of the Temporomandibular Joint can be diagnosed earlier using biomarkers and machine learning. Sci Rep 10:. https://doi.org/10.1038/S41598-020-64942-0

10) Bianchi J, Ruellas A, Prieto JC, et al (2021) Decision Support Systems in Temporomandibular Joint Osteoarthritis: A review of Data Science and Artificial Intelligence Applications. Semin Orthod 27:78–86. https://doi.org/10.1053/j.sodo.2021.05.004

11) Boffa A, Merli G, Andriolo L, et al (2020) Synovial Fluid Biomarkers in Knee Osteoarthritis: A Systematic Review and Quantitative Evaluation Using BIPEDs Criteria: https://doi.org/101177/1947603520942941 13:82S-103S. https://doi.org/10.1177/1947603520942941

12) Callahan LF, Cleveland RJ, Allen KD, Golightly Y (2021) Racial/Ethnic, Socioeconomic, and Geographic Disparities in the Epidemiology of Knee and Hip Osteoarthritis. Rheum Dis Clin North Am 47:1–20. https://doi.org/10.1016/J.RDC.2020.09.001

13) Chen K, Li Y, Li Y, et al (2023a) Stimuli-responsive electrospun nanofibers for drug delivery, cancer therapy, wound dressing, and tissue engineering. J Nanobiotechnology 21:237. https://doi.org/10.1186/S12951-023-01987-Z

14) Chen K, Li Y, Li Y, et al (2023b) Stimuli-responsive electrospun nanofibers for drug delivery, cancer therapy, wound dressing, and tissue engineering. Journal of Nanobiotechnology 2023 21:1 21:1–15. https://doi.org/10.1186/S12951-023-01987-Z

15) Chen X, Zhou G, Song P, et al (2014) Ultrasensitive electrochemical detection of prostate-specific antigen by using antibodies anchored on a DNA nanostructural scaffold. Anal Chem 86:7337–7342. https://doi.org/10.1021/AC500054X

16) Coradduzza D, Bellu E, Congiargiu A, et al (2022a) Role of Nano-miRNAs in Diagnostics and Therapeutics. International Journal of Molecular Sciences 2022, Vol 23, Page 6836 23:6836. https://doi.org/10.3390/IJMS23126836

17) Coradduzza D, Bellu E, Congiargiu A, et al (2022b) Role of Nano-miRNAs in Diagnostics and Therapeutics. Int J Mol Sci 23:6836. https://doi.org/10.3390/IJMS23126836

18) Cui A, Li H, Wang D, et al (2020) Global, regional prevalence, incidence and risk factors of knee osteoarthritis in population-based studies. EClinicalMedicine 29–30:. https://doi.org/10.1016/J.ECLINM.2020.100587

19) Deshmukh K, Sankaran S, Basheer Ahamed M, Khadheer Pasha SK (2019) Biomedical Applications of Electrospun Polymer Composite Nanofibres. Lecture Notes in Bioengineering 111–165. https://doi.org/10.1007/978-3-030-04741-2_5

20) Deshpande BR, Katz JN, Solomon DH, et al (2016) Number of Persons With Symptomatic Knee Osteoarthritis in the US: Impact of Race and Ethnicity, Age, Sex, and Obesity. Arthritis Care Res (Hoboken) 68:1743–1750. https://doi.org/10.1002/ACR.22897

21) Desantis, V., Saltarella, I., Lamanuzzi, A., Melaccio, A., Solimando, A. G., Mariggiò, M. A., Racanelli, V., Paradiso, A., Vacca, A., & Frassanito, M. A. (2020). MicroRNAs-based nano-strategies as new therapeutic approach in multiple myeloma to overcome disease progression and drug resistance. International Journal of Molecular Sciences, 21(9). https://doi.org/10.3390/ijms21093084

22) Fedoruk GV (2013) Arthroscopic anterior cruciate ligament plasty of the knee augmented hamstring graft

23) Fedoruk GV (2012) Modern technologies in arthroplasty of the anterior cruciate ligament. Zemsky vrach 21–23

24) Ford JA, Solomon DH (2019) Challenges in Implementing Treat to Target Strategies in Rheumatology. Rheum Dis Clin North Am 45:101. https://doi.org/10.1016/J.RDC.2018.09.007

25) Furuzawa-Carballeda J, Muñoz-Chablé OA, MacÍas-Hernández SI, Agualimpia-Janning A (2009) Effect of polymerized-type I collagen in knee osteoarthritis. II. In vivo study. Eur J Clin Invest 39:598–606. https://doi.org/10.1111/J.1365-2362.2009.02144.X

26) Garnero P, Piperno M, Gineyts E, et al (2001) Cross sectional evaluation of biochemical markers of bone, cartilage, and synovial tissue metabolism in patients with knee osteoarthritis: Relations with disease activity and joint damage. Ann Rheum Dis 60:619–626. https://doi.org/10.1136/ard.60.6.619

27) Guo Y, Wang X, Shen Y, et al (2022) Research progress, models and simulation of electrospinning technology: a review. J Mater Sci 57:58–104. https://doi.org/10.1007/S10853-021-06575-W/METRICS

28) Gómez-Hens, A., & Fernández-Romero, J. M. (2006). Analytical methods for the control of liposomal delivery systems. TrAC - Trends in Analytical Chemistry, 25(2), 167–178. https://doi.org/10.1016/j.trac.2005.07.006

29) Hassani S, Momtaz S, Vakhshiteh F, et al (2016) Biosensors and their applications in detection of organophosphorus pesticides in the environment. Archives of Toxicology 2016 91:1 91:109–130. https://doi.org/10.1007/S00204-016-1875-8

30) Henrotin Y (2022) Osteoarthritis in year 2021: biochemical markers. Osteoarthritis Cartilage 30:237–248. https://doi.org/10.1016/J.JOCA.2021.11.001

31) Henrotin Y, Gharbi M, Mazzucchelli G, et al (2012) Fibulin 3 peptides Fib3-1 and Fib3-2 are potential biomarkers of osteoarthritis. Arthritis Rheum 64:2260–2267. https://doi.org/10.1002/ART.34392

32) Henrotin Y, Sanchez C, Bay-Jensen AC, Mobasheri A (2016) Osteoarthritis biomarkers derived from cartilage extracellular matrix: Current status and future perspectives. Ann Phys Rehabil Med 59:145–148. https://doi.org/10.1016/J.REHAB.2016.03.004

33) Hosnijeh FS, Siebuhr AS, Uitterlinden AG, et al (2016) Association between biomarkers of tissue inflammation and progression of osteoarthritis: Evidence from the Rotterdam study cohort. Arthritis Res Ther 18:1–10. https://doi.org/10.1186/S13075-016-0976-3/FIGURES/2

34) Hua W, Verreault D, Allen HC (2014) Surface electric fields of aqueous solutions of NH4NO3, Mg(NO3)2, NaNO3, and LiNO3: Implications for atmospheric aerosol chemistry. Journal of Physical Chemistry C 118:24941–24949. https://doi.org/10.1021/JP505770T/SUPPL_FILE/JP505770T_SI_001.PDF

35) Hupfeld, S., Moen, H. H., Ausbacher, D., Haas, H., & Brandl, M. (2010). Liposome fractionation and size analysis by asymmetrical flow field-flow fractionation/multi-angle light scattering: influence of ionic strength and osmotic pressure of the carrier liquid. Chemistry and Physics of Lipids, 163(2), 141–147. https://doi.org/10.1016/J.CHEMPHYSLIP.2009.10.009

36) Kalogianni DP (2021) Nanotechnology in emerging liquid biopsy applications. 8:13. https://doi.org/10.1186/s40580-021-00263-w

37) Kjelgaard-Petersen C, Siebuhr AS, Christiansen T, et al (2015) Synovitis biomarkers: ex vivo characterization of three biomarkers for identification of inflammatory osteoarthritis. Biomarkers 20:547–556. https://doi.org/10.3109/1354750X.2015.1105497

38) Kralovic M, Vjaclovsky M, Kestlerova A, et al (2019) Electrospun nanofibers as support for the healing of intestinal anastomoses. Physiol Res 68:S517–S525. https://doi.org/10.33549/PHYSIOLRES.934387

39) Krasnokutsky S, Oshinsky C, Attur M, et al (2017) Serum Urate Levels Predict Joint Space Narrowing in Non-Gout Patients With Medial Knee Osteoarthritis. Arthritis Rheumatol 69:1213–1220. https://doi.org/10.1002/ART.40069

40) Kraus VB, Karsdal MA (2021) Osteoarthritis: Current Molecular Biomarkers and the Way Forward. Calcif Tissue Int 109:329–338. https://doi.org/10.1007/s00223-020-00701-7

41) Kraus VB, Sun S, Reed A, et al (2024) An osteoarthritis pathophysiological continuum revealed by molecular biomarkers. Sci Adv 10:eadj6814. https://doi.org/10.1126/SCIADV.ADJ6814

42) Kuhi L, Tamm AE, Tamm AO, Kisand K (2021) Risk Assessment of the Progression of Early Knee Osteoarthritis by Collagen Neoepitope C2C: A Longitudinal Study of an Estonian Middle-Aged Cohort. Diagnostics (Basel) 11:. https://doi.org/10.3390/DIAGNOSTICS11071236

43) Kumavat R, Kumar V, Malhotra R, et al (2021) Biomarkers of Joint Damage in Osteoarthritis: Current Status and Future Directions. Mediators Inflamm 2021:. https://doi.org/10.1155/2021/5574582

44) Li Y, Abedalwafa MA, Tang L, et al (2018) Electrospun nanofibers for sensors. Electrospinning: Nanofabrication and Applications 571–601. https://doi.org/10.1016/B978-0-323-51270-1.00018-2

45) Li YH, Tavallaee G, Tokar T, et al (2016) Identification of synovial fluid microRNA signature in knee osteoarthritis: differentiating early- and late-stage knee osteoarthritis. Osteoarthritis Cartilage 24:1577–1586. https://doi.org/10.1016/J.JOCA.2016.04.019

46) Liu K, Blokhuis AWP, Dijt SJ, et al (2024a) Molecular-scale dissipative chemistry drives the formation of nanoscale assemblies and their macroscale transport. Nature Chemistry 2024 17:1 17:124–131. https://doi.org/10.1038/s41557-024-01665-z

47) Liu K, Blokhuis AWP, Dijt SJ, et al (2024b) Molecular-scale dissipative chemistry drives the formation of nanoscale assemblies and their macroscale transport. Nature Chemistry 2024 17:1 17:124–131. https://doi.org/10.1038/s41557-024-01665-z

48) Longo UG, Candela V, Berton A, et al (2021) Biosensors for Detection of Biochemical Markers Relevant to Osteoarthritis. Biosensors 2021, Vol 11, Page 31 11:31. https://doi.org/10.3390/BIOS11020031

49) Lotz M, Martel-Pelletier J, Christiansen C, et al (2014) Republished: Value of biomarkers in osteoarthritis: current status and perspectives. Postgrad Med J 90:171–178. https://doi.org/10.1136/POSTGRADMEDJ-2013-203726REP

50) Lotz M, Martel-Pelletier J, Christiansen C (2013) Value of biomarkers in osteoarthritis: current status and perspectives. Ann Rheum Dis 72:1756–1763. https://doi.org/10.1136/annrheumdis-2013-203726

51) Mahmood Ansari S, Saquib Q, De Matteis V, et al (2021) Marine Macroalgae Display Bioreductant Efficacy for Fabricating Metallic Nanoparticles: Intra/Extracellular Mechanism and Potential Biomedical Applications. Bioinorg Chem Appl 2021:. https://doi.org/10.1155/2021/5985377

52) Mahmoudian A, Lohmander LS, Mobasheri A, et al (2021) Early-stage symptomatic osteoarthritis of the knee - time for action. Nat Rev Rheumatol 17:621–632. https://doi.org/10.1038/S41584-021-00673-4

53) Maren D, Tobias M, Frank Z, et al (2022) Relationship between different serum cartilage biomarkers in the acute response to running and jumping in healthy male individuals. Scientific Reports 2022 12:1 12:1–10. https://doi.org/10.1038/s41598-022-10310-z

54) Martino S, Yilmaz D, Tammaro C, et al (2025) Flexible 3D nanofiber-based SERS biosensor for detection of miRNA-223-3p in early Laryngeal Cancer diagnosis. Talanta 285:127293. https://doi.org/10.1016/J.TALANTA.2024.127293

55) McIlwraith CW, Kawcak CE, Frisbie DD, et al (2018) Biomarkers for equine joint injury and osteoarthritis. Journal of Orthopaedic Research® 36:823–831. https://doi.org/10.1002/JOR.23738

56) Meehan RT, Regan EA, Hoffman ED, et al (2021) Synovial Fluid Cytokines, Chemokines and MMP Levels in Osteoarthritis Patients with Knee Pain Display a Profile Similar to Many Rheumatoid Arthritis Patients. J Clin Med 10:. https://doi.org/10.3390/jcm10215027

57) Mohebbi M, Atabaki M, Tavakkol-Afshari J, et al (2022) Significant Effect of Crocin on the Gene Expression of MicroRNA-21 and MicroRNA-155 in Patients with Osteoarthritis. Iran J Allergy Asthma Immunol 21:. https://doi.org/10.18502/IJAAI.V21I3.9805

58) Mozafari, M. R., Johnson, C., Hatziantoniou, S., & Demetzos, C. (2008). Nanoliposomes and their applications in food nanotechnology. Journal of Liposome Research, 18(4), 309–327. https://doi.org/10.1080/08982100802465941

59) Munjal A, Bapat S, Hubbard D, et al (2019) Advances in Molecular biomarker for early diagnosis of Osteoarthritis. Biomol Concepts 10:111–119. https://doi.org/10.1515/BMC-2019-0014/XML

60) Murray CJL, Richards MA, Newton JN, et al (2013) UK health performance: findings of the Global Burden of Disease Study 2010. Lancet 381:997–1020. https://doi.org/10.1016/S0140-6736(13)60355-4

61) Naraoka T, Ishibashi Y, Tsuda E, et al (2013) Periodic knee injections of collagen tripeptide delay cartilage degeneration in rabbit experimental osteoarthritis. Arthritis Res Ther 15:. https://doi.org/10.1186/AR4181

62) Naresh V., Lee N (2021) A Review on Biosensors and Recent Development of Nanostructured Materials-Enabled Biosensors. A Review on Biosensors and Recent Development of Nanostructured Materials-Enabled Biosensors Sensors 21:1109. https://doi.org/10.3390/s21041109

63) Nganvongpanit K, Soponteerakul R, Kaewkumpai P, et al (2017) Osteoarthritis in two marine mammals and 22 land mammals: learning from skeletal remains. J Anat 231:140. https://doi.org/10.1111/JOA.12620

64) Nicu L, LechÍ T (2008) Biosensors and tools for surface functionalization from the macro- to the nanoscale: The way forward. J Appl Phys 104:. https://doi.org/10.1063/1.2973147

65) Nijhawan S, Quereshy F, Baur D, Horan M (2014) Patient standardization for diagnosis, treatment, and outcomes of osteoarthritis of the temporomandibular joint. Oral Surg Oral Med Oral Pathol Oral Radiol 117:e332–e333. https://doi.org/10.1016/J.OOOO.2014.01.008

66) Ohtsuki I, Morimoto S (2022) Troponin. Encyclopedia of Biological Chemistry: Second Edition 445–449. https://doi.org/10.1016/B978-0-12-378630-2.00195-X

67) Östlind E, Eek F, Stigmar K, et al (2022) Associations Between Physical Activity, Self-reported Joint Function, and Molecular Biomarkers in Working Age Individuals With Hip and/or Knee Osteoarthritis. Clin Med Insights Arthritis Musculoskelet Disord 15:11795441221081064. https://doi.org/10.1177/11795441221081063

68) Pal CP, Singh P, Chaturvedi S, et al (2016) Epidemiology of knee osteoarthritis in India and related factors. Indian J Orthop 50:518–522. https://doi.org/10.4103/0019-5413.189608

69) Pashchenko A, Stuchlíková S, Varvařovská L, et al (2022) Smart nanofibres for specific and ultrasensitive nanobiosensors and drug delivery system. Acta Veterinaria Brno 91:. https://doi.org/10.2754/avb202291020163

70) Pérez-García S, Calamia V, Hermida-Gómez T, et al (2021) Proteomic analysis of synovial fibroblasts and articular chondrocytes co-cultures reveals valuable vip-modulated inflammatory and degradative proteins in osteoarthritis. Int J Mol Sci 22:. https://doi.org/10.3390/ijms22126441

71) Poole AR (2003) Biochemical/immunochemical biomarkers of osteoarthritis: utility for prediction of incident or progressive osteoarthritis. Rheumatic Disease Clinics 29:803–818. https://doi.org/10.1016/S0889-857X(03)00056-5

72) Puigdellivol J, Comellas Berenger C, Pérez Fernández MÁ, et al (2019) Effectiveness of a Dietary Supplement Containing Hydrolyzed Collagen, Chondroitin Sulfate, and Glucosamine in Pain Reduction and Functional Capacity in Osteoarthritis Patients. J Diet Suppl 16:379–389. https://doi.org/10.1080/19390211.2018.1461726

73) Rasmussen DGK, Boesby L, Nielsen SH, et al (2019) Collagen turnover profiles in chronic kidney disease. Scientific Reports 2019 9:1 9:1–11. https://doi.org/10.1038/s41598-019-51905-3

74) Roemer FW, Guermazi A, Demehri S, et al (2021) Imaging in Osteoarthritis. Osteoarthritis Cartilage. https://doi.org/10.1016/J.JOCA.2021.04.018

75) Reimer, K., Vogt, P. M., Broegmann, B., Hauser, J., Rossbach, O., Kramer, A., Rudolph, P., Bosse, B., Schreier, H., & Fleischer, W. (2000). An innovative topical drug formulation for wound healing and infection treatment: in vitro and in vivo investigations of a povidone-iodine liposome hydrogel. Dermatology (Basel, Switzerland), 201(3), 235–241. https://doi.org/10.1159/000018494Runhaar J, Bierma-Zeinstra SMA (2022) The Challenges in the Primary Prevention of Osteoarthritis. Clin Geriatr Med 38:259–271. https://doi.org/10.1016/J.CGER.2021.11.012

76) Schadow S, Simons VS, Lochnit G, et al (2017) Metabolic Response of Human Osteoarthritic Cartilage to Biochemically Characterized Collagen Hydrolysates.

International Journal of Molecular Sciences 2017, Vol 18, Page 207 18:207. https://doi.org/10.3390/IJMS18010207

77) Sharma GK, James NR, Sharma GK, James NR (2022) Electrospinning: The Technique and Applications. Recent Developments in Nanofibers Research. https://doi.org/10.5772/INTECHOPEN.105804

78) Sharma TK, Ramanathan R, Rakwal R, et al (2015) Moving forward in plant food safety and security through NanoBioSensors: Adopt or adapt biomedical technologies? Proteomics 15:1680–1692. https://doi.org/10.1002/PMIC.201400503

79) Shen R, Ren X, Jing R, et al (2015) Rheumatoid Factor, Anti-Cyclic Citrullinated Peptide Antibody, C-Reactive Protein, and Erythrocyte Sedimentation Rate for the Clinical Diagnosis of Rheumatoid Arthritis. Lab Med 46:226–229. https://doi.org/10.1309/LMZYTSO5RHIHV93T

80) Sierakowski S, Cutolo M (2011) Morning symptoms in rheumatoid arthritis: a defining characteristic and marker of active disease. http://dx.doi.org/103109/030097422011566433 40:1–5. https://doi.org/10.3109/03009742.2011.566433

81) Smith WR, Hudson PW, Ponce BA, Rajaram Manoharan SR (2018) Nanotechnology in orthopedics: A clinically oriented review. BMC Musculoskelet Disord 19:1–10. https://doi.org/10.1186/S12891-018-1990-1/FIGURES/6

82) Sun X, Zhen X, Hu X, et al (2019) Osteoarthritis in the Middle-Aged and Elderly in China: Prevalence and Influencing Factors. Int J Environ Res Public Health 16:. https://doi.org/10.3390/IJERPH16234701

83) Talluri, S. V., Kuppusamy, G., Karri, V. V. S. R., Tummala, S., & Madhunapantula, S. R. v. (2016). Lipid-based nanocarriers for breast cancer treatment – comprehensive review. Drug Delivery, 23(4), 1291–1305. https://doi.org/10.3109/10717544.2015.1092183

84) Valpione S, Campana L (2019) Detection of circulating tumor DNA (ctDNA) by digital droplet polymerase chain reaction (dd-PCR) in liquid biopsies. Methods Enzymol 629:1–15. https://doi.org/10.1016/BS.MIE.2019.08.002

85) van der Molen HF, Visser S, Alfonso JH, et al (2021) Diagnostic criteria for musculoskeletal disorders for use in occupational healthcare or research: a scoping review of consensus- and synthesised-based case definitions. BMC Musculoskelet Disord 22:1–9. https://doi.org/10.1186/S12891-021-04031-Z/TABLES/1

86) Van Dorst B, Mehta J, Bekaert K, et al (2010) Recent advances in recognition elements of food and environmental biosensors: A review. Biosens Bioelectron 26:1178–1194. https://doi.org/10.1016/J.BIOS.2010.07.033

87) Vos T, Flaxman AD, Naghavi M, et al (2012) Years lived with disability (YLDs) for 1160 sequelae of 289 diseases and injuries 1990-2010: a systematic analysis for the Global Burden of Disease Study 2010. Lancet 380:2163–2196. https://doi.org/10.1016/S0140-6736(12)61729-2

88) Waluyo Y, Budu, Bukhari A, et al (2021) Changes in levels of cartilage oligomeric proteinase and urinary C-terminal telopeptide of type II collagen in subjects with knee osteoarthritis after dextrose prolotherapy: A randomized controlled trial. J Rehabil Med 53:. https://doi.org/10.2340/16501977-2835

89) Wang C, Wang J, Zeng L, et al (2019a) Fabrication of Electrospun Polymer Nanofibers with Diverse Morphologies. Molecules 2019, Vol 24, Page 834 24:834. https://doi.org/10.3390/MOLECULES24050834

90) Wang S, Su S, Yu C, et al (2021) Immunodetection of urinary C-terminal telopeptide fragment of type II collagen: An osteoarthritis biomarker analysis. Biotechnol Appl Biochem 68:726–731. https://doi.org/10.1002/BAB.1981

91) Wang XY, Zhang F, Zhang C, et al (2020) The Biomarkers for Acute Myocardial Infarction and Heart Failure. Biomed Res Int 2020:. https://doi.org/10.1155/2020/2018035

92) Wang Z, Ma B, Shen C, et al (2019b) Electrochemical Biosensing of Chilled Seafood Freshness by Xanthine Oxidase Immobilized on Copper-Based Metal–Organic Framework Nanofiber Film. Food Anal Methods 12:1715–1724. https://doi.org/10.1007/S12161-019-01513-8

93) Watson JL, Seinkmane E, Styles CT, et al (2023) Macromolecular condensation buffers intracellular water potential. Nature 623:842–852. https://doi.org/10.1038/S41586-023-06626-Z

94) Wiesing U (2019) Theranostics: is it really a revolution? Evaluating a new term in medicine. Med Health Care Philos 22:593–597. https://doi.org/10.1007/S11019-019-09898-3

95) Wongkaew N Nanofiber-integrated miniaturized systems: an intelligent platform for cancer diagnosis. https://doi.org/10.1007/s00216-019-01589-5

96) Yang, F., Huang, R., Ma, H., Zhao, X., & Wang, G. (2020). MiRNA-411 regulates chondrocyte autophagy in osteoarthritis by targeting hypoxia-inducible factor 1

alpha(HIF-1α). Medical Science Monitor, 26. https://doi.org/10.12659/MSM.921155

97) Zhang, X., & Wu, J. (2015). Prognostic role of microRNA-145 in prostate cancer: A systems review and meta-analysis. Prostate International, 3(3), 71–74. https://doi.org/10.1016/j.prnil.2014.09.001

98) ISO 80004-1:2023(en), Nanotechnologies – Vocabulary — Part 1: Core vocabulary. https://www.iso.org/obp/ui/en/#iso:std:iso:80004:-1:ed-1:v1:en. Accessed 11 Apr 2025a

99) European Observatory for Nanomaterials. https://euon.echa.europa.eu/. Accessed 11 Apr 2025b

100) BEST (Biomarkers, EndpointS, and other Tools) Resource [Internet] - PubMed. https://pubmed.ncbi.nlm.nih.gov/27010052/. Accessed 3 Jul 2022c

101) Prevalence and most common causes of disability among adults--United States, 2005 - PubMed. https://pubmed.ncbi.nlm.nih.gov/19407734/. Accessed 3 Jul 2022d

(2003) Origin.

102) Gnuplot: An Interactive Plotting Program. http://www.gnuplot.info/docs_4.0/gnuplot.html. Accessed 17 Mar 2025e

9. LIST OF PUBLICATIONS

a. Original scientific papers that are the basis of this dissertation

1. Pashchenko, A., Pospíšilová, M., Šaternová, J., Varvařovská, L., Jarošíková, R., Kalábová, H., Jarošíková, T., Beková, Š., Cruciani, S., Nečas, A., Novotný, P., Rulc, J., Tejral, G., Sopko, B., Maioli, M., & Amler, E. (2025). Fluorescent bionanosensor for picomolar detection of biomarkers in fluids. *PeerJ. Submitted March , 2025.* **IF: 3.2**

2. Bocková M, **Pashchenko A,** Stuchlíková S, Kalábová H, Divín R, Novotný P, Kestlerová A, Jelen K, Kubový P, Firment P, Fedačko J, Jarošíková T, Rulc J, Rosina J, Nečas A, Amler E, Hoch J. Low Concentrated Fractionalized Nanofibers as Suitable Fillers for Optimization of Structural-Functional Parameters of Dead Space Gel Implants after Rectal Extirpation. Gels. 2022 Mar 4;8(3):158. doi: 10.3390/gels8030158. PMID: 35323271**IF: 4.9**

3. VARVAŘOVSKÁ, Leontýna; SOPKO, Bruno; DIVÍN, Radek; **PASHSCHENKO, Aleksei**; FEDAČKO, Jan et al. Bacteria trapping effectivity on nanofiber membrane in liquids is exponentially dependent on the surface density.

("Bacteria trapping effectivity on nanofibre membrane in liquids is ...") Online. Acta Veterinaria Brno. 2023, roč. 92, č. 4, s. 435-441. ISSN 0001-7213. Dostupné z: https://doi.org/10.2754/avb202392040435.**IF: 0.817**

4. Amler E, Vojáček V, Sopko B, Divín R, **Pashchenko A**, Varga J, Nečas A, Celer V, Filipejova Z, Urbanová L, Rulc J, Krajníková M, Jarošíková T. Povidone-iodine functionalized nanofibers are prophylactic and protect against dissemination of SARS-CoV-2 infection. Epidemiol Mikrobiol Imunol. 2024;73(2):98-105. English. doi: 10.61568/emi/11-6306/20240424/137082. PMID: 39060100. **IF: 0.5**

5. Serra D, Garroni G, Cruciani S, Coradduzza D, **Pashchenko A,** Amler E, Pintore G, Satta R, Montesu MA, Kohl Y, Ventura C, Maioli M. Electrospun Nanofibers Encapsulated with Natural Products: A Novel Strategy to Counteract Skin Aging. Int J Mol Sci. 2024 Feb 5;25(3):1908. doi: 10.3390/ijms25031908. PMID: 38339184; PMCID: PMC10856659. **$IF_{2018-2023}$: 5.6**

6. Serra D, Bellu E, Garroni G, Cruciani S, Sarais G, Dessi D, **Pashchenko A**, Satta R, Montesu MA, Amler E, Floris M, Maioli M. Hydrolat of Helichrysum italicum promotes tissue regeneration during wound healing. ("Hydrolat of Helichrysum italicum promotes tissue regeneration during ...") Physiol Res. 2023 Dec 31;72(6):809-818. doi: 10.33549/physiolres.935101. PMID: 38215066; PMCID: PMC10805257**. IF:2.1**

7. Serra, D., Garroni, G., Cruciani, S., Coradduzza, D., **Pashchenko, A.**, Amler, E., Pintore, G., Parisse, P., Satta, R., Martini, F., Tognon, M., Brunetti, A., Ventura, C., & Maioli, M. (2024). Effects of nanofibers and essential oil in maintaining skin integrity, cell elasticity, and proliferation. Sci Rep. 2025 Mar 29;15(1):10864. doi: 10.1038/s41598-025-95788-z. PMID: 40158043. **IF: 3.8**

b. Review scientific papers that are the basis of this dissertation

1. **Pashchenko, A**., Stuchlíková, S., Varvařovská, L., Firment, P., Staňková, L., Nečasová, A., Filipejová, Z., Urbanová, L., Jarošíková, T., Nečas, A., & Amler, E. (2022). Smart nanofibres for specific and ultrasensitive nanobiosensors and drug delivery systems. In Acta Veterinaria Brno (Vol. 91, Issue 2, pp. 163–170). University of Veterinary Sciences Brno. https://doi.org/10.2754/avb202291020163 **IF: 0.817**
2. Coradduzza D, Bellu E, Congiargiu A, **Pashchenko A**, Amler E, Necas A, Carru C, Medici S, Maioli M. Role of Nano-miRNAs in Diagnostics and Therapeutics. Int J

Mol Sci. 2022 Jun 20;23(12):6836. doi: 10.3390/ijms23126836. PMID: 35743278;. **IF$_{2018-2023}$: 5.6**

3. Coradduzza D, Cruciani S, Arru C, Garroni G, **Pashchenko A**, Jedea M, Zappavigna S, Caraglia M, Amler E, Carru C, Maioli M. Role of miRNA-145, 148, and 185 and Stem Cells in Prostate Cancer. Int J Mol Sci. 2022 Jan 30;23(3):1626. doi: 10.3390/ijms23031626. PMID: 35163550;**IF$_{2018-2023}$: 5.6**
4. **PASHCHENKO, A.;** VARVAŘOVSKÁ, L.; CRUCIANI, S.; SOPKO, B.; JAROŠÍKOVÁ, T. et al. Ultrasensitive Bionanosensors from Functionalized Nanofibers for Musculoskeletal Disorders Diagnosis. Online. Osteoarthritis and Cartilage. 2023, roč. 31, s. S83-S84. ISSN 10634584. ttps://doi.org/10.1016/j.joca.2023.01.027. **IF: 7.507**
5. **PASHCHENKO, Aleksei;** PROKUPEK, Kristian; MARTINO, Sara; VARVAROVSKA, Leontyna; CRUCIANI, Sara et al. 155 OPTICAL AND ELECTRICAL BIONANOSENSORS FOR DETECTION OF STANDARD AND LOW-CONCENTRATED BIOMARKERS OF MUSCULOSKELETAL DISORDERS. Online. Osteoarthritis and Cartilage. 2024, roč. 32, s. S117-S118. ISSN 10634584. https://doi.org/10.1016/j.joca.2024.02.166.. **IF: 7.507**

c. Original scientific papers that are the basis of a dissertation without IF

1. PROKŮPEK, Kristián; **PASHCHENKO, Aleksei**; MARTINO, Sara; MLEJNEK, Pavel; CRUCIANI, Sara et al. NANOTECHNOLOGY FOR DISTANCE DIAGNOSTICS. Online. In: 2023, s. 0-0. Dostupné z: https://doi.org/10.37904/nanocon.2023.4804.
2. P. Novotný, J. Rulc, R. Divín, **A. Pashchenko**, J. Varga, M. Rogante, L.Varvařovská, R. Siroka, T. Jarosikova, E. Amler, Contactless collection of impurities on ultrasensitive nanofiber membrane, Proc. 12th International Conference “Mechanical Technologies and Structural Materials” MTSM 2023, Split, Croatia, 21-22/09/2023, N. Gjeldum, N. Čatipović, M. Mladineo, Eds., Croatian Society for Mechanical Technologies, Split, Croatia (2023), ISSN 1847-7917, pp. 229-235.

10. ATTACHMENTS

ELSEVIER LICENSE TERMS AND CONDITIONS Apr 08, 2025

This Agreement between Aleksei Pashchenko, Charles University, University of Sassari ("You") and Elsevier ("Elsevier") consists of your license details and the terms and conditions provided by Elsevier and Copyright Clearance Center.

License Number 6004301062460 License date Apr 08, 2025

Licensed Content Publisher Elsevier

Licensed Content Publication Elsevier Books

Licensed Content Title Electrospinning: anofabrication and Applications

Licensed C. AuthorYan Li,Mohammed Awad Abedalwafa,Liqin Tang,De Li,Lu Wang

Licensed Content Date Jan 1, 2019

Licensed Content Pages 31 Start Page 571 End Page 601

Type of Use reuse in a thesis/dissertation

Portion figures/tables/illustrations

Number of fgures/tables/illustrat. 2

Format both print and electronic

Are you the author of this Elsevier chapter? No

Will you be translating? No

Title of new work Bionanosensors in early-stage theragnostics

Institution name Charles University, University of Sassari

Portions FIGURE 18.1 Overview of NMs applications in sensors. NP, nanoparticle; QCM, quartz crystal microbalance. and FIGURE 18.2 Schematic illustration of the measures to endow NMs with sensing properties throughout the electrospinning process.

The Requesting Person / Organization to Appear on the License Aleksei Pashchenko, Charles University, University of Sassari Requestor Location Dr. Aleksei Pashchenko Ovocný trh 5 Prague, 11000 Czechia Publisher Tax ID GB 494 6272 12

SPRINGER NATURE LICENSE. TERMS AND CONDITIONS Apr 08, 2025

This Agreement between Aleksei Pashchenko, Charles University, University of Sassari ("You") and Springer Nature ("Springer Nature") consists of your license details and the terms and conditions provided by Springer Nature and Copyright Clearance Center.

License Number 6004321224174

License date Apr 08, 2025

Licensed Content Publisher Springer Nature

Licensed Content Publication Archives of Toxicology

Licensed Content Title Biosensors and their applications in detection of organophosphorus pesticides in the environment

Licensed Content Author Shokoufeh Hassani et al

Licensed Content Date Oct 19, 2016

Type of Use Thesis/Dissertation

Requestor type academic/university or research institute

Format print and electronic Portion figures/tables/illustrations

Number of figures/tables/illustrations 3

Will you be translating? No Circulation/distribution 1 - 29

Author of this Springer Nature content no

Title of new work Bionanosensors in early-stage theragnostics

Institution name Charles University, University of Sassari

Expected presentation date Jul 2025

Portions Fig. 1 Conceptual model of biosensing principle and Fig. 2 Typical structure of a biosensor (biorecognition, interface and transduction) and Fig. 3 Classification of biosensors based on transducer systems

The Requesting Person / Organization to Appear on the License Aleksei Pashchenko, Charles University, University of Sassari

Requestor Location Dr. Aleksei Pashchenko

BillingType InvoiceBilling Address Univerzita Karlova Ovocný trh 5Prague, 11000Czechia

SPRINGER NATURE LICENSE TERMS AND CONDITIONS Apr 08, 2025 This Agreement between Aleksei Pashchenko, Charles University, University of Sassari ("You") and Springer Nature ("Springer Nature") consists of your license details and the terms and conditions provided by Springer Nature and Copyright Clearance Center.

License Number 6004351177419

License date Apr 08, 2025

Licensed Content Publisher Springer Nature

Licensed Content Publication Analytical and Bioanalytical Chemistry

Licensed Content Title Nanofiber-integrated miniaturized systems: an intelligent platform for cancer diagnosis

Licensed Content Author Nongnoot Wongkaew

Licensed Content Date Feb 1, 2019

Type of Use Thesis/Dissertation

Requestor type academic/university or research institute

Format print and electronic

Portion figures/tables/illustrations

Number of figures/tables/illustrations 1

Will you be translating? no

Circulation/distribution 1 - 29

Author of this Springer Nature content no

Title of new work Bionanosensors in early-stage theragnostics

Institution name Charles University, University of Sassari

Expected presentation date Jul 2025

Portions Fig. 1 Nanofibers integrated microfluidic analytical systems and their application in clinical and point-of-care cancer diagnostics based on liquid biopsy. CSF = cerebrospinal fluid

The Requesting Person / Organization to Appear on the License Aleksei Pashchenko, Charles University, University of Sassari

Requestor Location Dr. Aleksei Pashchenko

Billing Type Invoice Billing Address Univerzita Karlova

Ovocný trh 5 Prague, Czechia 11000